5-1-2013

Protein carbonylation, protein aggregation and cell death in a murine model of multiple sclerosis

Anushka Dasgupta

Anushka Dasgupta

Candidate

Cell Biology and Physiology

Department

This disseration is approved, and it is acceptable in quality
and form for publication:

Dr. Oscar A. Bizzozero, Chairperson

Dr. Nora P. Bizzozero

Dr. Kevin K. Caldwell

Dr. Erin Milligan

PROTEIN CARBONYLATION, PROTEIN AGGREGATION AND NEURONAL CELL DEATH IN A MURINE MODEL OF MULTIPLE SCLEROSIS

By

ANUSHKA DASGUPTA

BSc-Biotechnology, Barkatullah University, Bhopal, 2003
MSc-Biotechnology, Barkatullah University, Bhopal, 2005
BEd-Science, Barkatullah University, Bhopal, 2007
PhD-Biomedical Sciences, University of New Mexico, Albuquerque, 2013

DISSERTATION

Submitted in Partial Fulfilment of the
Requirements for the Degree of

Doctor of Philosophy
Biomedical Science

The University of New Mexico
Albuquerque, New Mexico

May 2013

Acknowledgements

First and foremost, I would like to convey my gratitude to my mentor, Dr. Oscar A. Bizzozero for his constant help, support and guidance in almost everything I want to do. My journey to doctoral research began in June 2009 after meeting him for 20 minutes. I wanted to work on cell death while he was interested in the role of inflammatory demyelinating diseases and we came up with this idea of combining our interests. Despite continuous failures in the first year, he kept on inspiring me by giving gazillion solutions to approach the problems. His numerous informative discussions gave new directions to my thesis, while helping me have focus at the same time. I acknowledge my lab mates, Dr. Jianzheng Zheng (Jenny), Ms. Caludia Espinoza, Ms. Amelia Hilgart and Dr. Suzanne Smerjac for their company along my journey. I am grateful to Jenny for her timely suggestions in all my pursuits.

Secondly, I would like to extend my gratitude to Dr. Nora P. Bizzozero (NPB) for showing her concern in my professional and personal life. I thank her for her unending patience and willingness to help and prioritize any of my problems even when she was occupied with something else. Professionally, I greatly benefited from her expertise in PC12 cultures, which helped me develop a model to study the hypothesis for my doctoral research. On the personal side, I am obliged to her as she gave her precious time and effort for the treatment of my father's arm-fracture during his visit to Albuquerque last year. She considers and makes me feel like I am a part of her extended family at UNM.

I would like to thank Dr. Kevin K. Caldwell for his valuable critique on my research and experimental design, and also his praises; all of them intensified my passion for research. I got acquainted with him when he evaluated my qualifying exam in May 2009. Initially, I was scared with the constant bombardment of questions from the committee members in the exam. I still remember how Dr. Caldwell asked me more questions to lead me to correct answers while

commenting that he was confident that I knew the answers. I liked his style so much that soon, I requested him to continue evaluating my progress during my doctoral studies. His critical comments on my progress in subsequent meetings have always been thoughtful and knowledgeable.

I would also like to thank Dr. Milligan for her constructive ideas and skillful technical approaches that helped me of improving the presentation of my data. I met her briefly while presenting a poster at BSGP student research day in February 2009, and was inspired by her witty remarks. Few months later, she accepted my request to be a committee member for my doctoral research. Despite her busy schedule, she would find time to meet me whenever I needed. She has always helped me enhancing my knowledge base.

I am indebted to the Department of Cell Biology and Physiology (CBP), especially Dr. Paul McGuire and his lab members, CBP staff members: Ms. Melissa Nuttall, Ms. Yolanda Chacon-Aguilar and Ms. Tamara Howard for their valuable time and accessibility. I am also indebted to the Department of Neurosciences, Dr. Donald Partridge, Dr. Mike Wilson, NPB lab and Milligan lab for allowing me to use their facilities. I appreciate the help from Dr. Robert Rubin, Dr Clark Bird, Dr. Jenny Wilkerson and Dr. Weixiang Guo. Further, I also appreciate the help from the entire unit of Biomedical Sciences including Dr. Helen Hathaway. In particular, I cannot pass this opportunity to mention Mr. Ignacio Ortiz and Ms. Mary Fenton's endeavors, which helped me endure the experiences throughout my academic life at UNM with ease.

Finally, and most importantly, it was under the watchful eye of my parents that I gained the impetus and an ability to deal with challenges. This dissertation would not have been possible without the cooperation from my friends, family (particularly my sweet brother) and several individuals who directly or indirectly contributed to the preparation of this manuscript.

PROTEIN CARBONYLATION, PROTEIN AGGREGATION AND NEURONAL CELL DEATH IN A MURINE MODEL OF MULTIPLE SCLEROSIS

By

ANUSHKA DASGUPTA

BSc-Biotechnology, Barkatullah University, Bhopal, 2003
MSc-Biotechnology, Barkatullah University, Bhopal, 2005
BEd-Science, Barkatullah University, Bhopal, 2007
PhD-Biomedical Sciences, University of New Mexico, Albuquerque, 2013

Abstract

Many studies have suggested that oxidative stress plays an important role in the pathophysiology of both multiple sclerosis (MS) and its animal model experimental autoimmune encephalomyelitis (EAE). Yet, the mechanism by which oxidative stress leads to tissue damage in these disorders is unclear. Recent work from our laboratory has revealed that protein carbonylation, a major oxidative modification caused by severe and/or chronic oxidative stress conditions, is elevated in MS and EAE. Furthermore, protein carbonylation has been shown to alter protein structure leading to misfolding/aggregation. These findings prompted me to hypothesize that **carbonylated proteins, formed as a consequence of oxidative stress and/or decreased proteasomal activity, promote protein aggregation to mediate neuronal apoptosis *in vitro* and in EAE**. To test this novel hypothesis, I first characterized protein carbonylation, protein aggregation and apoptosis along the spinal cord during the course of

myelin-oligodendrocyte glycoprotein $(MOG)_{35-55}$ peptide-induced EAE in C57BL/6 mice [Chapter 2]. The results show that carbonylated proteins accumulate throughout the course of the disease, albeit by different mechanisms: increased oxidative stress in acute EAE and decreased proteasomal activity in chronic EAE. I discovered not only that there is a temporal correlation between protein carbonylation and apoptosis but also that carbonyl levels are significantly higher in apoptotic cells. A high number of juxta-nuclear and cytoplasmic protein aggregates containing the majority of the oxidized proteins are also present during the course of EAE, which seems to be due to reduced autophagy.

In chapter 3, I show that when gluthathione levels are reduced to those in EAE spinal cord, both neuron-like PC12 (nPC12) cells and primary neuronal cultures accumulate carbonylated proteins and undergo cell death (both by necrosis and apoptosis). Immunocytochemical and biochemical studies also revealed a temporal/spatial relationship between carbonylation, protein aggregation and cellular apoptosis. Furthermore, the effectiveness of the carbonyl scavenger hydralazine, histidine hydrazide and methoxylamine at preventing cell death identifies protein carbonyls as the toxic species. Experiments using well-characterized apoptosis inhibitors place protein carbonylation downstream of the mitochondrial transition pore opening and upstream of caspase activation. These in vitro studies demonstrate for the first time a causal relationship between carbonylation, protein aggregation and apoptosis of neurons undergoing oxidative damage. This relationship was further strengthened with the

experiments carried out in chapter 4, which show that inhibition of protein aggregation with congo red (CR) or 2-hydroxypropyl β-cyclodextrin (HPCD) significantly reduced neuronal cell death without affecting the levels of oxidized proteins. Interestingly, large, juxta-nuclear aggregates are not formed upon GSH depletion, suggesting that the small protein aggregates are the cytotoxic species. Together, our data suggest that protein carbonylation causes protein aggregation to mediate neuronal apoptosis *in vitro* and that a similar mechanism might be contributing to neuronal/glial apoptosis in EAE. These studies provide the basis for testing protein carbonylation scavengers and protein aggregation inhibitors for the treatment of inflammatory demyelinating disorders.

Table of Contents

List of figures

1. INTRODUCTION

1.1 Multiple sclerosis and experimental autoimmune encephalomyelitis

Multiple sclerosis (MS) is a highly heterogeneous, inflammatory disease of the central nervous system (CNS) affecting 350,000 people in US and 2.5 million worldwide (Fox, 2010). Although not firmly established, the occurrence of MS can be traced back to medieval times; however, Dr. Jean-Martin Charcott made the first official description of MS in 1868. The mean age for the onset of MS is 30 years, but can occur at any age. Women are twice as likely as men to be affected by MS in life, and the peak age of onset is about five years earlier for women than for men (Alonso and Hernan, 2008).

There are no symptoms exclusive to MS but many clinical features describe this demyelinating disorder, such as fatigue, depression, cognitive dysfunction, body aches, sleeping disorders, impairment of speech, vision and skeletal-muscle, coordination, failure of several organs (bowel/bladder/sexual dysfunction) and paralysis in severe episodes. There are several forms of MS based on the clinical course. Relapsing-remitting MS is the most common form of the disease, where patients experience a period of active symptoms (relapsing), after which the symptoms resolve spontaneously (remitting). With the continuous tissue damage that occurs over the years, patients develop the secondary progressive form of MS, in which symptoms become chronic and gradually worsen with no distinct remissions. In some patients MS symptoms become progressively worse from the onset without any clinical relapse, which defines primary progressive MS.

Progressive-relapsing MS is the least common type of MS, and refers to a steady worsening of symptoms over time accompanied by progressive relapses (McDonnel and Hawkins, 1996).

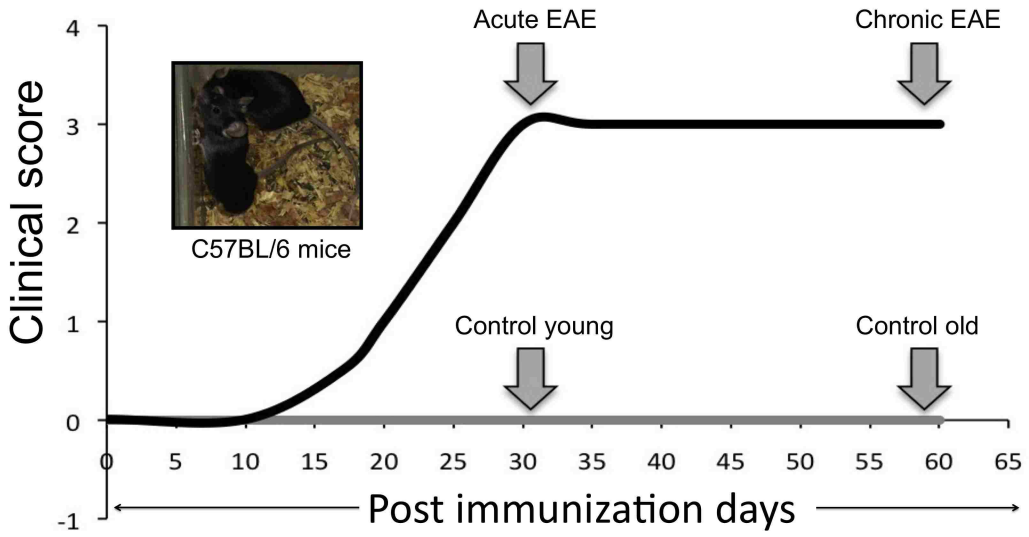

Figure 1: Female C57BL/6 mice representing EAE were monitored daily for disease signs (0-no disease, 1-4 for tail paralysis, hindlimb and forelimb paralysis respectively. Neurological symptoms reach a peak at 30 days post-immunization (DPI) and most animals remain ill throughout the entire experimental period (60 DPI). Control animals were sacrificed at 30 DPI (control young) and 60 DPI (control old).

MS is considered as a T cell-dependent immune disorder associated with inflammation and infiltration of T cells, B cells and macrophages into the CNS. T cell-mediated macrophage and microglial activation, driven by myelin-specific autoantigens (Witherick et al, 2011), leads to severe tissue injury and chronic neurodegeneration. Often these inflammatory infiltrated cells form a localized region around veins, which represent the highly heterogeneous MS-like lesions or MS plaques. Many reports demonstrate massive oligodendrocyte death

(Henderson, 2009) and neuronal destruction (Vercellino *et al.*, 2009) caused by inflammation and the ensuing oxidative stress (Keegan and Noseworthy, 2002).

Experimental autoimmune encephalomyelitis (EAE), also called experimental allergic encephalomyelitis, is frequently used as an animal model of MS because it closely shares both clinical and pathological features with the human disease. The use of EAE animals helps to explore the mechanistic basis of the disease and also to develop and test new therapeutic interventions for MS patients (Gold *et al.*, 2000; Constantinescu *et al.*, 2011). EAE in rodents is an acute or chronic-relapsing, inflammatory and demyelinating autoimmune disease. EAE can be induced by active immunization with myelin-specific antigens or by adoptive transfer of T-cells from immunized animals into naive animals. The animals used for this dissertation are female C57BL/6 mice in which EAE was induced by active immunization of myelin oligodendrocyte glycoprotein (MOG) peptide 35-55 in complete Freund's adjuvant (CFA). These animals were sacrificed at different times during the disease course to represent the acute or chronic phases of MS (Figure 1). Acute EAE was defined as having maximal neurological symptoms without any improvement for at least three consecutive days. Chronic EAE was defined arbitrarily as animals that remain in the stationary phase of the disease for 30 days (60 DPI). I used spinal cord of these animals for investigating the potential relationship between protein carbonylation and apoptosis because (1) both oxidative stress and cell death has been previously documented in this region (Smerjac and Bizzozero, 2008; Keegan and Noseworthy, 2002) and (2) this area is normally affected in MS. It is noteworthy that while there is evidence

validating cell death in EAE (Meyer *et al.*, 2001; Das *et al.*, 2008, Keegan and Noseworthy, 2002), a detailed characterization of cell death in EAE spinal cord in relation to specific biochemical and cellular alterations was lacking, which prompted me to initiate these studies.

1.2 Oxidative stress and cell death in MS and EAE

Reactive oxygen species (ROS) are the end products of normal aerobic cellular metabolism. Under normal conditions, these species are rapidly removed by the cellular antioxidant system to prevent their excessive buildup (Uttara *et al.*, 2009). However, when cellular antioxidant defenses are insufficient to keep ROS below a harmful threshold, oxidative stress (OS) develops (Schulz *et al.*, 2000). The outcomes of severe OS are molecular, cellular and tissue damage. Oxidative modification of intracellular lipids, proteins and DNA lead to cellular apoptosis and/or necrosis (Chandra, 2009). Apoptosis is characterized by cell shrinkage, membrane blebbing, nuclear condensation and DNA fragmentation while necrosis is differentiated by rapid cytoplasmic swelling, rupture of the plasma membrane and organelle breakdown (Figure 2), (Majno and Jorris, 1995). The extent and duration of the exposure to ROS determine the mechanism of cell death. It is believed that necrotic cell death occurs under more severe forms of OS than those necessary to elicit apoptotic cell death (Chandra, 2009). Excessive production of ROS damages the mitochondria depriving cells of ATP. ATP-depleted cells switch from apoptosis to necrosis since apoptosis is strictly energy driven. Apoptosis is considered advantageous because the apoptotic cells are eliminated by phagocytosis, preventing the release of intracellular

contents and the consequent damage to the surrounding tissues, as it occurs during necrosis (Troyano *et al.*, 2001).

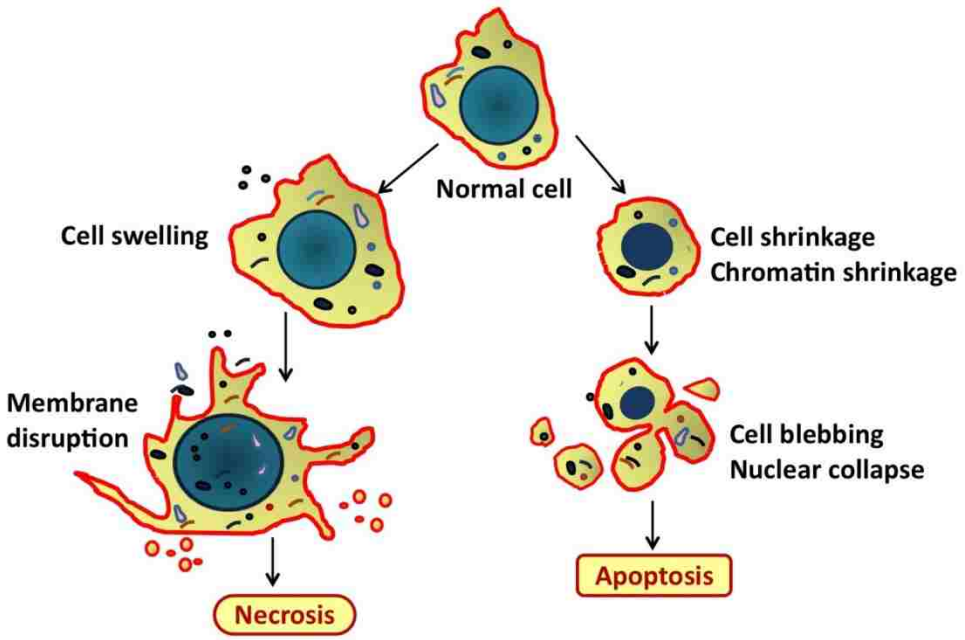

Figure 2: Cell death pathways – Necrosis takes place due to sudden injury leading to membrane disruption,, metabolic collapse, cell swelling and rupture resulting in inflammation. Apoptosis or programed cell death (PCD) involves membrane blebbing, cell shrinkage, chromatin condensation, nuclear fragmentation and collapse leading to the formation of apoptotic bodies that are phagocytosed.

The CNS is more vulnerable to OS than other tissues. It has been shown that CNS is predisposed to OS due, among other things, to its exceptionally active oxidative metabolism that generates relatively high levels of intracellular superoxide (Bast *et al.*, 1991). Also, low levels of antioxidant defenses, the presence of highly unsaturated lipids, and elevated iron content in CNS cells adds to the cellular vulnerability to oxidative damage. In recent years experimental evidence has accumulated suggesting that OS is a major player in the pathogenesis of inflammatory demyelination. As reviewed by Bizzozero

(2009), a number of findings support the critical role of ROS in MS. These include (1) the presence of the lipid peroxidation products in the CSF and plasma of MS patients, (2) reduced plasma levels of antioxidants and antioxidant enzymes in MS, (3) low levels of antioxidants like glutathione (GSH), α-tocopherol and uric acid in MS plaques, (4) the damage to mitochondrial DNA in active chronic plaques and (5) the effectiveness of various antioxidant treatments at ameliorating EAE. The above studies clearly suggest that oxidative damage has a causal role in the development of tissue injury in demyelinating disorders.

While MS and EAE were initially considered to be exclusively demyelinating disorders, studies in the last decade have provided clear evidence that axonal damage and neuronal cell death occur in these diseases (Meyer *et al.*, 2001; Aktas *et al.*, 2007. Further, neuronal damage in MS correlates with clinical disability (Meyer *et al.*, 2001; Aktas *et al.*, 2007) better than with demyelination. Neuronal cell death can be triggered in many stressors. One of them is GSH depletion, which is a characteristic feature of MS and EAE (Smerjac and Bizzozero, 2008; Zheng and Bizzozero, 2010a,b; Dasgupta and Bizzozero, 2011, Meyer *et al.*, 2001). In this dissertation, I used specific GSH-depleted neuronal cultures as a model of cell death to study the mechanistic aspects of apoptosis and necrosis that may be happening in EAE.

1.3 Protein carbonylation and cell death

Proteins are abundant cellular components that are highly susceptible to oxidation. Although the protein backbone and the side chains of most amino

acids may undergo oxidation, the direct metal-catalyzed introduction of aldehyde or ketone functional groups into proline, arginine, lysine and threonine (i.e. carbonylation) constitutes the major and most common oxidative alteration in aging (Berlett and Stadtman, 1997), EAE (Zheng and Bizzozero, 2010a) and MS (Bizzoero et al., 2005). Another alteration that generates carbonyl groups is through a non-oxidative pathway where the nucleophilic centers in cysteine, histidine or lysine react with reactive carbonyl species (RCS) derived from oxidized lipids such as 4-hydroxynonenal (4-HNE), malondialdehyde (MDA) and acrolein (ACR), or oxidized carbohydrates such as glyoxal and methylglyoxal (Figure 3). In some instances, rapid decomposition of hydroperoxides of valine and leucine can also result in protein carbonyl formation (Bizzozero, 2009). Because carbonyls are relatively difficult to induce compared to other oxidative modifications of proteins (e.g. oxidation of thiols), they are normally detected under more severe (e.g. neuroinflammation) and prolonged (e.g. neurodegeneration) OS conditions (Shacter, 2000). Our laboratory has recently found increased levels of protein carbonyls in both white matter and gray matter tissue of MS patients (Bizzozero *et al.*, 2005) and in the spinal cord and cerebellum of EAE rats and mice (Smerjac and Bizzozero, 2008; Zheng and Bizzozero, 2011; Dasgupta and Bizzozero, 2011), indicating that protein carbonylation is a factor present in inflammatory demyelinating disorders.

Protein carbonyls are believed to be toxic and might lead to cell death (Burcham and Fontaine, 2001). In this dissertation I studied whether or not inhibiting protein carbonylation has any consequence on the apoptosis of GSH-depleted neurons.

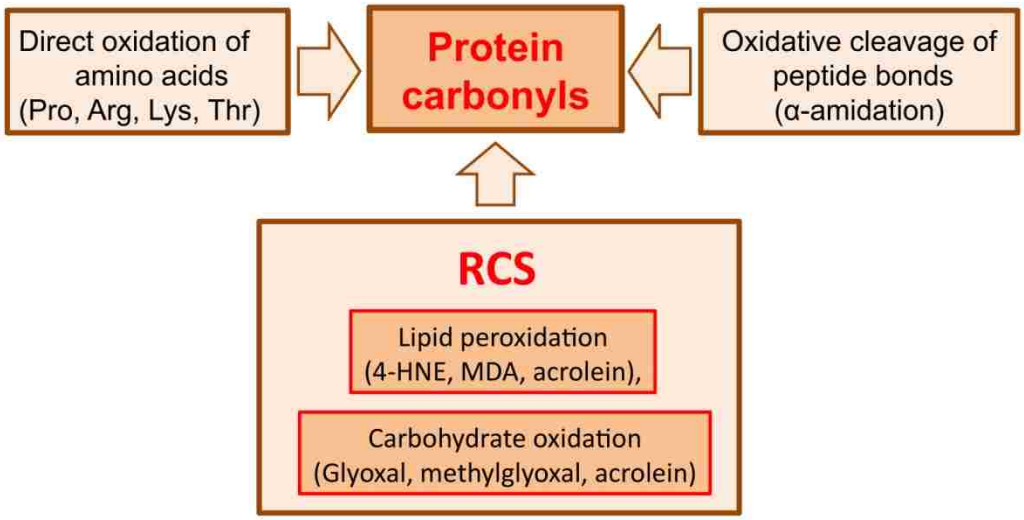

Figure 3: Mechanisms of formation of protein carbonyls (Modified from Bizzozero, O. A., Protein carbonylation inneurodegenerative and demyelinating CNS disease. Hanbook of neurochemistry and molecular neurobiology, 2009.

1.4 Protein carbonylation, protein aggregation and cell death

Protein aggregates are supra-molecular assemblies of misfolded, oxidized and damaged proteins that accumulate within cells. The presence of protein aggregates is typically considered undesirable because they are largely associated with cellular toxicity (Johansson *et al.,* 2012) and neuronal apoptosis (Estus *et al.*, 1997; Zhu *et al.,* 2000). Recently, protein aggregation has been implicated in the pathophysiology of many neurodegenerative diseases such as Alzheimer's disease (AD), Parkinson's disease (PD), Huntington's disease (HD) and amyotrophic lateral sclerosis (ALS) (Trzesniewska *et al.*, 2004; Hachiya *et al.,* 2008) and therefore became a subject of considerable investigation.

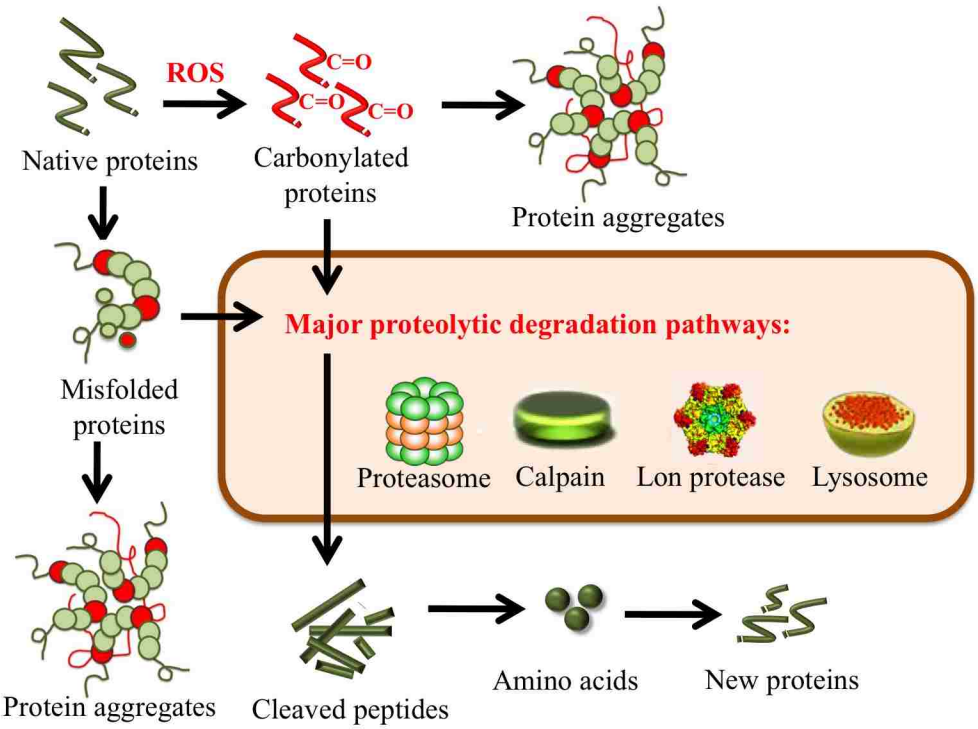

Figure 4: Protein damage and degradation. Modified and adapted from Faraout and Friguet (2006).Oxidized and misfolded proteins are digested by proteolytic degradation pathway. Protein aggregates are formed when damaged proteins escape the degradation system.

It is noteworthy that while protein aggregates are toxic to many cell types, a cytoprotective role in cancer cells has also been observed (Johansson *et al.,* 2012). The accumulation of protein aggregates is triggered by many factors. For example, in AD the production of beta amyloid proteins triggers protein aggregation in neurons leading to cytotoxic responses (Nilsberth *et al*., 2001; Etienne *et al.,* 2007). Other factors may include the overproduction of partially misfolded, carbonylated and damaged proteins, which after reaching high levels, cross-link and interact with each other to become a part of protein aggregates. Oxidized proteins have been demonstrated to induce changes in the tertiary

structure of proteins followed by exposure of hydrophobic domains that tend to aggregate if they are not degraded rapidly (Grune and Davies, 1997).

The proteolytic machinery in cells continuously degrades damaged and aggregated proteins to keep them at basal non-toxic levels and maintain homeostasis. Despite proteasomes target the majority of damaged proteins by recognizing increased hydrophobicity, some oxidized and aggregated proteins are degraded by other systems. The proteolytc systems include proteasomes (in cytosol and nucleus), cathepsins and other acid proteases in lysosomes or autophagosomes (in cytosol), lon-proteases (in mitochondria) and calpain (in cytosol). All of these proteases convert damaged proteins into small peptides (Grune et al., 2001) that are further cleaved to amino acids by amino- and carboxy-peptidases (Figure 4).

Proteasomes are large barrel shaped protein complexes that degrade carbonylated proteins independent of ubiquitin and ATP (Divald and Powell, 2006). Moderately oxidized proteins are selectively recognized and degraded by proteasomes while the susceptibility of heavily oxidized and cross-linked proteins to proteasomal hydrolysis is much lower (Grune *and* Davies, 1997). Calpain also preferentially degrades carbonylated proteins over the non-carbonylated counterparts (Troncoso *et al.*, 1995) and induces alterations in cell signaling. For example calpain cleaved carbonylated apoptosis inducing factor translocates from mitochondria to nucleus to trigger caspase dependent apoptotic pathway (Norberg et al., 2010).

Heavily oxidized proteins are targeted for lysosomal degradation or autophagy while protein aggregates rely only on autophagy for their clearance. Most protein aggregates are degraded by chaperone-mediated autophagy while aggregates containing ubiquitinated proteins are removed by selective autophagy. Clearance of protein aggregates by authophagy is called aggrephagy (Lamark and Johansen, 2012). Proteasome failure or loss of aggrephagy (impairment in autophagy) or both may result in the accumulation of degradation resistant protein complexes. Currently, the formation of large protein aggregates is considered cytoprotective (Arrastate *et al.*, 2004; Kopioto, 2000) or less cytotoxic than the small microaggregates dispersed within the cell (Arrastate *et al.*, 2004; Lamark and Johansen, 2012).

Protein carbonyls are known to trigger protein aggregation both in vitro and in yeast cells, thereby compromising cellular viability (Mirzaei and Regneir, 2008). Indeed, carbonylated proteins are highly enriched in protein aggregates in prokaryotes (Maissonneuve *et al.*, 2008) and in juxta-nuclear protein aggregates called aggresomes in yeast cells (Mirzaei and Regneir, 2008). Yet, despite this evidence, little is known about the relationship between protein carbonylation and aggregate formation in mammalian cells undergoing OS. Furthermore, since oxidized and cross-linked protein aggregates may inhibit the proteasome and progressively increase protein aggregation (Grune *et al.*, 2005), it is likely that carbonylation and protein aggregation might be mutually responsible for aggregation-associated proteotoxicity. In this dissertation, I used classical protein aggregate inhibitors to determine the cause-consequence relationship between

protein carbonylation and protein aggregation and their role in neuronal cell death triggered by GSH depletion.

1.5 Hypothesis and goals of the study

Based on reports from the scientific literature and previous studies in our laboratory, I hypothesize that **carbonylated proteins, formed as a consequence of oxidative stress and/or decrease proteasomal activity, promote protein aggregation to mediate neuronal apoptosis in vitro and in the spinal cord of EAE mice** (Figure 5). The major goals of the study were

1) To characterize cell death in EAE and determine if protein carbonylation and protein aggregation are related to neuronal apoptosis.
2) To determine if protein carbonylation, protein aggregation and cell death are also associated in GSH-depleted cultured neurons.
3) To investigate the causal role of protein carbonylation and protein aggregation in cell death.

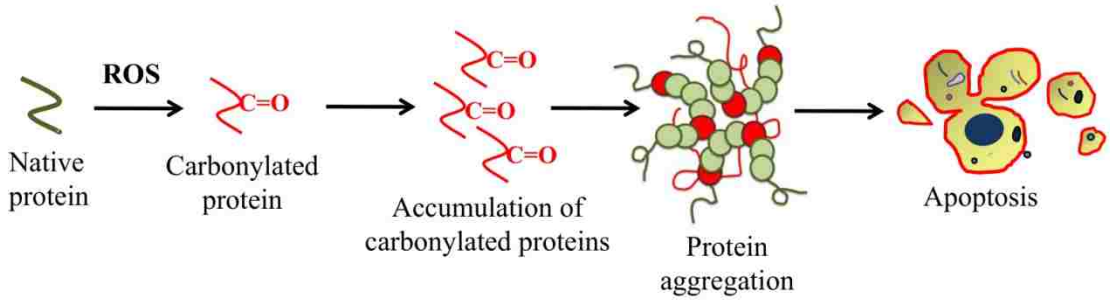

Figure 5: Hypothesis: Accumulation of protein carbonyls promote protein aggregation to mediate neuronal apoptosis.

1.6 Significance

In this dissertation, I will show that protein carbonylation and protein aggregation are linked to cell death in EAE. Further, protein carbonylation and aggregation precedes neuronal apoptosis in GSH-depleted cultured neurons. In the same system, Carbonyl scavengers and protein aggregation inhibitors prevent neuronal cell death. These novel data will serve as the basis for developing novel therapeutic strategy by either scavenging protein carbonyls and protein aggregates or both, or by stimulating the removal of oxidized proteins and protein aggregates. Future studies would test the effect of protein aggregate inhibitors in EAE to determine the role of protein aggregation in neuronal death during the disease progression. Furthermore, since OS, protein aggregation and neuronal cell death has been observed in PD, AD and ALS (Ross and Poirier, 2004), eliminating protein carbonyls and/or protein aggregates could be helpful in providing neuroprotection in these diseases as well.

2. Increased carbonylation, protein aggregation and apoptosis in the spinal cord of mice with experimental autoimmune encephalomyelitis

Anushka Dasgupta[1], Jianzheng Zheng[1], Nora I. Perrone-Bizzozero[2] and Oscar A. Bizzozero[1]*

[1]Deptartment of Cell Biology and Physiology and [2]Department of Neurosciences, University of New Mexico - Health Sciences Center, Albuquerque, New Mexico.

Abbreviations used: APC, adenomatous polyposis coli protein; DPI, days post-immunization; DNP, 2,4-dinitrophenyl; DNPH, 2,4-dinitrophenylhydrazine; EAE, experimental autoimmune encephalomyelitis; GFAP, glial fibrillary associated protein; GSH, reduced glutathione; GSSG, glutathione disulfide; LC3, Microtubule-associated protein light chain 3; MOG, myelin-oligodendrocyte glycoprotein; NeuN, neuronal nuclear antigen; PBS, phosphate-buffered saline; TBARS, thiobarbituric acid reactive substances; TUNEL, terminal deoxynucleotidyl transferase dUTP nick end labeling.

[Submitted to ASN Neuro 2013]

2.1 ABSTRACT

Previous work from our laboratory implicated protein carbonylation in the pathophysiology of both multiple sclerosis (MS) and its animal model experimental autoimmune encephalomyelitis (EAE). Subsequent *in vitro* studies revealed that the accumulation of protein carbonyls, triggered by glutathione deficiency or proteasome inhibition, leads to protein aggregation and neuronal cell death. These findings prompted us to investigate if their association can be also established *in vivo*. In this study, we characterized protein carbonylation, protein aggregation and apoptosis along the spinal cord during the course of myelin-oligodendrocyte glycoprotein $(MOG)_{35-55}$ peptide-induced EAE in C57BL/6 mice. The results show that protein carbonyls accumulate throughout the course of the disease, albeit by different mechanisms: increased oxidative stress in acute EAE and decreased proteasomal activity in chronic EAE. We also show a temporal correlation between protein carbonylation (but not oxidative stress) and apoptosis. Furthermore, carbonyl levels are significantly higher in apoptotic cells than in live cells. A high number of juxta-nuclear and cytoplasmic protein aggregates containing the majority of the oxidized proteins are present during the course of EAE. The LC3-II/LC3-I ratio is significantly reduced in both acute and chronic EAE indicating reduced autophagy and explaining why aggresomes accumulate in this disorder. Altogether, our data suggest a link between protein oxidation and neuronal/glial cell death *in vivo* and also demonstrate impaired proteostasis in this widely used murine model of MS.

Running Title: Carbonylation, protein aggregation and cell death in EAE

Key Words: Apoptosis, autophagy, experimental autoimmune encephalomyelitis, oxidative stress, protein carbonylation, protein aggregation, proteostasis.

2.2 INTRODUCTION

Experimental autoimmune encephalomyelitis (EAE) is an animal model of multiple sclerosis (MS) that is routinely employed to study the mechanistic basis of disease and to test therapeutic approaches (Gold et al., 2000). Both disorders are characterized by CNS inflammation, demyelination, axonal degeneration, and various degrees of oligodendrocyte and neuronal cell death (Luccinetti et al., 1996; Kornek and Lassmann, 1999, Kuerten et al., 2007). In recent years, several laboratories have obtained experimental evidence indicating that oxidative stress is a major player in the pathogenesis of inflammatory demyelination (Gilgun-Sherki et al., 2004; Bizzozero, 2009; Haider et al., 2011). Severe and/or prolonged oxidative stress conditions does lead to the non-enzymatic modification of specific amino acid residues resulting in the introduction of aldehyde or ketone functional groups (a.k.a. carbonylation) (Stadtman and Berlett, 1997). Thus, it is not surprising that large amounts of carbonylated proteins accumulate within CNS cells in many neurodegenerative disorders (Ferrante et al., 1997; Floor and Wetzel, 1998; Aksenov et al., 2001; Perluigi et al., 2005) as well as in neuroinflammatory disorders like MS

(Bizzozero et al., 2005) and EAE (Smerjac and Bizzozero, 2008; Zheng and Bizzozero, 2010a). However, the build-up of oxidized and other misfolded proteins is due not only to an increase in the rate of protein oxidation but also to their reduced proteolytic removal via the proteasome (Shringarpure et al., 2001; Divald and Powell, 2006). In fact, impaired proteasomal activity has been demonstrated in disorders where carbonylated proteins accumulate, including Alzheimer's disease (Keller et al., 2000), Parkinson's disease (McNaught et al., 2003), Huntington's disease (Seo et al., 2004) and more recently in MS (Zheng and Bizzozero, 2011) and EAE (Zheng and Bizzozero, 2010b; Zheng et al., 2012).

There is a substantial amount of data showing that the presence of carbonyl groups causes major changes in protein structure and function (Fucci et al., 1983; Starke et al., 1987; Dalle-Donne et al., 2001), which results in the loss of cell viability (England et al., 2004; Magi et al., 2004). In addition, carbonylation brings about the formation of protease-resistant protein aggregates, which are considered highly toxic and can mediate cell death (Nyström, 2005; Maisonneuve et al., 2008b). Indeed, we have recently shown that protein carbonylation, aggregation and cell death are linked during neuronal apoptosis triggered by glutathione deficiency (Dasgupta et al., 2012). These findings and the fact that both protein oxidation (Smerjac and Bizzozero, 2008; Zheng and Bizzozero, 2010a) and neuronal/oligodendrocyte apoptosis has been observed in EAE (Meyer et al., 2001; Das et al., 2008), prompted us to investigate if their association can be also established *in vivo*. In this study, and as a first step to

demonstrate such relationship, we measured the extent of protein carbonylation, protein aggregation and apoptosis along the spinal cord of mice with acute and chronic EAE. The results show for the first time (1) a temporal correlation between protein carbonylation (but not oxidative stress) and apoptosis, (2) an increased accumulation of carbonyl in apoptotic cells, (3) the presence in EAE of protein aggregates containing the majority of the oxidized proteins, and (4) a reduced autophagy in both acute and chronic EAE, which suggests impaired proteostasis in this murine model of MS. A preliminary account of these findings has been presented in abstract form (Dasgupta and Bizzozero, 2011).

2.2 MATERIAL AND METHODS

Induction of Experimental Autoimmune Encephalomyelitis (EAE)

Housing and handling of the animals as well as the euthanasia procedure were in strict accordance with the NIH Guide for the Care and Use of Laboratory Animals, and were approved by the Institutional Animal Care and Use Committee. Eight-week-old female C57BL/6 mice were purchased from Harlan Bioproducts (Indianapolis, IN) and housed at the UNM-animal resource facility. EAE was induced by active immunization with MOG_{35-55} peptide (AnaSpec, San Jose, CA) as described in our previous study (Zheng and Bizzozero, 2010a). Animals were weighed and examined daily for the presence of neurological signs. Acute disease was defined as having maximal neurological symptoms of EAE without any improvement for at least three consecutive days while chronic EAE was operationally defined as animals that remain in the stationary phase of

the disease for 30 days. Age-matched control animals for acute EAE (control young) and chronic EAE (control old) consisted of mice injected with complete Freund's adjuvant alone (i.e. without the MOG peptide). EAE and control mice were euthanized by decapitation, and the spinal cord was rapidly removed and divided into cervical, thoracic and lumbar regions. Sections were either fixed with methacarn (methanol : chloroform : acetic acid, 60 : 30 : 10 by vol) or homogenized in PEN buffer (20 mM sodium phosphate, pH 7.5, 1 mM EDTA, and 0.1 mM neocuproine) containing 2 mM 4,5 dihydroxy-1,3 benzene disulfonic acid and 1 mM dithiothreitol. Protein homogenates were stored at -80°C until use. Protein concentration was assessed with the Bio-Rad DCT™ protein assay (Bio-Rad Laboratories; Hercules, CA) using bovine serum albumin as a standard. For GSH determination, homogenates were prepared in PEN buffer without reducing agents and were processed immediately as described below.

Determination of GSH and lipid-peroxidation products

GSH levels were determined using the enzymatic recycling method (Shaik and Mehvar, 2006). Briefly, proteins from spinal cord homogenates were precipitated with 1% sulfosalicylic acid and removed by centrifugation at 10,000g for 15min. Aliquots of the supernatant were then incubated with 0.4U/ml glutathione reductase, 0.2mM NADPH, and 0.2mM 5,5'-dithiobis-(2-nitrobenzoic acid) in 1ml of 0.2M sodium phosphate buffer pH 7.5 containing 5mM EDTA. The rate of appearance of the thionitrobenzoate anion was measured spectrophotometrically at 412 nm. [GSH] was calculated by interpolation on a curve made with increasing concentrations of GSSG (0.1-10nmol).

Lipid peroxidation was estimated as the amount of thiobarbituric acid reactive substances (TBARS) (Okawa et al., 1979). Briefly, aliquots from the spinal cord homogenates were suspended in 10% (w/v) trichloroacetic acid containing 1% (w/v) thiobarbituric and 0.05% (w/v) butylated hydroxytoluene. Samples were incubated for 20 min at 90°C. Aggregated material was removed by centrifugation at 10,000g for 15 min and the absorbance of the supernatant was measured at 532 nm. The amount of TBARS was calculated using a standard curve prepared with 1,1,3,3-tetraethoxypropane.

Proteasome and calpain activity

The chymotrypsin-like activity of the 20S proteasome in the spinal cord homogenates was determined using a fluorescence assay (Rodgers and Dean, 2003). Briefly, 50µg protein was incubated for up to 2h at 25ºC with 50 µM of the 7-aminomethyl-4-coumarin (AMC)-labeled peptide Suc-Leu-Leu-Val-Tyr-AMC in the absence or presence of 10µM β-clasto-lactacystin-lactone (Enzo Life Sciences, Plymouth Meeting, PA). The proteasome activity was calculated as the difference in fluorescence intensity at 460 nm between the samples without and with inhibitor using excitation wavelength of 380nm. Calpain activity was also determined with a fluorescence assay using the substrate Suc-Leu-Leu-Val-Tyr-AMC in 100mM KCl, 10mM $CaCl_2$, 25mM Hepes buffer pH 7.5, and carrying out the incubation in the absence or presence of 40µg/ml calpeptin (Hassen et al., 2006).

Oxyblot analysis

Protein carbonyl groups were measured by oxyblot analysis as described earlier (Smerjac and Bizzozero, 2008). In brief, proteins (5µg) were incubated with 2,4-dinitrophenylhydrazine (DNPH) to form the 2,4-dinitrophenyl (DNP) hydrazone derivatives. Proteins were separated by electrophoresis and blotted to polyvinylidene difluoride membranes. DNP-containing proteins were detected using rabbit anti-DNP antiserum (1:500) and horseradish peroxidase-conjugated goat anti-rabbit IgG antibody (1:2,000). Blots were developed by enhanced chemiluminescence using the Western Lightning ECL™ kit from Perkin-Elmer (Boston, MA). Films were scanned in a Hewlett Packard Scanjet 4890 and the images were quantified using the NIH Image 1.63 imaging analysis program. The intensity of each lane on the film was normalized by the amount of coomassie blue staining in the corresponding lane.

Immunohistochemistry

Tissue specimens were fixed overnight in methacarn and then embedded in paraffin. Tissue was cross-sectioned (3-µm thick) and mounted on Vectabond™-treated slides (Vector Laboratories, Burlingame, CA). Sections were deparafinized with xylenes and a graded alcohol series, and then rinsed with phosphate-buffered saline (PBS) solution for 10 min. Apoptosis was detected using Click-iT® TUNEL Assay kit (Invitrogen). For carbonyl staining, sections were incubated for 15 min with 1 mg/ml DNPH prepared in 1N HCl to convert carbonyl groups into DNP-hydrazones. Sections were rinsed three times with

PBS, blocked with 10% (v/v) normal goat serum and incubated overnight with rabbit anti-DNP antibody (1:1000) (Sigma, St Louis, MO). After removing the primary antibody with 0.1% Triton X-100 in PBS, sections were incubated for 3h with Alexa Fluor® 647 goat anti-rabbit antibody (1:200, Molecular Probes, Eugene, OR). Sections were rinsed twice with PBS, and then mounted using DPX. Images were captured with a Zeiss 200m microscope (Carl Zeiss MicroImaging Inc., Thornwood, NY) equipped with a Hamamatsu C4742-95 digital camera (Hamamatsu Corp., Bridgewater, NJ).

For double immunofluorescence, DNPH-treated sections were incubated with the corresponding primary antibody, washed with PBS and followed by incubation with fluorescent secondary antibodies (Alexa Fluor® 647, 1:200, Molecular Probes). After washing, the sections were stained using Click-iT® TUNEL Assay kit (Invitrogen Corp., Carlsbad, CA), rinsed with PBS and mounted using DPX. The various cell types were detected by using antibodies against GFAP (1:250, mouse monoclonal; Sigma), adenomatous polyposis coli protein C-terminal (1:100, mouse monoclonal, Chemicon, Temecula, CA) and NeuN (1:200, mouse monoclonal, Chemicon) with corresponding secondary antibody conjugated to Alexa Fluor® 488.

For protein aggregation staining, methacarn fixed and paraffin embedded tissue sections were deparafinized and hydrated followed by washing with PBS. Samples were then incubated for 30 minutes with ProteoStat® Protein Aggregation Assay solution (Enzo Life Sciences) and destained using distilled water for 5 hours. Cellular nuclei were stained with DAPI (40ng/ml, Sigma).

Stained sections were mounted using 1,4-diazabicyclo[2.2.2]octane in polyvinyl alcohol (Sigma) as antifading agent.

Determination of autophagy index

Proteins (7.5 µg) were separated by sodium dodecyl sulfate–polyacrylamide gel electrophoresis on 15% gels and blotted to polyvinylidene difluoride membranes. LC3-I (18 kDa) and LC3-II (16 kDa) were detected using rabbit anti-LC3 antiserum (1:1000, Sigma) and horseradish peroxidase-conjugated goat anti-rabbit IgG antibody (1:2,000). Blots were developed by enhanced chemiluminescence as described above. The LC3-II/LC3-I ratio was determined by scanning densitometry of the films.

Protein aggregation assay

Assessment of protein aggregation was carried out as described by Maisonneuve et al., (2008a) with minor modifications. Spinal cord homogenates prepared in PEN buffer containing 1mM dithiothreitol and 150mM NaCl were centrifuged at 20,000x*g* for 30 min at 4°C. The pellets were then extracted with the same buffer containing 1% Triton X-100. Samples were kept on ice for 15 min and then centrifuged at 20,000x*g* for 30 min at 4°C. The final pellet, which contains some cytoskeleton structures but mostly aggregated proteins, was processed for oxyblot analysis as described above.

Statistical analysis

Results were analyzed for statistical significance with student *t*-test using GraphPad Prism® program (GraphPad Software incorporation, San Diego, CA).

2.3 RESULTS

Characteristic of mice with acute and chronic EAE

EAE in female C57BL/6 mice was induced by active immunization with MOG_{35-55} peptide as described under Materials and Methods. Symptoms were graded according to the following scale: 0, no symptoms; 1, tail weakness; 1.5, clumsy gait; 2, hind-limb paresis; 2.5, partial hind-limb dragging; 3, hind-limb paralysis; 3.5, hind-limb paralysis with fore-limb paresis; 4, complete paralysis; and 5, moribund. In this EAE model, neurological symptoms begin at 14 days post-immunization (DPI) (i.e. 7 days after the boost with MOG peptide) reaching a peak at 30 DPI, and most animals remain ill throughout the entire experimental period (60 DPI). Acute disease was defined as having maximal neurological symptoms of EAE without any improvement for at least three consecutive days. At this stage the spinal cord pathology is characterized by infiltration of inflammatory cells, mostly within the white matter and meninges. Chronic EAE was defined arbitrarily as animals that remain in the stationary phase of the disease for 30 days (60 DPI). At this stage there is very low perivascular and parenchymal inflammation, and almost no transmigration of inflammatory cells into the spinal cord. CFA-injected animals, which were sacrificed at 30 DPI (control young) and 60 DPI (control old), did not exhibit any neurological sign or

spinal cord pathology. For the present study we analyzed a total of 29 animals: 6 control-young, 11 acute EAE (clinical scores ranging from 1.0-3.5), 6 control-old and 6 chronic EAE (clinical scores ranging from 0.5-3.5) (Fig. 1a).

Increased neuronal and glial apoptosis in the spinal cord of mice with acute and chronic EAE

Using TUNEL staining we first measured the number of cells undergoing apoptosis in different spinal cord regions (cervical, thoracic and lumbar) during the course of EAE. As depicted in Fig. 1, the total number of apoptotic cells in the spinal cord of mice with acute EAE (panel b) was slightly higher than that with chronic EAE (panel c). In both cases, the lumbar section showed the highest number of apoptotic cells followed by the thoracic and cervical sections. These findings are in agreement with the notion that the extent of spinal cord lesions increases caudally (Müller et al., 2000). Similar results were obtained using active caspase-3 as a marker of apoptosis (data not shown).

Double staining of the lumbar spinal cord sections of acute EAE mice for TUNEL and cell-specific markers identified apoptotic cells as oligodendrocytes (48%), neurons (27%) and astrocytes (15%) (Fig. 2a,b). The identity of the remaining apoptotic cells (probably microglia and lymphocytes) was not determined. A similar distribution was found in chronic EAE animals, where 45%, 20% and 13% of the apoptotic cells were identified as oligodendrocytes, neurons and astrocytes, respectively. Stereological analysis of the same spinal cord region revealed that there is 27% neuronal loss, 15% oligodendrocyte loss and 36%

increase in the number of astrocytes (astrocytosis) in acute EAE (Fig. 2c). In chronic EAE, neuronal and oligodendrocyte deficits are 29% and 21%, respectively, while astrocyte number is almost unchanged (Fig. 2d).

Protein carbonylation, and not oxidative stress, correlates with apoptosis

As shown in Fig. 3a, GSH levels are reduced in all regions of the spinal cord of mice with acute EAE, with the largest decline (~46%) found in the lumbar section. In contrast, normal GSH concentrations are present in all the spinal cord areas of animals with chronic EAE (Fig. 3b). This data is consistent with a weakened cellular antioxidant defense system in acute EAE where inflammation is elevated. In agreement with the GSH data, levels of TBARS, a marker of lipid peroxidation, are elevated in all spinal cord segments of acute EAE (Fig. 3c) but not chronic EAE mice (Fig. 3d). Certainly, there is an almost perfect inverse relationship between GSH and TBARS levels throughout the length of the spinal cord. In contrast to lipid peroxidation, the amount of protein carbonyls is augmented in both acute EAE (Fig. 4a) and chronic EAE spinal cord (Fig. 4b) with the highest increase found in the lumbar area. Since protein carbonyls are not eliminated by enzymatic reduction to the corresponding alcohols (Bizzozero, 2009), the accumulation of protein carbonyls in chronic EAE in the absence of significant oxidative stress is most likely due to impaired proteolytic removal via the chymotrypsin-like activity of 20S proteasome (Ferrington et al., 2005). Indeed, this proteosomal activity, measured with a fluorogenic peptide substrate, was found normal in acute EAE but greatly decreased in all spinal cord regions of chronic EAE mice (Fig. 4c,d).

Apoptotic cells contain higher levels of protein carbonyls

Since protein carbonylation and cell death shows a similar temporal pattern, we sought to investigate if there is a spatial relationship between these two parameters as well. To this end, spinal cord sections were double stained with DNPH for carbonyls and TUNEL for apoptosis. Co-localization studies of carbonyls and annexin-V, a late marker in the apoptotic pathway, were not possible since sections for carbonyl detection had to be fixed in methacarn, which dissolves membrane phospholipids. Fig. 5 shows that apoptotic (TUNEL positive) cells are stained intensely with DNPH. Since this reagent also stains cell nuclei, likely due to its reactivity towards DNA oligonucleotides (Luo and Wehr, 2009), only the fluorescence present in the cytoplasm was quantified. As depicted in panel c, the fluorescence intensity in the cytoplasm of apoptotic cells from the lumbar spinal cord region of mice with acute EAE is ~ 2 times higher than that of non-apoptotic cells.

Carbonyls accumulate in all the major cell types of EAE spinal cord

Carbonyl levels in the various CNS cell types were determined by double-label immunofluorescence using antibodies against NeuN, APC and GFAP to identify neurons, oligodendrocytes and astrocytes, respectively. Carbonyl intensity in the control lumbar spinal cord region is the highest in astrocytes (150.7 ± 8.3) followed by oligodendrocytes (94.9 ± 6.7) and neurons (21.0 ± 1.3) (Fig 6). In acute EAE, carbonyl intensity in astrocytes, oligodendrocytes and neurons increase 2.8-, 2.1- and 4.3-fold, respectively. This suggests the occurrence of

different oxidative environments and/or proteasome activities in the various cell types.

The number of large protein aggregates is also increased in EAE.

Experiments were also conducted to determine the possible association between protein aggregation and cell death. Unfortunately, simultaneous staining for TUNEL and protein aggregation (ProteoStat®) was not possible due to the overlapping emission spectrum of the dyes in the corresponding kits. Nonetheless, we found a large increase in the number of protein aggregates, both juxta-nuclear (aggresomes) and cytoplasmic, in the lumbar spinal cord of mice with acute and chronic EAE as compared to controls (Fig. 7a,b). Furthermore, in acute EAE, linear regression curves predict a positive relationship between all three: protein carbonylation (r^2 = 0.97), protein aggregation (r^2=0.83) and cell death (r^2=0.88) and the clinical score (Fig. 7c). The presence of aggresomes in EAE also suggested an impairment of autophagy, the major degradation system responsible for the turnover of bulky cellular components. Indeed, we found that the LC3-II/LC3-I ratio (a.k.a. autophagy index) was significantly reduced in both acute and chronic EAE (Fig. 8).

Most carbonylated proteins are present in insoluble protein aggregates.

To determine if carbonylated proteins are part of protein aggregates, we fractionated the spinal cord homogenates by differential centrifugation as described by Maisonneuve et al., (2008a). This method is based on the large sedimentation coefficient of protein aggregates relative to other cellular protein

complexes and on their insolubility in high ionic-strength buffers containing the non-denaturing detergent triton X-100. As shown in Fig. 9, carbonylated proteins are highly enriched in the detergent insoluble protein fraction both in control and EAE samples suggesting that, like in other aerobic systems (Maisonneuve et al., 2008b), oxidized proteins are the major substrates for aggregation.

2.4 DISCUSSION

The present study reveals a positive correlation between protein carbonylation (but not oxidative stress) and neuronal and glial apoptosis in the spinal cord of EAE mice. As we found in glutathione-depleted or proteasome-inhibited cultured neurons (Dasgupta et al., 2012), apoptotic cells have increased carbonyl accumulation suggesting a cytotoxic role for this modification. We also describe for the first time the presence of protein aggregates in EAE, which contain the majority of the oxidized proteins. Furthermore, the build-up of these inclusion bodies may result not only from augmented carbonylation but also from reduced clearance by autophagy. The proteasome deficiency in chronic EAE and the decrease of autophagy in both acute and chronic EAE clearly points to an impaired proteostasis in this murine model of inflammatory demyelination. A schematic model summarizing our experimental findings is shown in Fig. 10.

Consistent with previous studies (Pender et al., 1991; Akassoglou et al., 1998; Anderson et al., 2008; Vogt et al., 2009; Toft-Hansen et al., 2011) we found significant neuronal and oligodendrocyte loss in acute EAE along with astrocytosis. The latter involves astrocyte activation, hypertrophy and

proliferation, which are considered to be a characteristic response to inflammation or autoimmune injury of the CNS (Toft-Hansen et al., 2011). Interestingly, the extent of neuronal and oligodendrocyte loss in chronic EAE is similar to that in acute EAE despite apoptosis continues throughout the disease process. While oligodendrocytes have some regenerating capacity that could explain these findings (Arenella et al., 1984; Tripathi et al., 2010), the mitotic rate of neurons is almost nil (Tripathi et al., 2010). Thus, we can conclude that (1) the majority of neurons, and possibly oligodendrocytes, die during the acute (inflammatory) phase and (2) only a small, yet significant, fraction of cell death occurs by apoptosis. The notion that most cell death occurs early in the disease is supported by the finding that calpain activity, a marker of both necrosis and apoptosis (Guyton et al., 2005), is elevated in acute EAE but not in chronic EAE (Fig. S1).

Like in most neurodegenerative disorders, oxidative stress is also a significant player in the pathogenesis of inflammatory demyelination (Smith et al., 1999; Gilgun-Sherki et al., 2004). At the peak of the disease, and concomitant with the rise in inflammation, there is increased oxidative stress with the ensuing depletion of cellular GSH and accumulation lipid peroxides and protein carbonyls. There are several, and not mutually exclusive, reasons underlying the reduction of GSH in acute EAE. These include (1) oxidation of GSH to glutathione disulfide (GSSG); (2) conjugation of GSH with reactive α,β-unsaturated aldehydes derived from lipid peroxidation (e.g. acrolein, 4-hydroxynonenal); (3) reduced cellular uptake of cysteine, required for GSH synthesis, due to high levels of glutamate

(Sagara and Schubert, 1998); (4) decreased activity of enzymes involved in the GSH synthesis (e.g. glutathione synthetase) and/or recycling of GSSG via glutathione reductase; and (5) diminished amount of NADPH, which is needed for GSSG reduction. However, regardless of the mechanism responsible for the decrease in low-molecular-weight thiols, GSH levels return to normal values in the chronic phase of the disease as inflammation also subsides. As expected, the amount of lipid peroxidation products is high in acute EAE and decreases to normal levels in the chronic phase. In contrast, protein carbonyls are also elevated in chronic EAE and likely the result of the lower proteasome proteolytic activity in this stage of the disease. Thus, cell death in the spinal cord of EAE mice exhibits a better temporal correlation with the build-up of oxidized proteins than with oxidative stress. Furthermore, while carbonyls are also present in live cells during the course of EAE, their levels are much higher in apoptotic cells demonstrating a spatial correlation between these two parameters.

It is interesting to note that in both control and EAE spinal cord, astrocytes contain the highest levels of carbonyls, followed by oligodendrocytes and neurons. This result is not totally unexpected since astrocytes produce large amounts of ROS (Keller et al., 1999) that could generate significant amounts of carbonyls within these cells. Nonetheless, it was somewhat surprising to find that the basal carbonyl staining in neurons and oligodendrocytes are significantly lower, particularly when these two cell types are considered to be highly susceptible to oxidative stress (Halliwell, 2006; Benarroch, 2009). Interestingly, the notion that astrocytes are less sensitive to oxidative damage than other CNS

cells has been recently challenged. It has been found that astrocytes in the unperturbed mouse brain contain significantly lower levels of reduced glutathione than neurons and oligodendrocytes (Miller et al., 2009). An alternative possibility is that oligodendrocytes and neurons may have a more efficient proteolytic machinery to remove oxidized proteins thus reducing the build up of carbonylated proteins in these cells. Studies are underway to determine GSH and proteasome levels in individual cells during the course of EAE.

Carbonylation is known to cause inappropriate inter- and intra-protein cross-links as well as protein misfolding, which in turn results in the formation of high-molecular-weight aggregates (Grune et al., 1997; Mirzaei and Regnier, 2008). As these aggregates get larger they precipitate, become resistant to proteolytic degradation and reduce cell viability (Nyström, 2005; Maisonneuve et al., 2008a). The precise relationship between protein aggregate formation and apoptosis, or whether the aggregates are themselves cytotoxic is unclear. It has been recently discovered that protein aggregates, as they form, sequester multiple preexistent and newly synthesized proteins that have essential cellular functions and thus are critical for cell survival (Olzscha et al., 2011). The presence in EAE tissues of a significant number of cells containing large protein aggregates is noteworthy and may be due not only to an increase in the amount of carbonylated proteins but also to a deficient removal. In this regard, we found that autophagy, the major mechanism for protein aggregate clearance (Son et al., 2012), is significantly reduced in both acute and chronic EAE thereby explaining the presence of juxta-nuclear protein aggregates throughout the disease. While it is tempting to

speculate that these inclusion bodies contribute significantly to cell death, there is some evidence suggesting aggresomes may instead provide a cytoprotective function by sequestering the toxic, aggregated proteins (Tyedmers et al., 2010). Some of the same studies also propose that the smaller protein aggregates are the cytotoxic species. Thus, in the future, it will be important to determine the size-distribution of protein aggregates during the course of the disease as we may find that the presence of small rather than large aggregates correlates better with the changes in pathology and disease activity. Indeed, the occurrence in EAE of protein aggregates with a size smaller than those detected by histochemical analysis is very likely since protein carbonyls, which are enriched in the aggregates isolated by high-speed centrifugation, do not co-localize with the ProteoStat-positive aggresomes and large cytoplasmic inclusion bodies.

Using neuronal cultures, we have recently found that a moderate depletion of glutathione (GSH), similar to that observed in EAE (this study), leads to increased protein carbonylation, protein aggregation and cell death, all of which are temporally correlated (Dasgupta et al., 2012). Furthermore, several protein carbonyl scavengers (hydralazine, histidine hydrazide and methoxylamine) prevented protein aggregation and cell death, suggesting that during GSH depletion oxidized proteins are critical for aggregate formation and cytotoxicity. In that study, we also found that protein aggregates are not made of carbonylated proteins exclusively since the cellular amount of oxidized species is roughly 1-2% of that of the aggregates. However, protein carbonylation may expose hydrophobic surfaces that can mediate aberrant interactions with other (non-

oxidized) proteins, resulting in their functional impairment and sequestration as was recently proposed for several cerebral proteopathies (Walker and LeVine, 2012). Preliminary studies in our laboratory also show that inhibition of protein aggregation with Congo Red and 2-hydroxypropyl-β-cyclodextrin reduce neuronal cell death induced by partial GSH depletion without affecting oxidative stress or protein carbonylation, which suggests a direct link between protein oxidation, protein aggregation and cell death (Dasgupta and Bizzozero, unpublished results). In the future, it will be important to examine whether carbonyl scavengers and aggregation inhibitors prevent or reduce cell death and ameliorate disease activity in EAE. Interestingly, it has been recently found that the reactive carbonyl scavenger hydralazine reduces disease activity in acute EAE mice (Leung et al., 2011). Yet, while encouraging, these findings should be interpreted with caution since hydralazine is also a potent antioxidant (Zheng and Bizzozero, 2010) and it is well known that reduction of oxidative stress ameliorates EAE (Marracci et al., 2002; Penkowa and Hidalgo, 2003; Hendricks et al., 2004; Offen et al., 2004). Studies using carbonyl scavengers lacking antioxidant and anti-inflammatory properties are thus needed to elucidate the role of protein oxidation in inflammatory demyelination.

2.5 FUNDING

This work was supported by PHHS grant NS057755 from the National Institutes of Health.

2.6 REFERENCES

Arenella LS, Herndon R. (1984) Mature oligodendrocytes: division following experimental demyelination in adult animals. Arch Neurol 41:1162-1165.

Akassoglou K, Bauer J, Kassiotis G, Pasparakis M, Lassmann H, Kollias G, Probert L (1998) Oligodendrocyte apoptosis and primary demyelination induced by local TNF/p55TNF receptor signaling in the central nervous system of transgenic mice models for multiple sclerosis with primary oligodendrogliopathy. Am J Pathol 153:801–813.

Aksenov MY, Aksenova MV, Butterfield DA, Geddes JW, Markesbery WR (2001) Protein oxidation in the brain in Alzheimer's disease. Neurosci 103:373-383.

Anderson JM, Hampton DW, Patani R, Pryce G, Crowther RA, Reynolds R, Franklin RJM, Giovannoni G, Compston DA, Baker D, Spillantini MG, Chandran S (2008) Abnormally phosphorylated tau is associated with neuronal and axonal loss in experimental autoimmune encephalomyelitis and multiple sclerosis. Brain 131:1736-1748.

Benarroch EE (2009) Oligodendrocytes: Susceptibility to injury and involvement in neurologic disease. Neurology 72, 1779-1785.

Bizzozero OA (2009) Protein carbonylation in neurodegenerative and demyelinating CNS diseases. In “Handbook of Neurochemistry and Molecular Neurobiology” (Lajtha A, Banik N, Ray S, eds) Springer, pp. 543-562.

Bizzozero OA, DeJesus G, Callahan K, Pastuszyn A (2005) Elevated protein carbonylation in the brain white matter and gray matter of patients with multiple sclerosis. J Neurosci Res 81:687–695.

Dalle-Donne I, Rossi R, Giustarini D, Gagliano N, Lusini L, Milzani A, Di Simplicio P, Colombo R (2001) Actin carbonylation: from a simple marker of protein oxidation to relevant signs of severe functional impairment. Free Radic Biol Med 31:1075–1083.

Das A, Guyton MK, Matzelle DD, Ray SK, Banik NL (2008) Time-dependent increases in protease activities for neuronal apoptosis in spinal cords of Lewis rats during development of acute experimental autoimmune encephalomyelitis. J Neurosci Res 86:2992-3001.

Dasgupta A, Bizzozero OA (2011) Positive correlation between protein carbonylation and apoptosis in EAE. Trans Am Soc Neurochem 42:PSM08-01.

Dasgupta A, Zheng J, Bizzozero OA (2012) Protein carbonylation and aggregation precede neuronal apoptosis induced by partial glutathione depletion. ASN NEURO 4(3):art:e00084.doi:10.1042/AN20110064.

Divald A, Powell S. (2006) Proteasome mediates removal of proteins oxidized during myocardial ischemia. Free Radic Biol Med 4:156-164.

England K, O'Driscoll C, Cotter TG (2004) Carbonylation of glycolytic proteins is a key response to drug-induced oxidative stress and apoptosis. Cell Death Differ 11:252–260.

Ferrante RJ, Browne SE, Shinobu LA, Bowling AC, Baik MJ, MacGarvey U, Kowall NW, Brown RH, Beal MF (1997) Evidence of increased oxidative damage in both sporadic and familial amyotrophic lateral sclerosis. J Neurochem 69:2064-2074.

Ferrington DA, Husom AD, Thompson LV (2005) Altered proteasome structure, function and oxidation in aged muscle. FASEB J 19:644-646.

Floor E, Wetzel MG (1998) Increased protein oxidation in human sustantia nigra pars compacta in comparison with basal ganglia and prefrontal cortex measured with an improved dinitrophenylhydrazine assay. J Neurochem 70:268-275.

Fucci L, Oliver CN, Coon MJ, Stadtman ER (1983) Inactivation of key metabolic enzymes by mixed-function oxidation reactions: possible implication in protein turnover and ageing. Proc Nat Acad Sci USA 80:1521-1525.

Gilgun-Sherki Y, Melamed E, Offen D (2004) The role of oxidative stress in the pathogenesis of multiple sclerosis: the need for effective antioxidant therapy. J Neurol 251:261-268.

Gold R, Hartung HP, Toyka KV (2000) Animal models for autoimmune demyelinating disorders of the nervous system. Mol Med Today 6:88-91.

Grune T, Reinheckel T, Davies KJ (1997) Degradation of oxidized proteins in mammalian cells. FASEB J 11:526- 534.

Guyton MK, Wingrave JM, Yallapragada AV, Wilford GG, Sribnick EA, Matzelle DD, Tyor WR, Ray SK, Banik NL (2005) Upregulation of calpain correlates with increased neurodegeneration in acute experimental autoimmune encephalomyelitis. J Neurosci Res 81:53–61.

Haider L, Fischer MT, Frischer JM, Bauer J, Höftberger R, Botond G, Esterbauer H, Binder CJ, Witztum JL, Lassmann H (2011) Oxidative damage in multiple sclerosis lesions. Brain 134:1914–1924

Halliwell B (2006) Oxidative stress and neurodegeneration: where are we now? J Neurochem 97:1634-1658.

Hassen GW, Feliberti J, Kesner L, Stracher A, Mokhtarian F (2006) A novel calpain inhibitor for the treatment of acute experimental autoimmune encephalomyelitis. J Neuroimmunol 180:135-146.

Hendriks JJ, Alblas J, van der Pol SM, van Tol EA, Dijkstra CD, de Vries HE (2004) Flavonoids influence monocytic GTPase activity and are protective in experimental allergic encephalitis. J Exp Med 200:1667-1672.

Keller JN, Hanni KB, Gabbita SP, Friebe V, Mattson MP, Kindy MS (1999) Oxidized lipoproteins increase reactive oxygen species formation in microglia and astrocyte cell lines. Brain Res 830: 10-15.

Keller JN, Hanni KB, Marksberry WR (2000) Impaired proteasome function in Alzheimer's disease. J Neurochem 75:436-439.

Kornek B, Lassmann H (1999) Axonal pathology in multiple sclerosis: a historical note. Brain Pathol 9:651–656.

Kuerten S, Kostova-Bales DA, Frenzel LP, Tigno JT, Tary-Lehmann M, Angelov DN, Lehmann PV (2007) MP4- and MOG:35-55-induced EAE in C57BL/6 mice differentially targets brain, spinal cord and cerebellum. J Neuroimmunol 189:31-40.

Leung G, Sun W, Zheng L, Brookes S, Tully M, Shi R (2011) Anti-acrolein treatment improves behavioral outcome and alleviates myelin damage in experimental autoimmune encephalomyelitis mouse. Neurosci 173:150-155.

Lucchinetti CF, Bruck W, Rodriguez M, Lassmann H (1996) Distinct patterns of multiple sclerosis pathology indicate heterogeneity in pathogenesis. Brain Pathol 6:259-274.

Luo S, Wehr NN (2009) Protein carbonylation: avoiding pitfalls in the 2,4-dinitrophenylhydrazine assay. Redox Rep 14:159-166.

McNaught KS, Belizaire R, Isacson O, Jenner P, Olanow CW (2003) Altered proteasomal function in sporadic Parkinson's disease. Exp Neurol 179:38-46.

Magi B, Ettorre A, Liberatori S, Bini L, Andreassi M, Frosali S, Neri P, Pallini V (2004) Selectivity of protein carbonylation in the apoptotic response to oxidative stress associated with photodynamic therapy: a cell biochemical and proteomic investigation. Cell Death Differ 11:842-852.

Maisonneuve E, Ezraty B, Dukan S (2008a) Protein aggregates: an aging factor involved in cell death. J Bacteriol 190:6070–6075.

Maisonneuve E, Fraysse L, Lignon S, Capron L, Dukan S (2008b) Carbonylated proteins are detectable only in a degradation-resistant aggregate state in Escherichia coli. J Bacteriol 190:6609–6614.

Marracci GH, Jones RE, McKeon GP, Bourdette DN (2002) Alpha-lipoic acid inhibits T cell migration into the spinal cord and suppresses and treats experimental autoimmune encephalomyelitis. J Neuroimmunol 131:104-114.

Meyer R, Weissert R, Diem R, Storch MK, de Graaf KL, Kramer B, Bahr M (2001) Acute neuronal apoptosis in a rat model of multiple sclerosis. J Neurosci 21:6214–6220.

Miller VM, Lawrence DA, Mondal TK, Seegal RF (2009) Reduced glutathione is highly expressed in white matter and neurons in the unperturbed brain - Implication for oxidative stress associated with neurodegeneration. Brain Res 1276:22-30.

Mirzaei H, Regnier F (2008) Protein:protein aggregation induced by protein oxidation. J Chromatogr 873:8-14.

Müller DM, Pender MP, Greer JM (2000) A neuropathological analysis of experimental autoimmune encephalomyelitis with predominant brain stem and cerebellar involvement and differences between active and passive induction. Acta Neuropathol 100:174-182.

Nyström T (2005) Role of oxidative carbonylation in protein quality control and senescence. EMBO J 24:1311-1317.

Offen D, Gilgun-Sherki Y, Barhum Y, Benhar M, Grinberg L, Reich R, Melamed E, Atlas D (2004) A low molecular weight copper chelator crosses the blood-brain barrier and attenuates experimental autoimmune encephalomyelitis. J Neurochem 89:1241-1251.

Ohkawa H, Ohishi N, Yagi K (1979) Assay for lipid peroxides in animal tissues by thiobarbituric acid reaction. Anal Biochem 95:331-358.

Olzscha H, Schermann SM, Woerner AC, Pinket S, Hecht MH, Tartaglia GG, Vendruscolo M, Hayer-Hartl M, Hartl FU, Vabulas RM (2011) Amyloid-like aggregates sequester numerous metastable proteins with essential cellular functions. Cell 144:67–78.

Pender MP, Nguyen KB, McCombe PA, Kerr JF (1991) Apoptosis in the nervous system in experimental allergic encephalomyelitis. J Neurol Sci 104:81-87.

Penkowa M, Hidalgo J (2003) Treatment with metallothionein prevents demyelination and axonal damage and increases oligodendrocyte precursors and tissue repair during experimental autoimmune encephalomyelitis. J Neurosci Res 72:574-586.

Perluigi M, Poon HF, Maragos W, Pierce WM, Klein JB, Calabrese V, Cini C, DeMarco C, Butterfield DA (2005) Proteomic Analysis of protein expression and oxidative modification in R6/2 transgenic mice - a model of Huntington's disease. Mol Cell Proteomics 4:1849-1861.

Rodgers KJ, Dean RT (2003) Assessment of proteasome activity in cell lysates and tissue homogenates using peptide substrates. Int J Biochem Cell Biol 35:716-727.

Sagara Y, Schubert D (1998) The activation of metabotropic glutamate receptors protects nerve cells from oxidative stress. J Neurosci 18:6662-6671.

Seo H, Sonntag KC, Isacson O (2004) Generalized brain and skin proteasome inhibition in Huntington's disease. Ann Neurol 56:319-328.

Shaik IH, Mehvar R (2006) Rapid determination of reduced and oxidized glutathione levels using a new thiol-masking reagent and the enzymatic recycling method: application to the rat liver and bile samples. Anal Bioanal Chem 385:105–113.

Shringarpure R, Grüne T, Davies KJ (2001) Protein oxidation and 20S proteasome-dependent proteolysis in mammalian cells. Cell Mol Life Sci 58:1442-1450.

Smerjac SM, Bizzozero OA (2008) Cytoskeletal protein carbonylation and degradation in experimental autoimmune encephalomyelitis. J Neurochem 105:763-772.

Smith KJ, Kapoor R, Felts PA (1999) Demyelination: the role of reactive oxygen and nitrogen species. Brain Pathol 9:69-92.

Son JH, Shim JH, Kim KH, Ha JY, Han JY (2012) Neuronal autophagy and neurodegenerative diseases. Exp Mol Med 44:89-98.

Stadtman ER, Berlett BS (1997) Reactive oxygen-mediated protein oxidation in aging and disease. Chem Res Toxicol 10:485-494.

Starke PE, Oliver CN, Stadtman ER (1987) Modification of hepatic proteins in rats exposed to high oxygen concentration. FASEB J 1:36–39.

Toft-Hansen H, Füchtbauer L, Owens T (2011) Inhibition of reactive astrocytosis in established experimental autoimmune encephalomyelitis favors infiltration by myeloid cells over T cells and enhances severity of disease. Glia 59:166-176.

Tripathi RB, Rivers LE, Young KM, Jamen F, Richardson WD (2010) PDGFRA/NG2 glia generate new oligodendrocytes but few astrocytes in a murine EAE model of demyelinating disease. J Neurosci 30:16383-16390.

Tyedmers J, Mogk A, Bukau B (2010) Cellular strategies for controlling protein aggregation. Nature Rev 11:777-788.

Vogt J, Paul F, Aktas O (2009) Lower motor neuron loss in multiple sclerosis and experimental autoimmune encephalomyelitis. Annals Neurol 66:310–322.

Walker LC, LeVine H (2012) Corruption and spread of pathogenic proteins in neurodegenerative diseases. J Biol Chem 287:33109-33115.

Zheng J, Bizzozero OA (2010a) Accumulation of protein carbonyls within cerebellar astrocytes in murine experimental autoimmune encephalomyelitis. J Neurosci Res 88:3376-3385.

Zheng J, Bizzozero OA (2010b) Reduced proteasomal activity contributes to the accumulation of carbonylated proteins in chronic experimental autoimmune encephalomyelitis. J Neurochem 115:1556–1567.

Zheng J, Bizzozero OA (2011) Decreased activity of the 20S proteasome in the brain white matter and gray matter of patients with multiple sclerosis. J Neurochem 117:143-153.

Zheng J, Dasgupta A, Bizzozero OA (2012) Changes in 20S subunit composition are largely responsible for altered proteasomal activities in experimental autoimmune encephalomyelitis. J Neurochem 121:486-494.

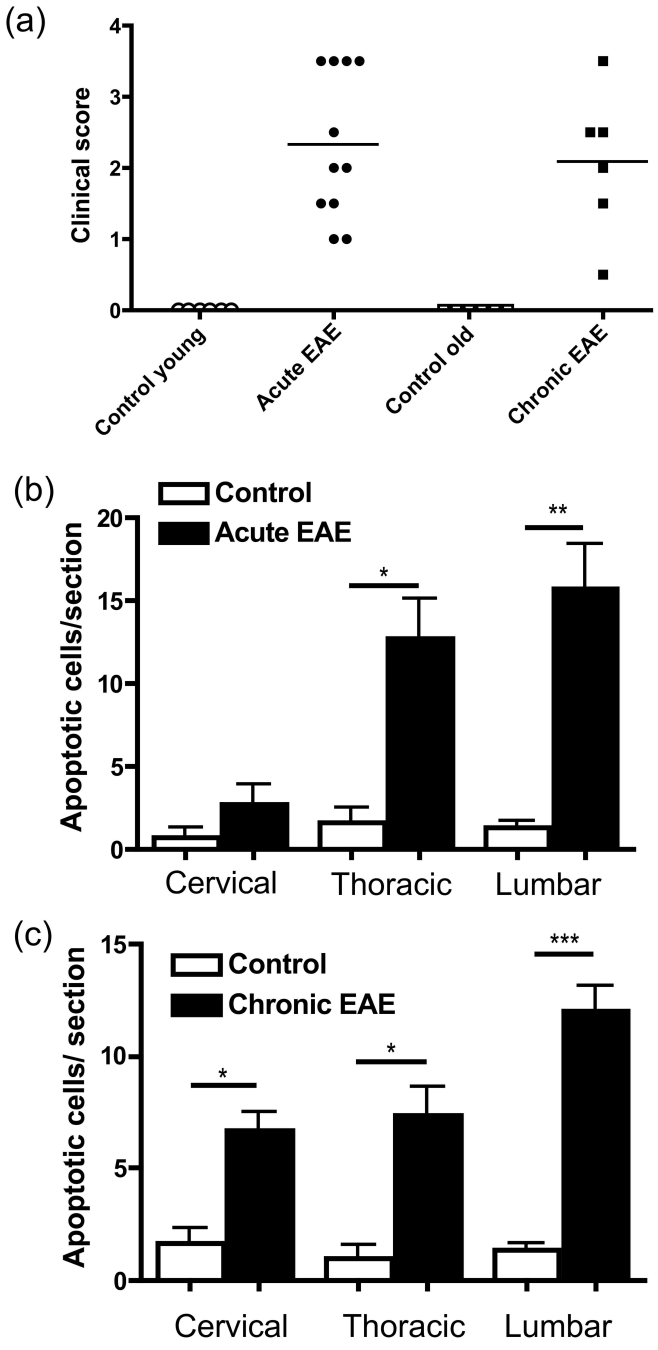

Fig. 1 – Apoptosis along the spinal cord is high in both acute and chronic EAE – (a) Clinical scores of animals used in the study. (b, c) Number of apoptotic cells determined by TUNEL staining in the different spinal cord regions (cervical, thoracic and lumbar) of acute and chronic EAE mice, respectively. A total of 5-8 non-consecutive (30μm apart) 3μm-thick sections per animal were analyzed and averaged. Values represent the mean ± SEM of 3 animals per experimental group. Clinical scores (mean ± SEM) of acute and chronic EAE mice were 2.2 ± 0.7 and 1.8 ± 0.7, respectively. *p<0.05, **p<0.005, ***p<0.0005.

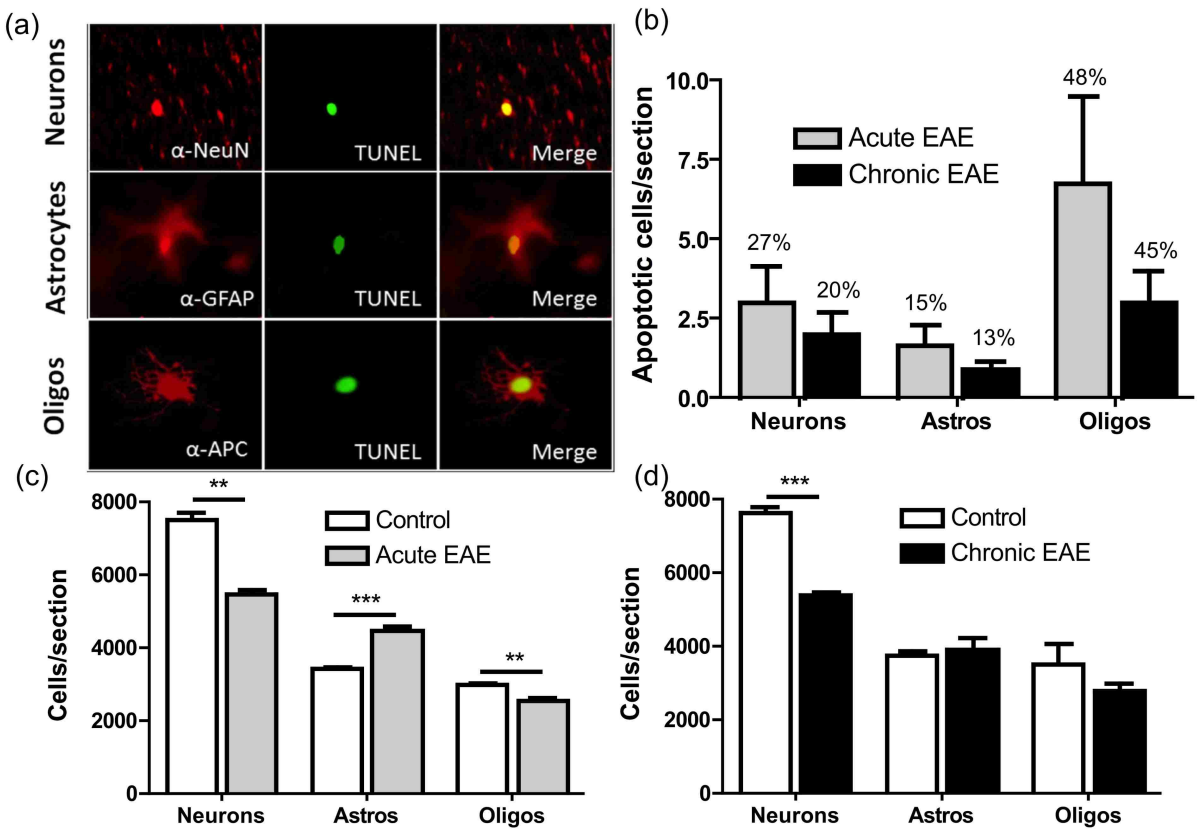

Fig. 2 - Significant neuronal and glial apoptosis occurs in acute and chronic EAE. (a) High-magnification, double-label immunofluorescence images of lumbar spinal cord sections of acute EAE mice depicting an apoptotic neuron, astrocyte and oligodendrocyte. Immunohistochemical detection of cellular apoptosis was determined using TUNEL (green channel) and antibodies against specific cell types (neurons: NeuN, astrocytes: GFAP, oligodendrocytes: APC). (b) Number of TUNEL-positive cells in the lumbar spinal cord of acute and chronic EAE mice that are identified as neurons, astrocytes and oligodendrocytes. A total of 5 non-consecutive (30μm apart) 0.3μm-thick sections per animal were analyzed and averaged. Values are the mean ± SEM of 3-6 animals per experimental group. Clinical scores (mean ± SEM) of acute and chronic EAE mice were 2.2 ± 0.7 and 1.8 ± 0.7, respectively. Numbers on top of the bars are the values expressed as percentage of TUNEL-positive cells. Note that those numbers do not add up to 100% since there are other unidentified apoptotic cells. (c, d) Average number of neurons, astrocytes and oligodendrocytes per section in the lumbar spinal cord region of acute and chronic EAE mice, respectively. Cells were identified using the same markers as indicated above and DAPI staining. A total of 5 non-consecutive (30μm apart) 3μm-thick sections per animal were analyzed and averaged. Values represent the mean ± SEM of 3 mice per experimental group. **p<0.005, ***p<0. 0005.

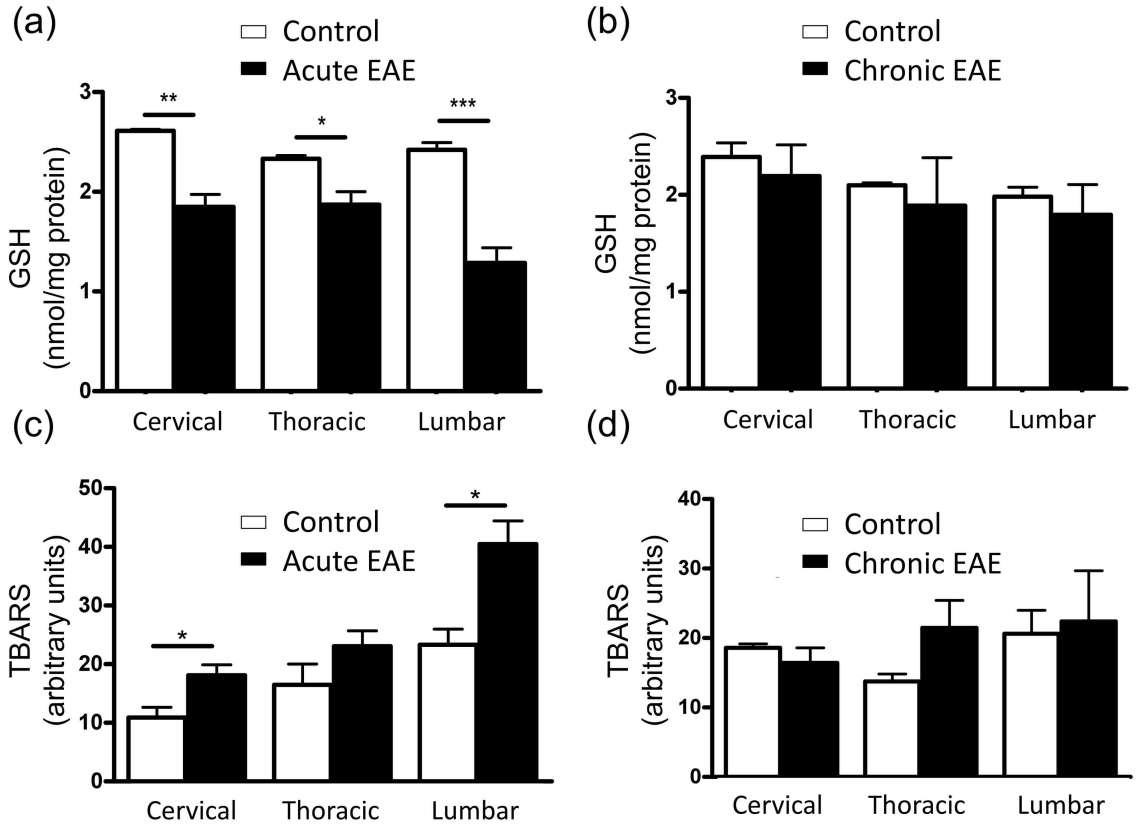

Fig. 3 –Diminished GSH levels and increased lipid peroxidation are found only in acute EAE. (a, b) GSH levels in the various spinal cord regions (cervical, thoracic and lumbar) of acute and chronic EAE mice, respectively. Values represent the mean ± SEM of 3-4 animals per experimental group. Clinical scores (mean ± SEM) of acute and chronic EAE mice were 2.0 ± 0.5 and 1.7 ± 0.6, respectively. (c, d) TBARS levels in the different spinal cord regions of acute and chronic EAE mice, respectively. Values represent the mean ± SEM of 3-5 animals per experimental group. Clinical scores (mean ± SEM) of acute and chronic EAE mice were 2.3 ± 0.5 and 1.7 ± 0.6, respectively. *p<0.05, **p<0.005, ***p<0.0005.

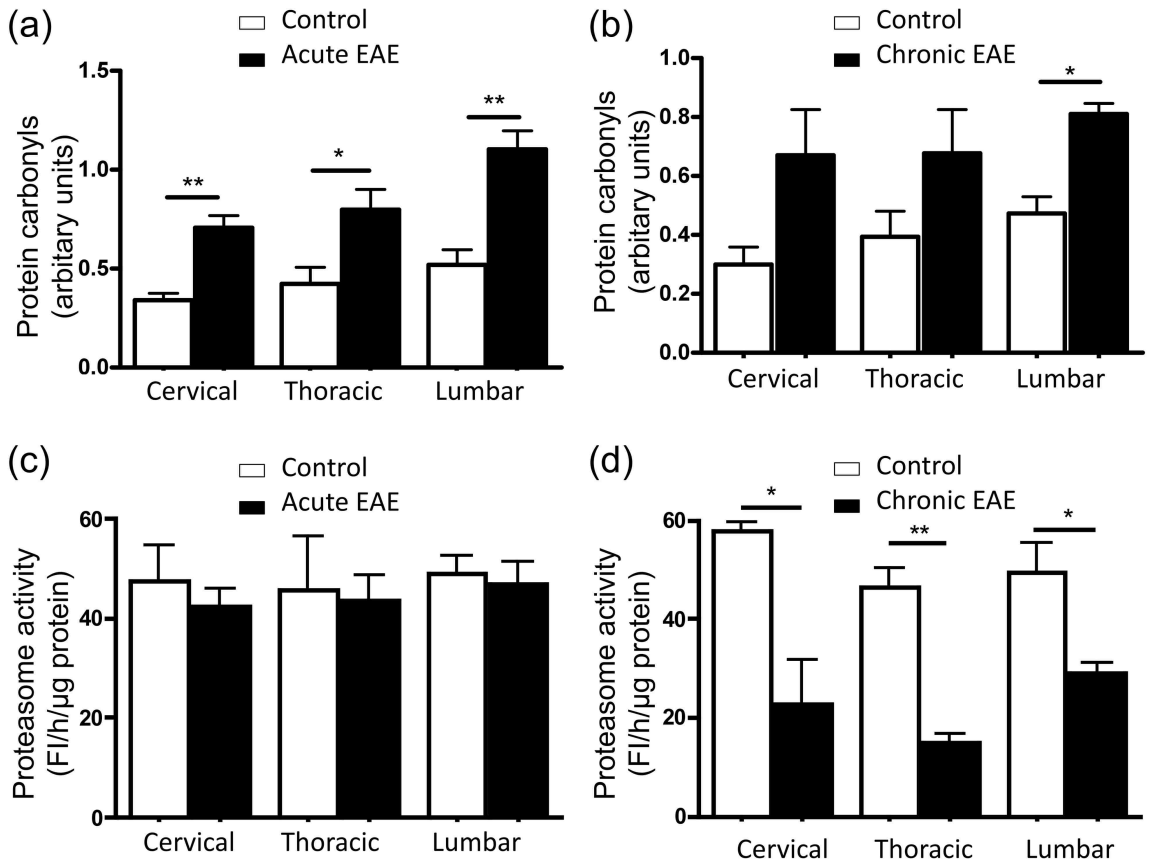

Fig. 4 - Protein carbonyls accumulate in both acute and chronic EAE. (a, b) Protein carbonyl levels in the various spinal cord regions (cervical, thoracic and lumbar) of acute and chronic EAE mice, respectively. (c, d) Proteasome chymotrypsin-like activity in the different spinal cord regions of acute and chronic EAE mice, respectively. FI, fluorescence units. Values represent the mean ± SEM of 3 animals per experimental group. Clinical scores (mean ± SEM) of acute and chronic EAE mice were 2.2 ± 0.7 and 1.8 ± 0.7, respectively. *$p<0.05$, **$p<0.005$.

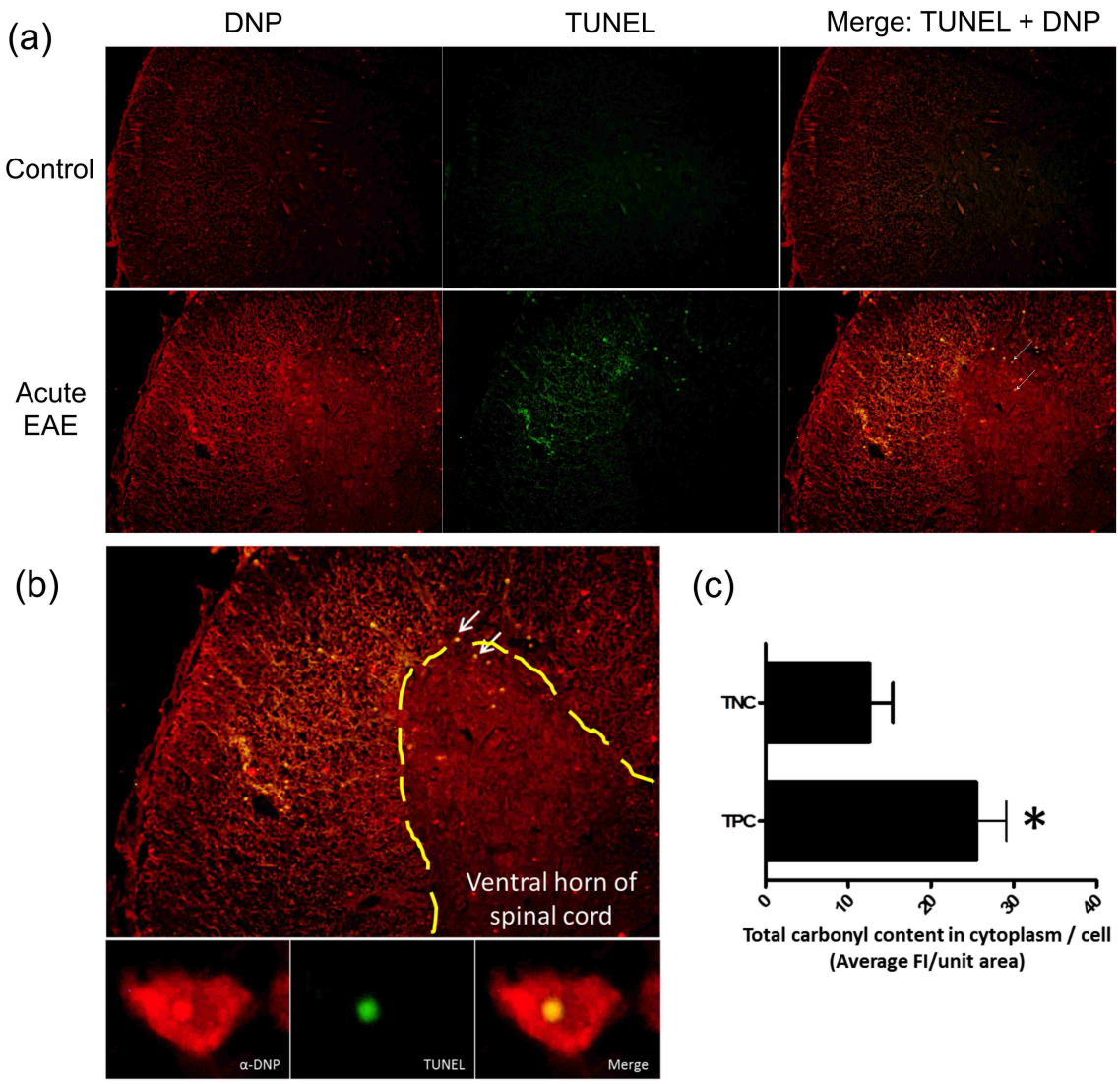

Fig. 5 - Carbonylation levels are higher in apoptotic than in non-apoptotic cells. (a) Double-label immunofluorescence images of lumbar spinal cord sections from control and acute EAE mice. Carbonyls were detected by anti-DNP labeling after derivatization with DNPH (red channel) and apoptotic cells were identified by TUNEL staining (green channel). (b) High-magnification image depicting a TUNEL-positive cell containing extensive carbonyl staining in the cytoplasm. (c) Bar graph showing carbonyl levels in the cytoplasm of TUNEL-positive cells (TPC) and TUNEL-negative cells (TNC) in the lumbar spinal cord region of acute EAE mice. A total of 10 non-consecutive (30μm apart) 3μm-thick sections per animal were analyzed and averaged. Values represent the mean ± SEM of 5 animals per experimental group. Clinical scores (mean ± SEM) of acute EAE mice were 2.3 ± 0.5. *$p<0.05$. FI, fluorescence intensity.

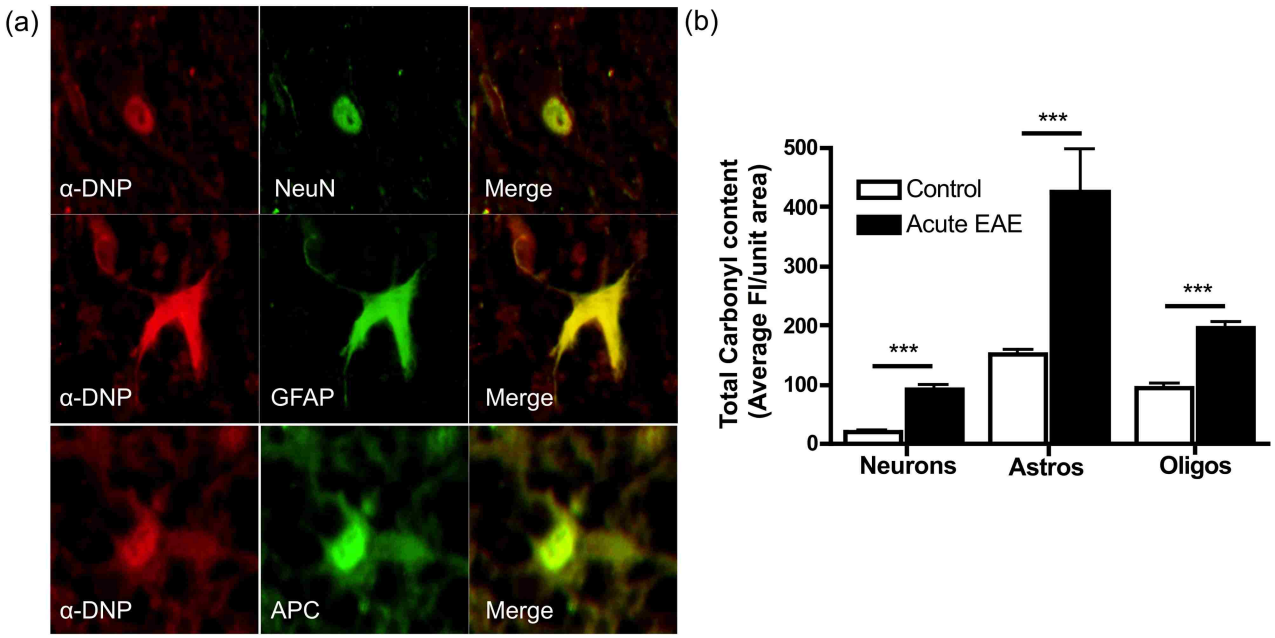

Fig. 6 - Carbonyls accumulate in all the major cell types present in the EAE spinal cord. (a) Double-label immunofluorescence images of cells from the lumbar spinal cord region of acute EAE mice depicting carbonyl staining in the red channel (anti-DNP labeling after derivatization with DNPH) and cell type markers in the green channel (NeuN for neurons, GFAP for astrocytes and APC for oligodendrocytes). (b) Carbonyl content in different cell types in the lumbar spinal cord of control and acute EAE mice. A total of 5-8 non-consecutive (30μm apart) 3μm-thick sections per animal were analyzed and averaged. Values represent the mean ± SEM of 5 animals per experimental group. Clinical scores (mean ± SEM) of acute EAE mice were 2.3 ± 0.5. ***$p<0.0005$. FI, fluorescence intensity.

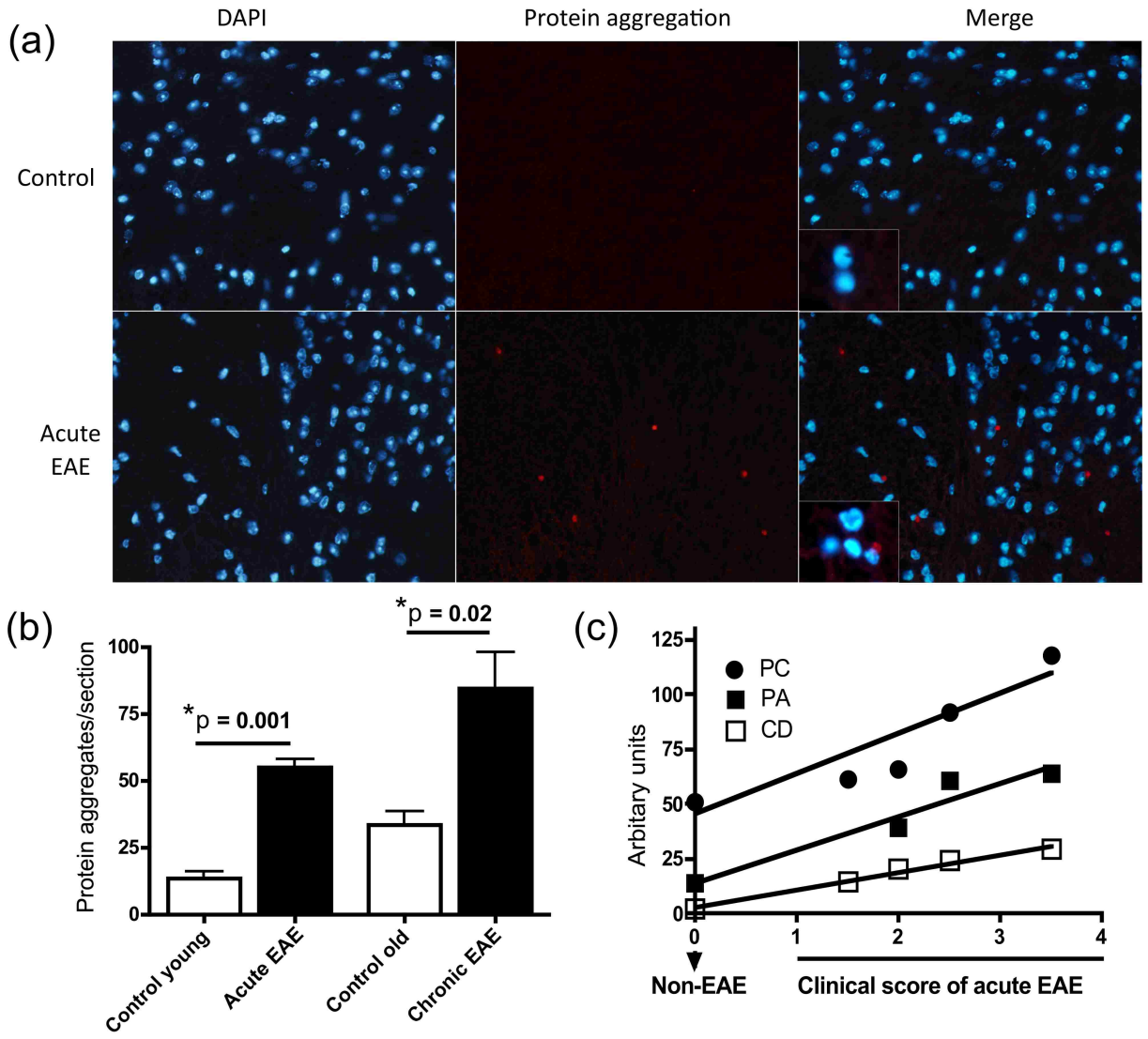

Fig. 7 – The number of protein aggregates augments in both acute and chronic EAE. (a) Representative images of lumbar spinal cord of control and acute EAE mice stained with the ProteoStat® protein aggregation dye (red) and DAPI (light blue) for nuclear identification. (b) Bar diagram showing the number of large protein aggregates in cross-section of the lumbar spinal cord. A total of 9-15 non-consecutive (30µm apart) 3µm-thick sections per animal were analyzed and averaged. Values represent the mean ± SEM of 3-5 animals per experimental group. Clinical scores (mean ± SEM) of acute and chronic EAE mice were 2.4 ± 0.5 and 2.5 ± 0.6, respectively. (c) Linear regression curves predicting a positive relationship between protein carbonylation (PC, r^2 = 0.97), protein aggregation (PA, r^2=0.83) and cell death (CD, r^2=0.88) with the clinical score. Each point represents the average of 2-3 EAE mice per experimental group.

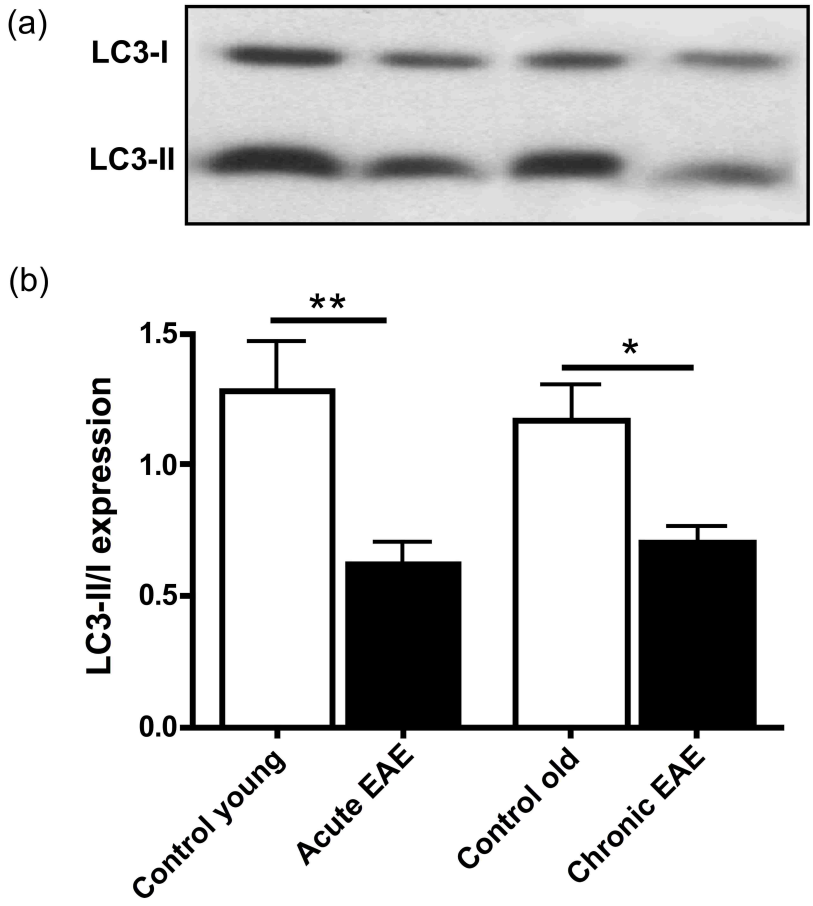

Fig. 8 – Autophagy is impaired in both acute and chronic EAE. (a) A representative western blot depicting the expression of LC3-I and its shorter and lipidated form (LC3-II) in the spinal cord of control and EAE mice. (b) Authophagy index (i.e. LC3-II/LC3-I expression) was determined by densitometric scanning of the western blots. Values represent the mean ± SEM of 4-6 animals per experimental group. Clinical scores (mean ± SEM) of acute and chronic EAE mice were 3.0 ± 0.3 and 2.8 ± 0.5, respectively. *$p<0.05$, **$p<0.005$.

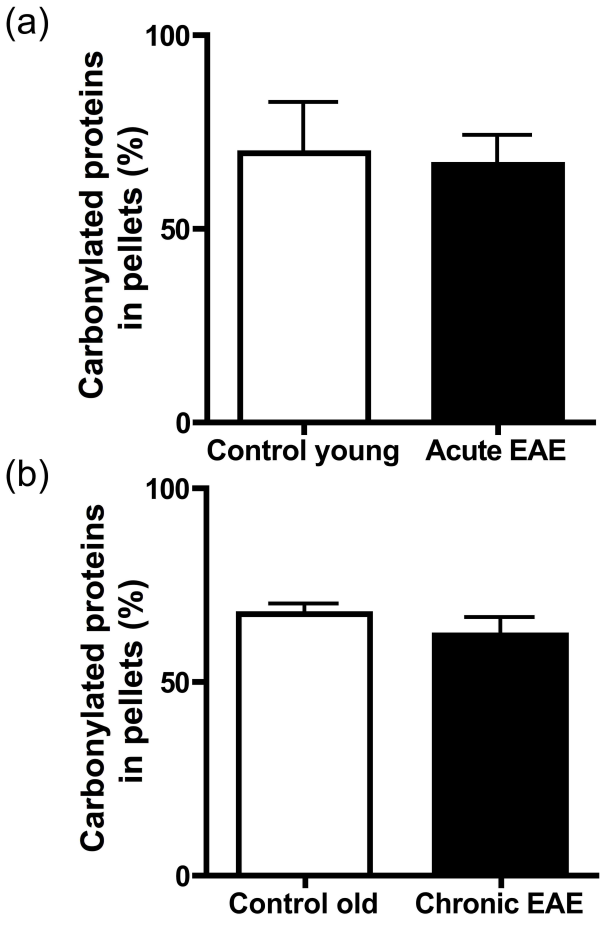

Fig. 9 – Carbonylated proteins partition into the aggregated protein fraction. Levels of protein carbonyls in the spinal cord homogenates and the triton-insoluble aggregated protein fraction were quantified by oxyblot analysis. Values are expressed as the percentage of total protein carbonyls present in the aggregated protein fraction and represent the mean ± SEM of 3 animals per experimental group. Clinical scores (mean ± SEM) of acute and chronic EAE mice were 3.5 ± 0.0 and 2.2 ± 0.3, respectively. Note that the triton-insoluble fraction, which has less than 20% of the protein present in the initial spinal cord homogenate, contains between than 60%-70% of the protein carbonyls.

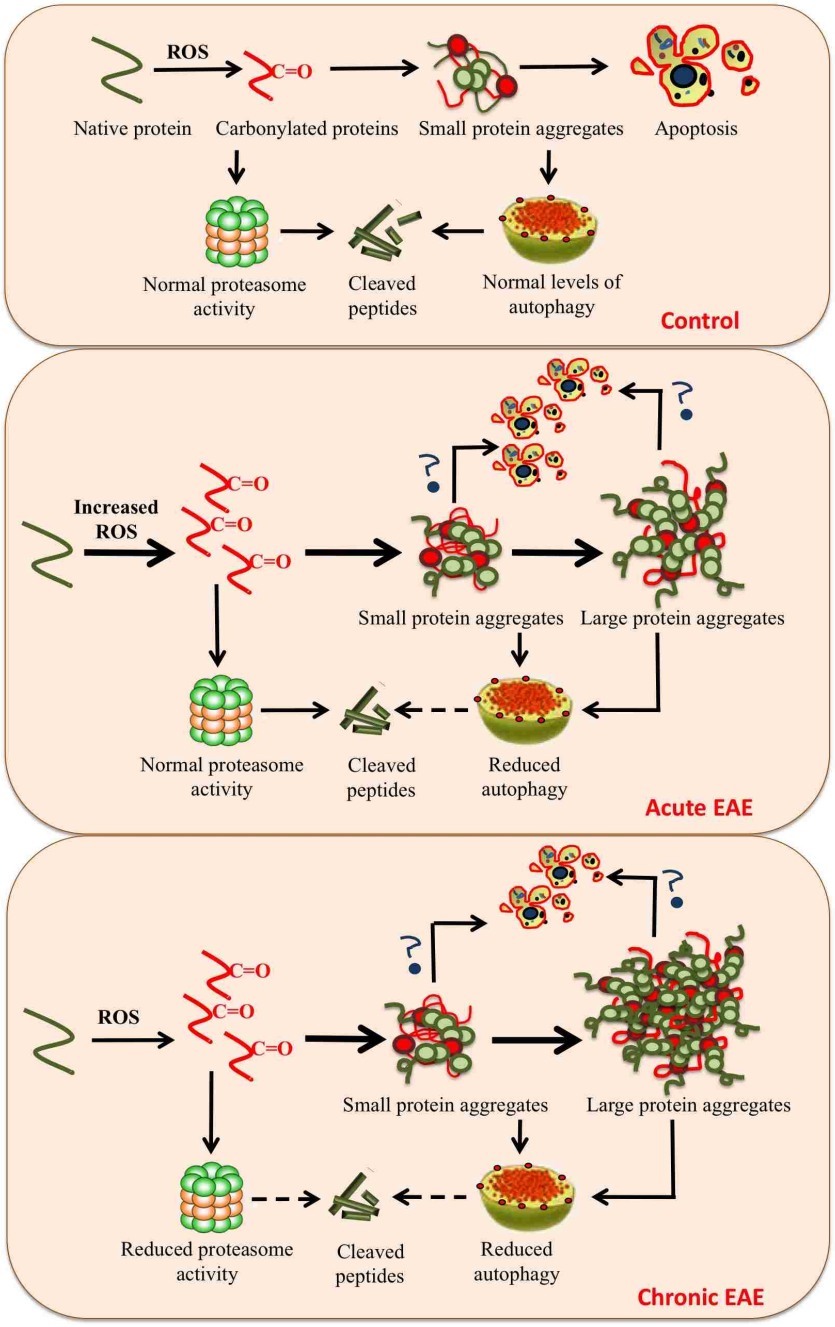

Fig. 10 – Schematic diagram that incorporates the major findings of this study. Carbonylated proteins accumulate in the spinal cord of both acute and chronic EAE mice, albeit by different mechanisms: increased oxidative stress in acute EAE and decreased proteasomal activity in chronic EAE. Augmented protein carbonyl levels and diminished authophagy lead to the formation of protein aggregates throughout the course of the disease. The occurrence of small and/or large protein aggregates may be responsible for the increased neuronal and glial apoptosis.

SUPPLEMENTAL INFORMATION

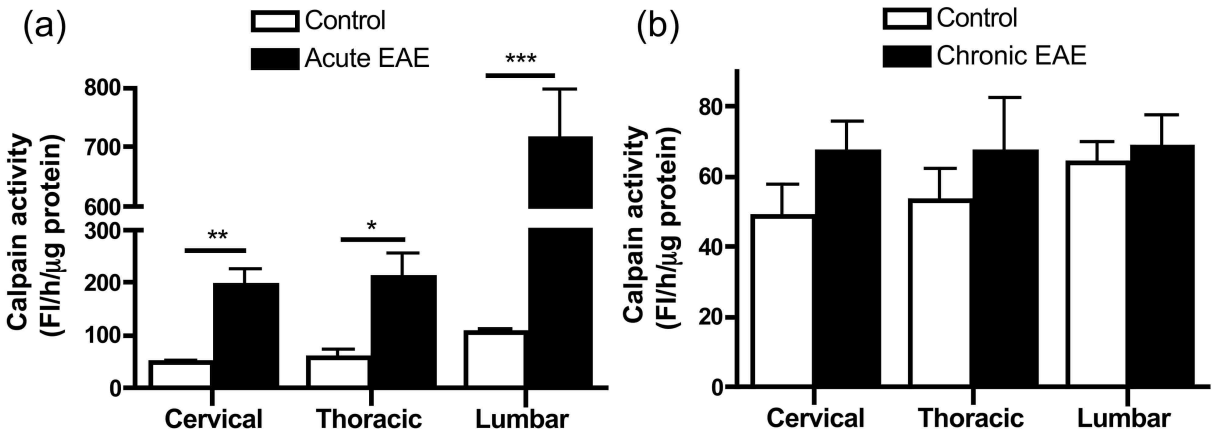

Fig. S1- Calpain activity is increased only in acute EAE. (a, b) Calpain activity in the different mouse spinal cord regions (cervical, thoracic, lumbar) in acute and chronic EAE, respectively. FI, fluorescence intensity. Values represent the mean ± SEM of 4-5 animals per experimental group. Clinical scores (mean ± SEM) of acute and chronic EAE mice were 2.3 ± 0.5 and 2.7 ± 0.5, respectively. *p<0.05, **p<0.005, **p<0.0005.

3. Protein carbonylation and aggregation precede neuronal apoptosis induced by partial GSH depletion

Anushka Dasgupta, Jianzheng Zheng and Oscar A. Bizzozero*

Dept. of Cell Biology and Physiology, University of New Mexico - Health Sciences Center, Albuquerque, New Mexico.

Abbreviations used: ACR, acrolein; BSO, buthionine sulfoximine; DEM, diethyl maleate; DNP, 2,4-dinitrophenyl; DNPH, 2,4-dinitrophenylhydrazine; EAE, experimental autoimmune encephalomyelitis; GSH, glutathione; 4-HNE, 4-hydroxynonenal; MDA, malondialdehyde; MPTP, mitochondrial permeability transition pore; NGF, nerve growth factor; nPC12 cells, NGF-treated rat adrenal medullary pheochromocytoma cells; PBS, phosphate-buffered saline; PCO, protein carbonyl; ROS, reactive oxygen species; TBARS, thiobarbituric acid reactive substances.

3.1 ABSTRACT

While the build-up of oxidized proteins within cells is believed to be toxic, there is currently no evidence linking protein carbonylation and cell death. In this study we show that incubation of neuron-like PC12 (nPC12) cells with 50μM diethyl maleate (DEM) leads to a partial and transient depletion of glutathione (GSH). Concomitant with GSH disappearance there is increased accumulation of protein carbonyls (PCOs) and cell death (both by necrosis and apoptosis). Immunocytochemical studies also revealed a temporal/spatial relationship between carbonylation and cellular apoptosis. In addition, the extent of all three PCO accumulation, protein aggregation and cell death augments if oxidized proteins are not removed by proteasomal degradation. Furthermore, the effectiveness of the carbonyl scavengers hydralazine, histidine hydrazide and methoxylamine at preventing cell death identifies PCOs as the toxic species. Experiments using well-characterized apoptosis inhibitors place protein carbonylation downstream of the mitochondrial transition pore opening and upstream of caspase activation. While the study focused mostly on nPC12 cells, experiments in primary neuronal cultures yielded the same results. The findings are also not restricted to DEM-induced cell death since a similar relationship between carbonylation and apoptosis was found in staurosporin- and buthionine sulphoximine-treated nPC12 cells. In sum, the above results show a causal relationship between carbonylation and apoptosis of neurons undergoing oxidative damage.

3.2 INTRODUCTION

Many neurological disorders are characterized by severe and/or prolonged oxidative stress conditions, which play a significant pathophysiological role (Reynolds et al., 2007; Jomova et al., 2010). The major outcome of oxidative stress is the irreversible damage of cell macromolecules by reactive oxygen species (ROS). Proteins are the major target for oxidants as a result of their abundance and their elevated reaction rate constants (Davies, 2005). Although the polypeptide backbone and the side chains of most amino acids are susceptible to oxidation, the non-enzymatic introduction of aldehyde or ketone functional groups to specific amino acid residues (i.e. carbonylation) constitutes the most common oxidative alteration of proteins (Bizzozero, 2009). Accumulation of protein carbonyls does not only occur but has also been implicated in the etiology and/or progression of several CNS disorders, including Alzheimer's disease (Aksenov et al., 2001), Parkinson's disease (Floor and Wetzel, 1998), amyotrophic lateral sclerosis (Ferrante et al., 1997) and multiple sclerosis (Bizzozero et al., 2005).

Carbonylation is believed to have deleterious effects on both protein function and cell viability. However, while there is ample experimental evidence demonstrating that the presence of carbonyl groups leads to changes in protein structure and function (Fucci et al., 1983; Starke et al., 1987; Dalle-Donne et al., 2001), a direct relationship between protein carbonylation and cell death has not been conclusively established. The major problem lies on the difficulty to differentiate the effect(s) of carbonylation from that of other protein modifications that occur

simultaneously under oxidative stress conditions (e.g. oxidation of cysteine thiols, nitration of tyrosine residues). Nonetheless, a number of studies have recently surfaced suggesting a link between increased protein carbonylation and loss of cell viability. For instance, carbonylation of critical glycolytic enzymes in etopside-treated HL60 cells seems to decrease glucose utilization and cause cell death (England et al., 2004), while oxidation of several chaperones has been associated to apoptosis of irradiated HL60 human leukemia cells (Magi et al., 2004). In addition, carbonylation may lead to the formation of large, protease-resistant protein aggregates, which are considered highly cytotoxic (Nyström, 2005; Maisonneuve et al., 2008).

Because of the potential cellular toxicity that results from the accumulation of carbonylated proteins, their intracellular levels are normally maintained very low by proteolytic removal. Among the various cellular proteases, the 20S proteasome, via it chymotrypsin-like activity and in an ATP-independent manner, has been shown responsible for digesting oxidized proteins (Shringarpure et al., 2003; Divald and Powell, 2006). Indeed, failure of this proteolytic system, as it happens in many neurodegenerative disorders, results in the build up of oxidized proteins that likely contributes cellular dysfunction and tissue damage (Rinaudo and Piccinini, 2007).

In recent years, our laboratory has been investigating the mechanism of protein carbonylation and the metabolic/cellular impact of increased protein oxidation in inflammatory demyelinating disorders. We have found that protein carbonyls accumulate in the CNS of patients with multiple sclerosis (Bizzozero et al., 2005)

and of animals with experimental autoimmune encephalomyelitis (EAE) (Smerjac and Bizzozero, 2008; Zheng and Bizzozero, 2010b). Recent immunohistochemical studies in the spinal cord of EAE mice have demonstrated a positive correlation between carbonylation levels and neuronal/oligodendrocyte apoptosis (Dasgupta and Bizzozero, 2011). Based on these findings we set up to investigate whether a relationship, causal or otherwise, exists between protein carbonylation and neuronal cell death *in vitro*. To this end, the concentration of GSH in nerve growth factor (NGF)-treated PC12 cells or primary neurons was reduced to levels similar to those found in the spinal cord of EAE animals. Under these oxidative stress conditions, we discovered a close temporal/spatial relationship between protein carbonylation and apoptosis. Experiments combining GSH depletion, proteasome inhibition and carbonyl scavenging strengthened the link between protein damage in the form of carbonyls and loss of cell viability.

3.3 Material and Methods

Neuronal cultures and drug treatments

Rat adrenal medullary pheochromocytoma (PC12) cells were cultured on poly-L-lysine-coated 6-well plates (BioCoat™, BD Biosciences, Bedford, MA) in RPMI-1640 media containing 10% serum (7.5% donor horse and 2.5% fetal calf serum; Sigma, St. Louis, MO) and an antibiotic/antimycotic mixture (Invitrogen Corp., Carlsbad, CA). Cells grown at 60-70% confluence were differentiated into a neuronal phenotype by incubation with 100 ng/ml of NGF (Sigma) for either 1 or

7 days. Primary neuronal cultures were established from cerebral cortices of C57BL/6 mice and grown for 7 days as described by Harms et al. (2010). Cells were treated with the GSH depletor diethylmaleate (DEM, Sigma) for 1-24 hours. Control cells were left untreated after incubation with NGF. In some cases, DEM-treated cells were incubated with the proteasome inhibitors lactacystin (Enzo Life Sciences, Plymouth Meeting, PA) and epoxomycin (Enzo) in the absence or presence of various compounds including trolox (Sigma), hydralazine (Sigma), methoxylamine (Sigma), z-histidine hydrazide (Peninsula Laboratories, San Carlos, CA). Other drugs tested were the mitochondrial permeability transition pore (MPTP) inhibitor cyclosporin A (Calbiochem; La Jolla, CA), the pan-caspase inhibitor zVAD-fmk (Sigma), the apoptosis initiator staurosporine (Sigma) and the GSH depletor buthionine sulfoximine (BSO) (Sigma). After incubation, cells were homogenized in PEN buffer (20 mM sodium phosphate, pH 7.5, 1 mM EDTA, and 0.1 mM neocuproine) containing 2 mM 4,5 dihydroxy-1,3-benzene disulfonic acid and 1 mM dithiothreitol. For GSH determination, cells were homogenized in PEN buffer without reducing agents and were processed immediately as described below. Protein homogenates were stored at -80°C until use. Protein concentration was assessed with the Bio-Rad DC™ protein assay (Bio-Rad Laboratories; Hercules, CA) using bovine serum albumin as standard.

Determination of GSH and lipid-peroxidation products

GSH levels were determined using by enzymatic recycling method (Shaik and Mehvar, 2006). Lipid peroxidation in the cell homogenates was estimated as the

amount of thiobarbituric acid reactive substances (TBARS) (Ohkawa et al., 1979).

Proteasome activity

The chymotrypsin-like activity of the 20S proteasome was determined in the cell homogenates using a fluorescence assay (Rogers and Dean, 2003). Briefly, 50µg protein was incubated for 2h at 25ºC with 50 µM of the 7-aminomethyl-4-coumarin (AMC)-labeled peptide Suc-Leu-Leu-Val-Tyr-AMC (Enzo) in the absence or presence of 10µM β-*clasto*-lactacystin-lactone (Enzo). The proteasome activity was calculated as the difference in fluorescence intensity at 460 nm between the samples without and with inhibitor using excitation wavelength of 380nm.

Calpain activity

Calpain activity was also determined with a fluorescence assay using the substrate Suc-Leu-Leu-Val-Tyr-AMC. In this case, incubation was carried out in 25mM Hepes buffer pH 7.5 containing 100mM KCl and 10mM $CaCl_2$, in the absence or presence of 10 µg calpeptin (Hassem et al., 2006).

Western blot and oxyblot

Proteins (5 µg) were separated by sodium dodecyl sulfate–polyacrylamide gel electrophoresis on 10% gels and blotted to polyvinylidene difluoride membranes. Blots then were incubated overnight at 4°C with monoclonal (mAb) or polyclonal antibodies (Ab) against spectrin (mAb, 1:2,000; Sigma), GAP-43 (Ab, 1:2,000, a

gift from Dr. Perrone-Bizzozero), γ-enolase (Ab, 1:2000; Sigma), active caspase-3 (mAb, 1:1,000; Cell Signaling, Danvers, MA), 20S proteasome α-subunit (mAb, 1:2,000; Enzo), 4-hydroxynonenal (4-HNE) (Ab, 1:1,000; Abcam, Cambridge, MA), malondialdehyde (MDA) (Ab, 1:1,000; Abcam) and acrolein (ACR) (Ab, 1:1,000; Abcam). Membranes were rinsed three times in phosphate-buffered saline (PBS) containing 0.05% Tween-20, and then incubated for 2h with the appropriate horseradish peroxidase (HRP)-conjugated secondary antibody. Blots were developed by enhanced chemiluminescence using the Western Lightning ECL™ kit from Perkin-Elmer (Boston, MA).

Protein carbonyl groups were measured by oxyblot analysis as described earlier (Smerjac and Bizzozero, 2008). In brief, proteins (5µg) were incubated with 2,4-dinitrophenylhydrazine (DNPH) to form the 2,4-dinitrophenyl (DNP) hydrazone derivatives. Proteins were separated by electrophoresis and blotted to membranes as above. DNP-containing proteins were detected using rabbit anti-DNP antiserum (1:500) and HRP-conjugated goat anti-rabbit IgG antibody (1:2,000). Developed films were scanned in a Hewlett Packard Scanjet 4890 and the images were quantified using the NIH Image 1.63 imaging analysis program. The intensity of each lane on the film was normalized by the amount of coomassie blue staining in the corresponding lane.

Immunohistochemistry

Cells, cultured on 12 mm round poly-lysine coated coverslips (BD BioCoat™) were fixed with 4% paraformaldehyde for 20 min. For carbonyl staining, fixed

cells were incubated for 15 min with 1 mg/ml DNPH prepared in 1N HCl to convert carbonyl groups into DNP-hydrazones. Cells were rinsed with PBS, blocked with 10% (v/v) normal goat serum and incubated overnight with rabbit anti-DNP antibody (1:1000; Sigma). After removing the primary antibody with 0.1% triton-X-100 in PBS, slides were incubated for 3h with Alexa Fluor® 647 goat anti-rabbit antibody (1:100, Molecular Probes, Eugene, OR). Cells were rinsed twice with 0.1% Triton X-100 in PBS. For double immunofluorescence staining using Click-iT® TUNEL Assay kit (Invitrogen), DNPH-treated specimens were incubated with terminal deoxynucleotidyl transferase and dNTPs conjugated to Alexa Fluor®488 azide, rinsed twice with 0.1% Triton X-100 in PBS, once with PBS, and then mounted using DPX. Images were captured with a Zeiss 200m microscope (Carl Zeiss MicroImaging Inc., Thornwood, NY) equipped with a Hamamatsu C4742-95 digital camera (Hamamatsu Corp., Bridgewater, NJ). **Please note that images obtained using paraformaldehyde and methacarn fixatives were similar** (Supplemental Fig. 1). **Incubation with HCl did not affect the TUNEL staining** (Supplemental Fig. 2)**. Damaged-nuclei reacted with DNPH, therefore we titrated the DNPH intensity of the cytoplasm for our study** (Supplemental Fig. 3)**.** Necrotic cells were identified on the basis of morphological features such as swollen cell bodies with many holes while apoptotic cells were identified by DNA fragmentation.

For NFH staining, fixed cells were incubated overnight with mouse anti-NFH antibody (mAb, 1:250; Sigma) followed by a 3h-incubation with Alexa Fluor® 488 rabbit anti-mouse antibody (Ab, 1:100; Molecular Probes).

Cell viability assays

For trypan blue exclusion assay, floating and adherent cells were diluted in PBS, stained with 0.4% trypan blue for 5 min, and counted in a Nebauer hemocytometer (Altman et al., 1993). Cell death was also determined by measuring lactate dehydrogenase (LDH) activity on a 10µl-aliquot from the cell supernatant using the LDH-cytotoxicity assay kit II (ABCAM, Cambridge, MA).

Protein aggregation assay

Cell homogenates prepared in PEN buffer containing 1mM dithiothreitol and 150mM NaCl were centrifuged at 20,000x*g* for 30 min at 4°C. The pellets were then extracted with the same buffer containing 1% triton X-100. Samples were kept on ice for 15 min and were centrifuged at 20,000x*g* for 30 min at 4°C. The final pellet, which contains some cytoskeleton structures but mostly aggregated proteins, was re-suspended in PEN buffer for protein determination.

Statistical analysis

Results were analyzed for statistical significance with student *t*-test using GraphPad Prism® program (GraphPad Software incorporation, San Diego, CA).

3.4 RESULTS

Low doses of DEM causes partial and transient GSH depletion in neuronal cells

PC12 cells were differentiated into a neuronal phenotype by incubation with NGF for 24h. These cells, which we termed neuron-like PC12 or nPC12, developed neurites that stained positive for neurofilament heavy chain (NFH) (Fig. 1a) and expressed the neuron-specific markers α-spectrin, GAP-43 and γ-enolase (Fig. 1b). Reduction of intracellular GSH levels was attained with DEM. This membrane-permeable electrophilic agent depletes intracellular GSH by directly conjugating with GSH through glutathione-S-transferase (Buchmüller-Rouiller et al., 1995), leading to mitochondrial production of reactive oxygen species (ROS) and oxidative stress (Bizzozero et al., 2006). As shown in Fig. 2a, DEM dose-dependently reduced the concentration of GSH in nPC12 cells. For this study, we chose a concentration of 50μM DEM to achieve a reduction in GSH levels similar to that observed in the spinal cord of EAE mice (Dasgupta and Bizzozero, 2011). At 50μM DEM, GSH levels decreased progressively, reaching the lowest values between 3h and 12h of incubation. By 24h, the concentration of GSH was back to normal (Fig. 2b). Since the thioether linkage between GSH and DEM is metabolically stable, the recovery of GSH levels at longer incubation times is likely due to *de novo* synthesis of the tripeptide. Similar results were obtained in more differentiated cells such as PC12 cells treated with NGF for 7 days (Fig. 2c) and primary cortical neurons (Fig. 2d).

Protein carbonylation and GSH depletion are correlated in DEM-treated nPC12 cells

Lipid peroxidation and protein oxidation were evaluated by measuring TBARS and PCO levels, respectively. As shown in Fig 3a, TBARS levels do not change

during the incubation of nPC12 cells with 50μM DEM, although the mean values were higher at the peak of oxidative stress (3-12h). In contrast, the amount of protein carbonyls increased progressively from 2h to 12h and then diminished significantly by 24h of incubation (Fig. 3b). Again, similar results were obtained in PC12 cells treated with NGF for 7 days and in primary cortical neurons (data not shown).

Protein carbonyls are not eliminated by enzymatic reduction to the corresponding alcohols (Bizzozero, 2009). Instead, they are removed by degradation via the chymotrypsin-like activity of 20S proteasome (Ferrington et al., 2005). We found that this activity, measured with a fluorogenic peptide substrate, increases 3-4-fold at 3h-12h of incubation to decline thereafter (Fig. 3c). Interestingly, the amount of 20S proteasome, as determined by the levels of the constitutive α-subunits, followed the same temporal pattern as that of proteasome activity (Fig 3c, inset). This suggests that oxidative stress causes up-regulation in proteasome expression most likely to remove the potentially toxic misfolded and oxidized proteins that build up in cells.

DEM-treatment leads to apoptosis and necrosis of nPC12 cells

We next investigated if partial GSH depletion is toxic to nPC12 cells. As shown in Fig. 4, the viability of DEM-treated nPC12 cells, as determined by the trypan blue exclusion test (panel a) and the LDH cytotoxicity assay (panel b), gradually decreases up to 12 h of incubation and by 24h the proportion of dead cells

decreases significantly. Similar temporal patterns of cell death were obtained for detached and adherent cell populations (data not shown), suggesting that dying cells do not automatically detach from the poly-lysine coated plates. Increased calpain activity, a marker of both apoptosis and necrosis (Guyton et al., 2005), was observed between 3-12 h to decline thereafter (Fig. 4c). The increase in calpain activity is also evident from the reduction in the amount of NFH, one of its proteolytic targets, (Fig. 4d) and from the retraction of neurites (not shown). Active caspase-3 expression, a marker of apoptosis (Namura et al., 1998), was measured by western blotting using an antibody that detects the p17 subunit of this enzyme but not the full-length 32kDa procaspase-3. As shown in Fig. 4e, active caspase-3 levels follow an identical temporal pattern as that of the other two cell-death markers, suggesting that apoptosis accounts for at least a fraction of the dead cells. Indeed, morphological analysis revealed that approximately half of the dead cells contain the extensive nuclear fragmentation typical of apoptotic cells (Fig. 4f). There is, however, an equal amount of cells with swollen cytoplasm and intracellular vacuoles that are characteristic of necrosis.

Temporal/spatial correlation between protein carbonylation and apoptosis in GSH depleted nPC12 cells

Since protein carbonylation and cell death shows a similar temporal pattern, we sought to investigate if there is a spatial relationship between these two parameters as well. To this end, DEM-treated cells were double stained with DNPH for protein carbonyls and TUNEL or annexin-V for apoptosis. Consistent with the results from oxyblot analysis (Fig. 3), the average DNP staining intensity

per cell reaches a maximum between 3 h and 12 h after addition of DEM to decline thereafter (Fig. 5a,b). As shown in Fig. 5c, apoptotic (TUNEL positive) cells stained intensely with DNPH. Since DNPH also stained the nuclei, likely due to its reactivity towards DNA oligonucleotides (Luo and Wehr, 2009), we quantified the fluorescence in the cytoplasm. As depicted in panel d, the fluorescence intensity in the cytoplasm of apoptotic cells was ~ 2 times higher than that of non-apoptotic cells (Fig. 5d). While there is a significant variation in DNP staining among the cells, it is clear that the proportion of cells with the highest cytoplasmic carbonyl content is elevated between 3h and 12h (Fig. 5e). The temporal/spatial positive relationship between apoptosis and protein oxidation was further demonstrated by extensive co-localization annexin-V, a late marker of apoptosis, and DNP immunoreactivity (Fig. 6).

Impaired removal of PCOs increases DEM-induced cell death

To determine if accumulation of oxidized/misfolded proteins plays a role in cell death, we incubated DEM-treated cells with the proteasome inhibitors epoxomicin and lactacystin. At a concentration of 1μM, these drugs were found to reduce the chymotrypsin-like activity of the 20S proteasome by 90.6 ± 13.7% (lactacystin) and 98.9 ± 7.2% (epoxomicin). Proteasome inhibitors were added to nPC12 cells 12h after addition of DEM and incubation continued until 24 h. As depicted in Fig. 7a, cells incubated with the inhibitors have significantly higher levels of protein carbonyls, indicating that in this system proteasomes are largely responsible for the degradation of most oxidized proteins. Levels of GSH in the epoxomicin- and lactacystin-treated cells at 24h of incubation are similar to that

in untreated cells (Fig. 7b). Under these conditions we found a large increase in cell death as measured by LDH release (Fig. 7c) and trypan blue exclusion assay (Fig. 7d). A correlation between protein carbonylation and cell death was also observed by α-DNP/TUNEL double staining of proteasome inhibited DEM-treated cells (Fig. 7e). These results further support our hypothesis of a strong relationship between protein damage and neuronal apoptosis. It is noteworthy that, in the absence of DEM, epoxomicin and lactacystin do not cause cell death, suggesting that toxicity of the drug is probably due to its ability to inhibit the removal of oxidized proteins.

Carbonyl scavengers reduce cell death and protein aggregation in epoxomicin-treated GSH-depleted cells

The role of protein carbonylation in cell death was further explored using the classical reactive carbonyl species (RCS) scavengers hydralazine, z-histidine hydrazide and methoxylamine. These compounds form Schiff bases with the carbonyl groups and, with the exception of hydralazine, they have no antioxidant properties (Zheng and Bizzozero, 2010a). In this series of experiments the RCS scavengers were added together with epoxomicin to cells that had been treated with DEM for 12h and incubation continued for another 12h. As shown in Fig. 8, all three drugs reduced protein carbonylation, protein aggregation and cell death, indicating that (1) protein carbonyls are indeed cytotoxic and (2) protein aggregation is induced, directly or indirectly, by carbonylation. Preliminary western blot studies revealed that MDA-, ACR- and 4-HNE-protein adducts are not formed to any appreciable degree during incubation with DEM, suggesting

that carbonylation takes place by direct oxidation of amino acid side chain residues rather than by attachment of reactive carbonyl species to the protein backbone (data not shown). The effectiveness of the vitamin E analogue trolox at preventing protein carbonylation and cell dead even when added 12h after DEM suggests that there is still significant oxidative stress during the recovery phase (Fig. 8).

Differential effects of cyclosporin A and zVAD-fmk on cell death and protein carbonylation.

Finally, attempts were made to localize the site of protein oxidation within the apoptotic pathway. To this end, nPC12 cells were incubated with DEM and either the MPTP inhibitor cyclosporin A or the pan-capase inhibitor zVAD-fmk. As shown in Fig. 9, addition of 5μM cyclosporin A prevented all three cell death, protein carbonylation and protein aggregation induced by GSH depletion. In contrast, pan-caspase inhibition reduced cell death but has no effect on protein carbonylation or aggregation (Fig.10). These findings suggest that protein oxidation/aggregation occurs after MPTP opening but before caspase activation.

3.5 DISCUSSION

In this study we show that a moderate and transient depletion of GSH in nPC12 cells leads to increased accumulation of protein carbonyls and cell death. Both the amount of PCOs and the proportion of dead cells diminish as GSH is biosynthetically replenished. However, cell death persists if oxidized proteins are not removed by the proteasome. These results suggest that the build-up of

oxidized and/or misfolded proteins is responsible for the loss of cell viability in this system. Furthermore, the effectiveness of several RCS scavengers at preventing cell death suggests that protein carbonyls are indeed the toxic species. Experiments using cyclosporin A and zVAD-fmk place protein carbonylation downstream of the MPTP opening and upstream of caspase activation. While the study focused on nPC12 cells, experiments using more differentiated PC12 cells and primary neuronal cultures yielded the same results, indicating that the above findings are not circumscribed to partially differentiated dopaminergic neurons. A schematic model summarizing our experimental findings is shown in Fig. 11.

DEM is commonly used to deplete both cytoplasmic and mitochondrial GSH and to cause oxidative stress and cell death (Freeman and Meredith, 1988). At millimolar concentrations, DEM is highly toxic and causes cell death mostly by necrosis (Nagai et al., 2002). Our study employed a much lower concentration (i.e. 50μM) of DEM to achieve the partial GSH depletion detected in the spinal cord of EAE mice, where there is significant neuronal apoptosis (Dasgupta and Bizzozero, 2011). Under these conditions, ~50% of the dead cells measured after 12 h of incubation with DEM displayed morphological features that are characteristic of apoptosis with the rest being necrotic cells. A switch from apoptosis to necrosis in models with severe oxidative stress has been attributed to reduction in ATP levels below a threshold level that is insufficient to support apoptosis, an energy-depended process (Eguchi et al., 1997). The mechanism linking GSH depletion and increased production of ROS by mitochondria has

been studied extensively (Armstrong and Jones, 2002; Shen et al., 2005). It is generally accepted that a decline in the GSH/GSSG ratio leads to the opening of the MPTP by oxidation of a critical dithiol in the voltage-sensing region of this protein complex (Petronilli et al., 1994). When GSH falls below a certain level, permeability transition occurs followed by a collapse in mitochondrial membrane potential. This event causes enhanced production of superoxide either from the rise in redox cycling of ubiquinone within complex III (Chen et al., 2003) or from the reverse electron transport from succinate to NADH within complex I (Lambert and Brand, 2004). Loss of cytochrome c from mitochondria, after permeability transition and swelling, can also augment the production of oxygen free radicals by reducing the redox centers upstream of complex IV (Votyakova and Reynolds, 2005). Our data are in agreement with this model since MPTP inhibition with cyclosporin A reduces protein oxidation and cell death (both apoptosis and necrosis). They also indicate that carbonylation occurs after MPTP opening and as the result of the ensuing high degree of oxidative stress. It should be emphasized that our findings are not restricted to DEM-induced cell death as a similar relationship between carbonylation and apoptosis was established in staurosporine- and BSO-treated nPC12 cells (Supplemental Fig.4 and Fig. 5). It is also interesting that by 24h of incubation, the surviving cells are able to replenish the GSH pool completely. Recovery of GSH levels has also been observed in the brain of rats treated with DEM (Gupta et al., 2000) and in cultured astrocytes incubated with the DEM-analogue dimethyl fumarate (Lin et al., 2011), and it is generally ascribed to an antioxidant response that increases

the amount of γ-glutamylcysteine synthetase, the rate-limiting enzyme of GSH biosynthesis (Lewerenz and Maher, 2011).

The incorporation of aldehyde and ketone functional groups into proteins takes place by direct and indirect mechanisms (Bizzozero, 2009). Direct protein carbonylation involves the metal ion-catalyzed oxidation of Thr, Lys, Arg, and Pro to α-amino-β-ketobutyric acid, α-aminoadipic semialdehyde and glutamic semialdehyde, respectively. In contrast, indirect carbonylation entails the reaction of the nucleophilic centers in Cys, His or Lys residues with RCS, bifunctional carbonyl-containing molecules derived from the oxidation of lipids (e.g. 4-HNE, MDA, ACR) and carbohydrates (e.g. glyoxal, methylglyoxal) (Bizzozero, 2009). Our finding that the RCS scavengers hydralazine, methoxylamine, histidine hydrazide prevented the formation of protein carbonyls initially suggested that carbonylation is occurring by an indirect mechanism. However, we were unable to detect RCS-protein adducts, implying that direct oxidation of amino acids residues is the most likely process and that the scavengers are able to form stable adducts with oxidized proteins. It is noteworthy that direct carbonylation appears to be also the major mechanism underlying the formation of carbonyls in the CNS of EAE mice (Zheng and Bizzozero, 2010b).

Carbonylated proteins in mitochondria and cytoplasm are digested by the Lon protease (Bota and Davies, 2002) and the 20S proteasome (Grune et al., 1997), respectively. While lactacystin is capable of inhibiting both of these proteolytic systems, epoxomicin is highly specific for the proteasome (Kisselev and Goldberg, 2001). Thus, our findings suggest that cytoplasmic oxidized proteins

are likely responsible for damage of nPC12 cells during GSH depletion. The 20S proteasome by itself plays a critical protective role during oxidative stress by digesting oxidized proteins via its chymotrypsin-like activity and without requirement for ubiquitin or energy (Shringarpure et al., 2003). We have observed a rapid and large rise in proteasome expression and activity upon GSH depletion. This is in agreement with a recent study showing increased expression of 20S proteasome, immunoproteasome and the P28α/β regulatory particle upon incubation of murine embryonic fibroblasts with hydrogen peroxide, which was interpreted as an oxidative stress adaptation mechanism designed to reduce the load of oxidized protein in the cell (Pickering et al., 2010). In our system, however, the elevation in proteasomal chymotrysin-like activity was not sufficient to prevent the accumulation of PCOs that occurs during first 12h of incubation with DEM, and addition of epoxomixin or lactacystin results in a further build-up of oxidized proteins. Interestingly, incubation of nPC12 cells with epoxomicin or lactacystin alone (i.e. in the absence of DEM) does not lead to any appreciable increase in protein carbonylation, protein aggregation or cell death, indicating that basal protein oxidation in these neuron-like cells is quite low. In liver cells, however, proteasome inhibition causes increased carbonyl formation and protein aggregation, even in the absence of an obvious oxidative challenge (Demasi and Davies, 2003). This discrepancy could be attributed to differences in the cell type, the turnover rate of damaged proteins and the incubation conditions.

It has been shown that carbonylation causes inappropriate inter- and intra-protein cross-links as well as protein misfolding, which in turn results in the formation of

high-molecular-weight aggregates (Grune et al., 1997; Mirzaei and Regnier, 2008). As these aggregates get larger they precipitate, become resistant to proteolytic degradation and reduce cell viability (Nyström, 2005; Maisonneuve et al., 2008). The precise relationship between protein aggregate formation and apoptosis, or whether the aggregates are in and of themselves cytotoxic is unclear. However, it has been recently discovered that protein aggregates, as they form, sequester multiple preexistent and newly synthesized proteins that have essential cellular functions and are critical for cell survival (Olzscha et al., 2011). Our results show that various carbonylation scavengers are able to prevent protein aggregation and cell death, suggesting that during GSH depletion oxidized proteins are critical for aggregate formation and cytotoxicity. In our system, protein aggregates clearly are not made of carbonylated proteins alone since the cellular amount of carbonylated proteins is roughly 1-2% of that of the aggregates. However, protein carbonylation may expose hydrophobic surfaces that can mediate aberrant interactions with other (non-oxidized) proteins, resulting in their functional impairment and sequestration. Future studies will test whether agents capable of preventing protein aggregation can also reduce cell death even in the presence of abundant protein oxidation.

Carbonylation of specific proteins has been found to be toxic as well. For instance, the occurrence of carbonyls in GAPDH, ANT and Bcl-2 has been shown to play a role in nitric oxide-induced apoptosis in insulin-producing RINm5F cells (Cahuana et al., 2004). Carbonyl modification of several chaperones, including glucose-regulated protein-78, heat-shock protein-60, heat-

shock protein cognate-71, phosphate disulphide isomerase and calreticulin, has been linked to apoptosis of irradiated HL60 human leukemia cells (Magi et al., 2004). Furthermore, apoptosis of etopside-treated HL60 cells is caused by reduced rate of glycolysis, which likely results from the extensive carbonylation of several glycolytic enzymes including aldolase, enolase, triose phosphate isomerase and phosphoglycerate mutase (England et al., 2004). Characterization of the carbonyl proteome of PC12 cells will determine if similar metabolic pathways or cellular processes are affected during GSH depletion.

In sum, the present study identifies protein oxidation as an important step in neuronal cell death triggered by GSH depletion. While it is clear that other cytotoxic mechanisms may be at play in EAE, it is tempting to speculate that the reduced levels of GSH and the accumulation of protein carbonyls observed in this disease (Dasgupta and Bizzozero, 2011) play a significant pathophysiological role.

3.6 ACKNOWLEDGEMENTS

The authors wish to thank Mr. Clark Bird (Dept. of Neurosciences, UNM) for his help with the primary neuronal cultures and Dr. Robert Rubin (Dept. of Molecular Genetics and Microbiology, UNM) for the use of his plate centrifuge.

3.7 FUNDING

This work was supported by PHHS grant NS057755 from the National Institutes of Health.

3.8 REFERENCES

Altman SA, Randers L, Rao G (1993) Comparison of trypan blue dye exclusion and fluorometric assays for mammalian cell viability determinations. Biotechnol Prog 9:671-674.

Armstrong JS, Jones DP (2002) Glutathione depletion enforces the mitochondrial permeability transition and causes cell death in Bcl-2-overexpressing HL60 cells. FASEB J 16:1263-1265.

Aksenov MY, Aksenova MV, Butterfield DA, Geddes JW, Markesbery WR (2001) Protein oxidation in the brain in Alzheimer's disease. Neuroscience 103:373-383.

Bizzozero OA (2009) Protein carbonylation in neurodegenerative and demyelinating CNS diseases. In “Handbook of Neurochemistry and Molecular Neurobiology” (Lajtha A, Banik N, Ray S, eds) Springer, New York, NY. pp. 543-562.

Bizzozero OA, Dejesus G, Callahan K, Pastuszyn A (2005) Elevated protein carbonylation in the brain white matter and gray matter of patients with multiple sclerosis. J Neurosci Res 81:687-695.

Bizzozero OA, Ziegler JL, De Jesus G, Bolognani F (2006) Acute depletion of reduced glutathione causes extensive carbonylation of rat brain proteins. J Neurosci Res 83:656-667.

Bota DA, Davies KJ (2002) Lon protease preferentially degrades oxidized mitochondrial aconitase by an ATP-stimulated mechanism. Nat Cell Biol 4:674-680.

Buchmuller-Rouiller Y, Corrandin SB, Smith J, Schneider P, Ransijn A, Jongeneel CV, Mauel J (1995) Role of glutathione in macrophage activation: effect of cellular glutathione depletion on nitrite production and leishmanicidal activity. Cell Immunol 164:73-80.

Cahuana GM, Tejedo JR, Jiménez J, Ramírez R, Sobrino F, Bedoya FJ (2004) Nitric oxide-induced carbonylation of Bcl-2, GAPDH and ANT precedes apoptotic events in insulin-secreting RINm5F cells. Exp Cell Res 293:22-30.

Chen Q, Vazquez EJ, Moghaddas S, Hoppel CL, Lesnefsky EJ (2003) Production of reactive oxygen species by mitochondria: central role of complex III. J Biol Chem 278:36027-36031.

Dalle-Donne I, Rossi R, Giustarini D, Gagliano N, Lusini L, Milzani A, Di Simplicio P, Colombo R. (2001) Actin carbonylation: from a simple marker of protein oxidation to relevant signs of severe functional impairment. Free Radic Biol Med 31:1075–1083.

Dasgupta A, Bizzozero OA (2011) Positive correlation between protein carbonylation and apoptosis in EAE. Trans Am Soc Neurochem 42:PSM08-01.

Davies MJ (2005) The oxidative environment and protein damage. Biochim Biophys Acta 1703:93-109.

Demasi M, Davies KJ (2003) Proteasome inhibitors induce intracellular protein aggregation and cell death by an oxygen-dependent mechanism. FEBS Lett 542:89-94.

Divald A, Powell SR (2006) Proteasome mediates removal of proteins oxidized during myocardial ischemia. Free Radic Biol Med 40:156-164.

Eguchi Y, Shimizu S, Tsujimoto Y (1997) Intracellular ATP levels determine cell death fate by apoptosis or necrosis. Cancer Res 57:1835-1840.

England K, O'Driscoll C, Cotter TG (2004) Carbonylation of glycolytic proteins is a key response to drug-induced oxidative stress and apoptosis. Cell Death and Differentiation 11:252–260.

Ferrante RJ, Browne SE, Shinobu LA, Bowling AC, Baik MJ, MacGarvey U, Kowall NW, Brown RH, Beal MF (1997) Evidence of increased oxidative damage in both sporadic and familial amyotrophic lateral sclerosis. J Neurochem 69:2064-2074.

Ferrington DA, Husom AD, Thompson LV (2005) Altered proteasome structure, function and oxidation in aged muscle. FASEB J 19:644-646.

Floor E, Wetzel MG (1998) Increased protein oxidation in human sustantia nigra pars compacta in comparison with basal ganglia and prefrontal cortex measured with an improved dinitrophenylhydrazine assay. J Neurochem 70:268-275.

Freeman ML, Meredith MJ (1988) Subcellular localization of glutathione and thermal sensitivity. Radiat Res 115:461-471.

Fucci L, Oliver CN, Coon MJ, Stadtman ER (1983) Inactivation of key metabolic enzymes by mixed-function oxidation reactions: possible implication in protein turnover and ageing. Proc Nat Acad Sci 80:1521-1525.

Grune T, Reinheckel T, Davies KJ (1997) Degradation of oxidized proteins in mammalian cells. FASEB J 11:526- 534.

Gupta A, Datta M, Shukla GS (2000) Cerebral antioxidant status and free radical generation following glutathione depletion and subsequent recovery. Mol Cell Biochem 209:55-61.

Guyton MK, Wingrave JM, Yallapragada AV, Wilford GG, Sribnick EA, Matzelle DD, Tyor WR, Ray SK, Banik NL (2005) Upregulation of calpain correlates with increased neurodegeneration in acute experimental autoimmune encephalomyelitis. J Neurosci Res 81:53–61

Harms KM, Li L, Cunningham LA (2010) Murine neural stem/progenitor cells protect neurons against ischemia by HIF-1a–Regulated VEGF signaling. PLoS ONE 5:e9767.

Hassen GW, Feliberti J, Kesner L, Stracher A, Mokhtarian F (2006) A novel calpain inhibitor for the treatment of acute experimental autoimmune encephalomyelitis. J Neuroimmunol 180:135-146.

Jomova K, Vondrakova D, Lawson M, Valko M (2010) Metals, oxidative stress and neurodegenerative disorders. Mol Cell Biochem 345:91-104.

Kisselev AF, Goldberg AL (2001) Proteasome inhibitors: from research tools to drug candidates. Chem Biol 8:739-758.

Lambert AJ, Brand MD (2004) Superoxide production by NADH:ubiquinone oxidoreductase (complex I) depends on the pH gradient across the mitochondrial inner membrane. Biochem J. 382:511-517.

Lewerenz J, Maher P (2011) Control of redox state and redox signaling by neural antioxidant systems. Antiox Redox Signal 14:1449-1465.

Lin S, Lisi L, Russo CD, Polak PE, Sharp A, Weinberg G, Kalinin S, Feinstein DL (2011) The anti-inflammatory effects of dimethyl fumarate in astrocytes involve glutathione and haem oxygenase-1. ASN NEURO 3(2):art:e00055.doi:10.1042/AN 20100033.

Luo S, Wehr NN (2009) Protein carbonylation: avoiding pitfalls in the 2,4-dinitrophenylhydrazine assay. Redox Rep 14:159-166.

Magi B, Ettorre A, Liberatori S, Bini L, Andreassi M, Frosali S, Neri P, Pallini V (2004) Selectivity of protein carbonylation in the apoptotic response to oxidative stress associated with photodynamic therapy: a cell biochemical and proteomic investigation. Cell Death Differ 11:842-852.

Maisonneuve E, Ezraty B, Dukan S (2008) Protein aggregates: an aging factor involved in cell death. J Bacteriol 190: 6070-6075.

Mirzaei H, Regnier F (2008) Protein:protein aggregation induced by protein oxidation. J Chromatogr 873:8-14.

Nagai H, Matsumaru K, Feng G, Kaplowitz N (2002) Sensitization to tumor necrosis factor-α-induced apoptosis in cultured mouse hepatocytes. Hepatology 36:55-64.

Namura S, Zhu J, Fink K, Endres M, Srinivasan A, Tomaselli K, Yuan J, Moskowitz MA (1998) Activation and cleavage of caspase-3 in apoptosis induced by experimental cerebral ischemia. J Neurosci 18:3659-3668.

Nyström T (2005) Role of oxidative carbonylation in protein quality control and senescence. EMBO J 24:1311-1317.

Ohkawa H, Ohishi N, Yagi K (1979) Assay for lipid peroxides in animal tissues by thiobarbituric acid reaction. Anal Biochem 95:351 – 358.

Olzscha H, Schermann SM, Woerner AC, Pinket S, Hecht MH, Tartaglia GG, Vendruscolo M, Hayer-Hartl M, Hartl FU, Vabulas RM (2011) Amyloid-like aggregates sequester numerous metastable proteins with essential cellular functions. Cell 144:67–78.

Petronilli V, Costantini P, Scorrano L, Colonna R, Passamonti S, Bernardi P (1994) The voltage sensor of the mitochondrial permeability transition pore is tuned by the oxidation-reduction state of vicinal thiols. Increase of the gating potential by oxidants and its reversal by reducing agents. J Biol Chem 269:16638-16642.

Pickering AM, Koop AL, Teoh CY, Ermak G, Grune T, Davies KJ (2010) The immunoproteasome, the 20S proteasome and the PA28αβ proteasome regulator are oxidative-stress-adaptive proteolytic complexes. Biochem J 432:585-594.

Reynolds A, Laurie C, Mosley RL, Gendelman HE (2007) Oxidative stress and the pathogenesis of neurodegenerative disorders. Int Rev Neurobiol 82:297-325.

Rinaudo MT, Piccinini M (2007) Immunoproteasome activity in the nervous system. In “Handbook of Neurochemistry and Molecular Neurobiology: Neuroimmunology. (Lajtha A, Galoya A, Besedorsky H, eds) Springer, New York, NY. Vol 12, pp. 223-235.

Rodgers KJ, Dean RT (2003) Assessment of proteasome activity in cell lysates and tissue homogenates using peptide substrates. Int J Biochem Cell Biol 35:716-727.

Shaik IH, Mehvar R (2006) Rapid determination of reduced and oxidized glutathione levels using a new thiol-masking reagent and the enzymatic recycling method: Application to the rat liver and bile samples. Anal Bioanal Chem 385:105–113

Shen D, Dalton TP, Nebert DW, Shertzer HG (2005) Glutathione redox state regulates mitochondrial reactive oxygen production. J Biol Chem 280:25305-25312.

Shringarpure R, Grune T, Mehlhase J, Davies KJ (2003) Ubiquitin conjugation is not required for the degradation of oxidized proteins by proteasome. J Biol Chem 278:311-318.

Smerjac SM, Bizzozero OA (2008) Cytoskeletal protein carbonylation and degradation in experimental autoimmune encephalomyelitis. J Neurochem 105:763-772.

Starke PE, Oliver CN, Stadtman ER (1987) Modification of hepatic proteins in rats exposed to high oxygen concentration. FASEB J 1:36–39.

Votyakova TV, Reynolds IJ (2005) Ca^{2+}-induced permeabilization promotes free radical release from rat brain mitochondria with partially inhibited complex I. J Neurochem 93:526-537.

Zheng J, Bizzozero OA (2010a) Traditional reactive carbonyl scavengers do not prevent the carbonylation of brain proteins induced by acute glutathione depletion. Free Radic Res 44:258-266.

Zheng J, Bizzozero OA (2010b) Accumulation of protein carbonyls within cerebellar astrocytes in murine experimental autoimmune encephalomyelitis. J Neurosci Res 88:3376-3385.

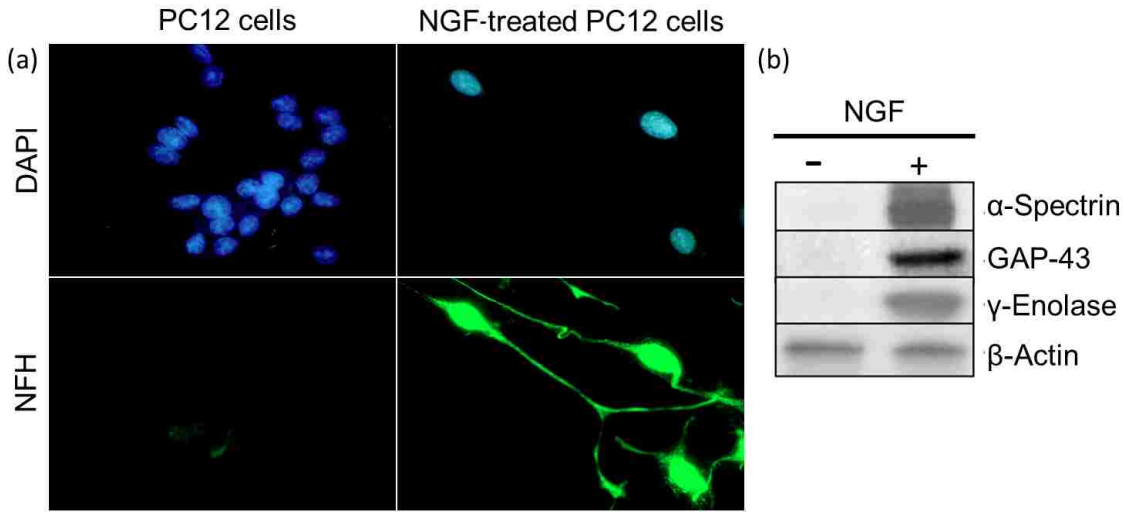

Fig. 1 - PC12 cells are differentiated into neuron-like cells upon treatment with NGF. PC12 cells were incubated in the absence or presence of NGF for 24 h as described in Materials and methods section. (a) Representative immunofluorescence picture of untreated and NGF-treated cells. Nuclear [4′,6-diamidino-2-phenylindole (DAPI)] and NFH staining are shown in blue and green respectively. Note that, 12 h after NGF treatment, cells are no longer round and flat but show NFH-positive processes that are characteristic of neurons. (b) Western blots depicting the expression of the neuron-specific markers α-spectrin, GAP-43 and γ-enolase only in NGF-treated PC12 cells.

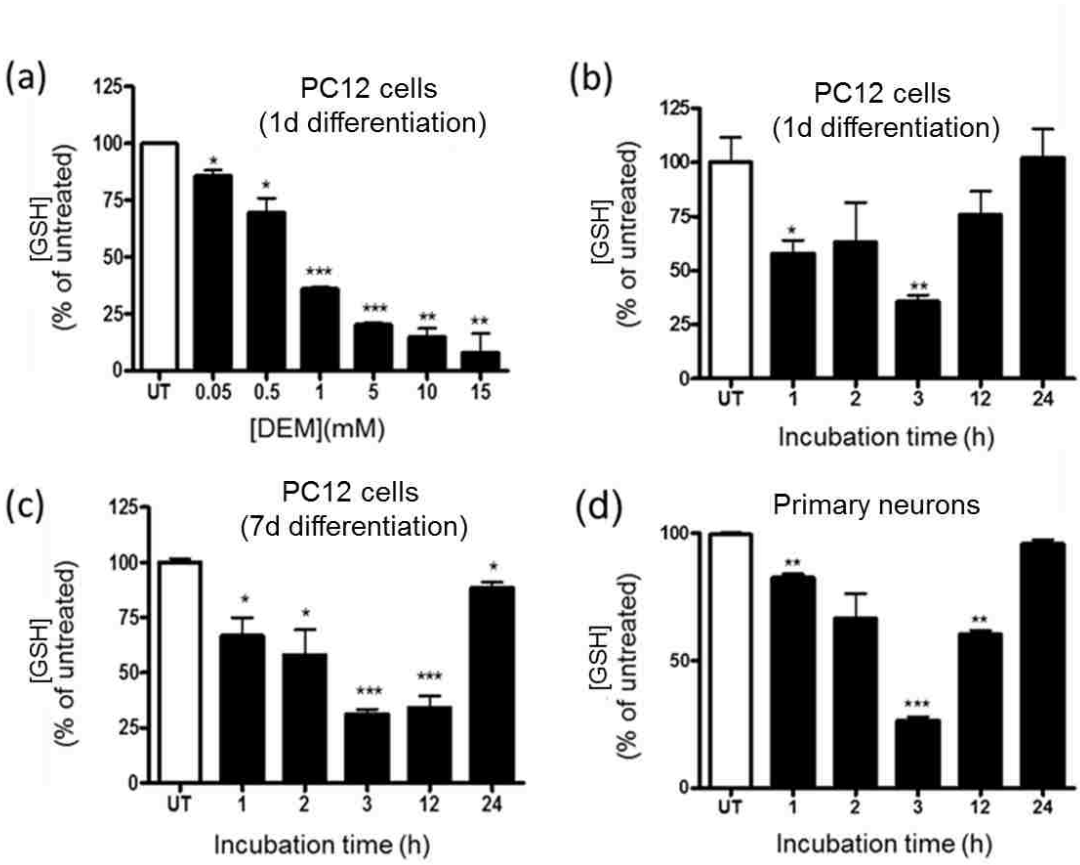

Fig. 2 – DEM induces GSH depletion in nPC12 cells and primary neurons. (a) Effect of various concentrations of DEM on GSH levels in nPC12 cells at 15 min of incubation. (b–d) Time course of GSH depletion after addition of 50 μM DEM to PC12 cells differentiated for 1 or 7 days (d) with NGF and to primary neurons. Values represent the means±S.E.M of 4–9 experiments. Asterisks denote values that are significantly different from those obtained in untreated (UT) cells; *P<0.05, **P<0.01, ***P<0.001.

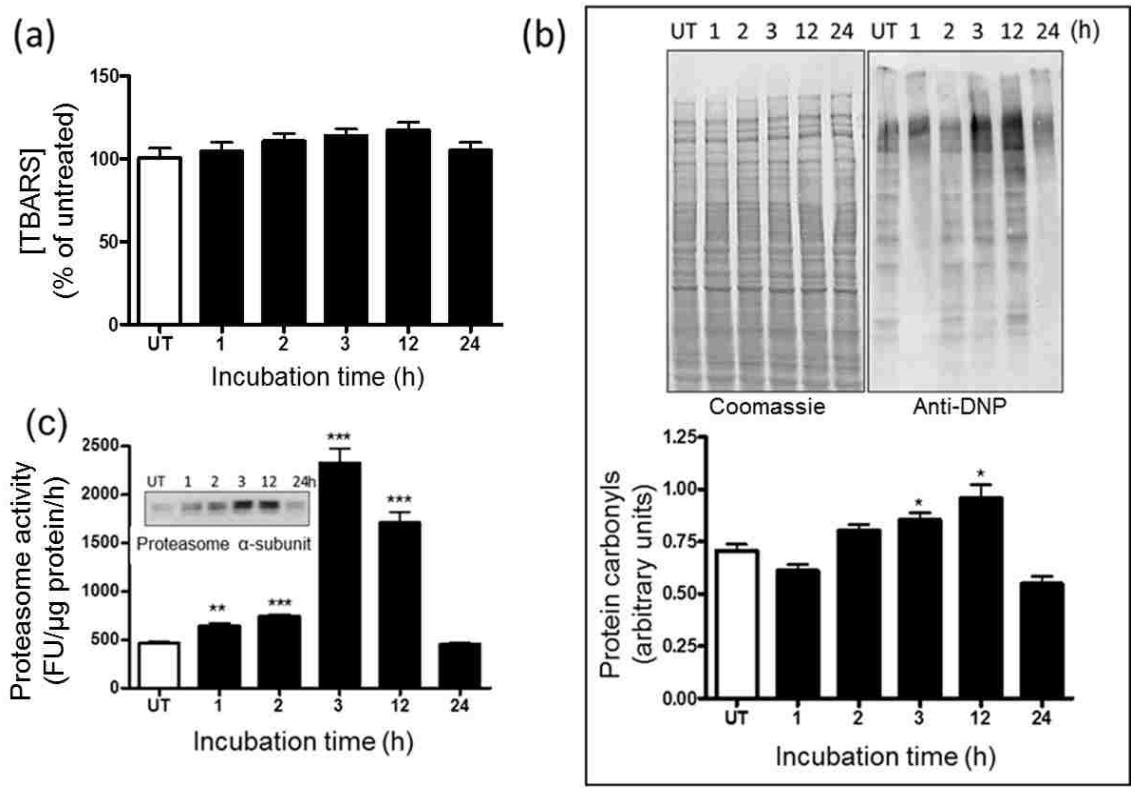

Fig. 3 – Protein carbonylation and proteasome expression in nPC12 cells increase upon GSH depletion. (a) Levels of TBARS during the course of DEM-induced GSH depletion. (b) Representative oxyblot of total cell proteins during the course of DEM-induced GSH depletion (upper panel). Lane intensities were measured by scanning densitometry and were used to calculate protein carbonyl levels as described in Materials and Methods (lower panel). (c) Proteasome chymotrypsin-like activity and proteasome α-subunit expression (inset) in DEM-treated nPC12 cells. Values represent the mean ± SEM of 4 experiments. Asterisks denote values that are significantly different from those obtained in untreated (UT) cells; *p<0.05, **p<0.01, ***p<0.001.

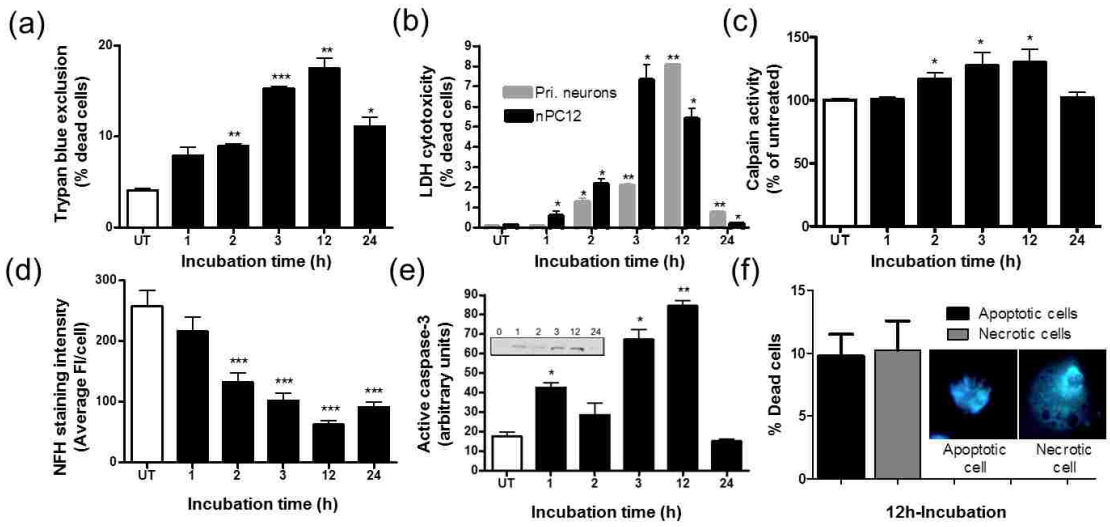

Fig. 4 – Partial GSH depletion leads to apoptosis and necrosis of nPC12 cells. Cells were incubated with 50µM DEM for various periods of time as described under Materials and Methods. (a) Cell death quantified using the trypan blue exclusion assay and (b) LDH release. (c) Temporal pattern of calpain activity, a marker of apoptosis and necrosis. (d) NFH immunostaining intensity. (e) Levels of active caspase-3 were determined by western blot anaysis (inset). (f) Quantification of apoptotic and necrotic cell death after 12h of DEM treatment using morphologic analysis. Values represent the mean ± SEM of 4 experiments. Asterisks denote values that are significantly different from those obtained in untreated (UT) cells; *p<0.05, **p<0.01, ***p<0.001.

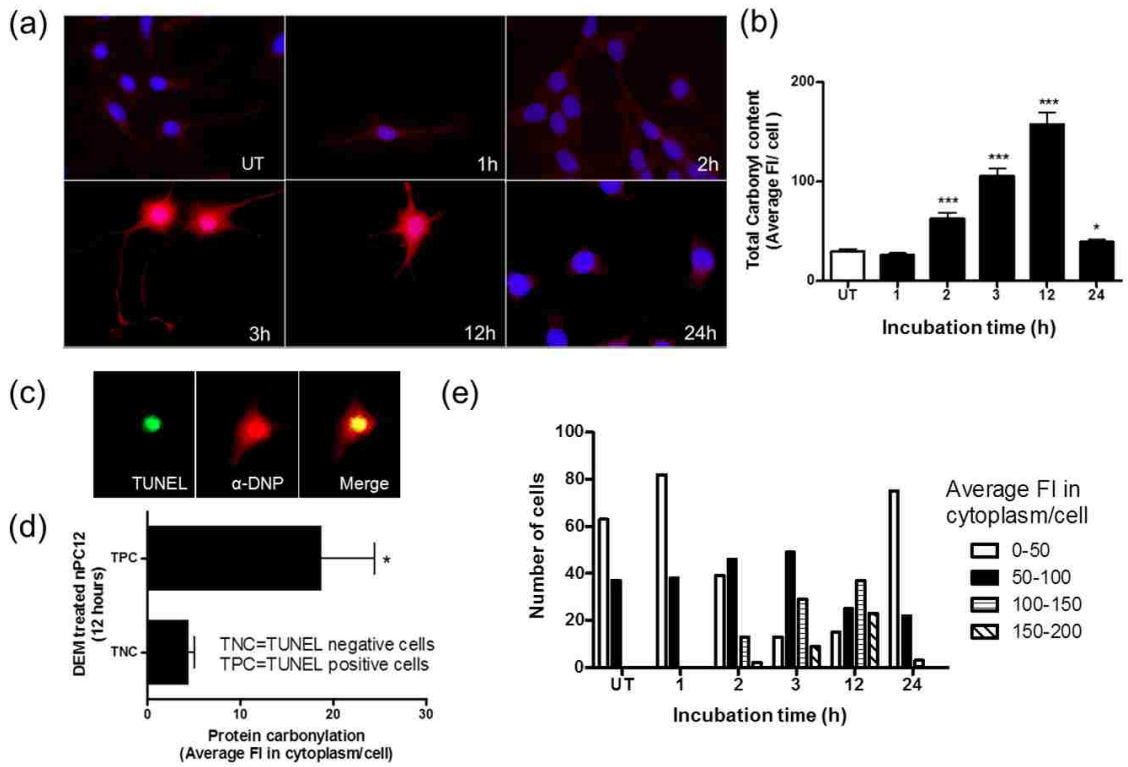

Fig. 5 – Temporal and spatial correlation between carbonylation and apoptosis in DEM-treated nPC12 cells. (a) Immunocytochemical detection of carbonyls in DEM-treated nPC12 cells at different time points. Carbonyls were detected with anti-DNP antibodies after derivatization with DNPH (red). TUNEL staining for apoptosis and 4′,6-diamidino-2-phenylindole (DAPI) staining for nuclei are shown in green and blue respectively. (b) Total carbonyl content of DEM-treated nPC12 cells determined by immunocytochemistry. Asterisks denote values that are significantly different from those obtained in untreated (UT) cells; *P<0.05, ***P<0.001. (c) Anti-DNP staining in the nucleus and cytoplasm of TUNEL positive cells. (d) PCO levels in the cytoplasm of TUNEL positive cells (TPC) and TUNEL negative cells (TNC) at 12 h of treatment with DEM. *P<0.05. (e) Average fluorescence intensity (FI) in the cytoplasm of nPC12 cells increases between 3 and 12 h of incubation with DEM. Values represent the means±S.E.M. of 100–200 cells per experiment.

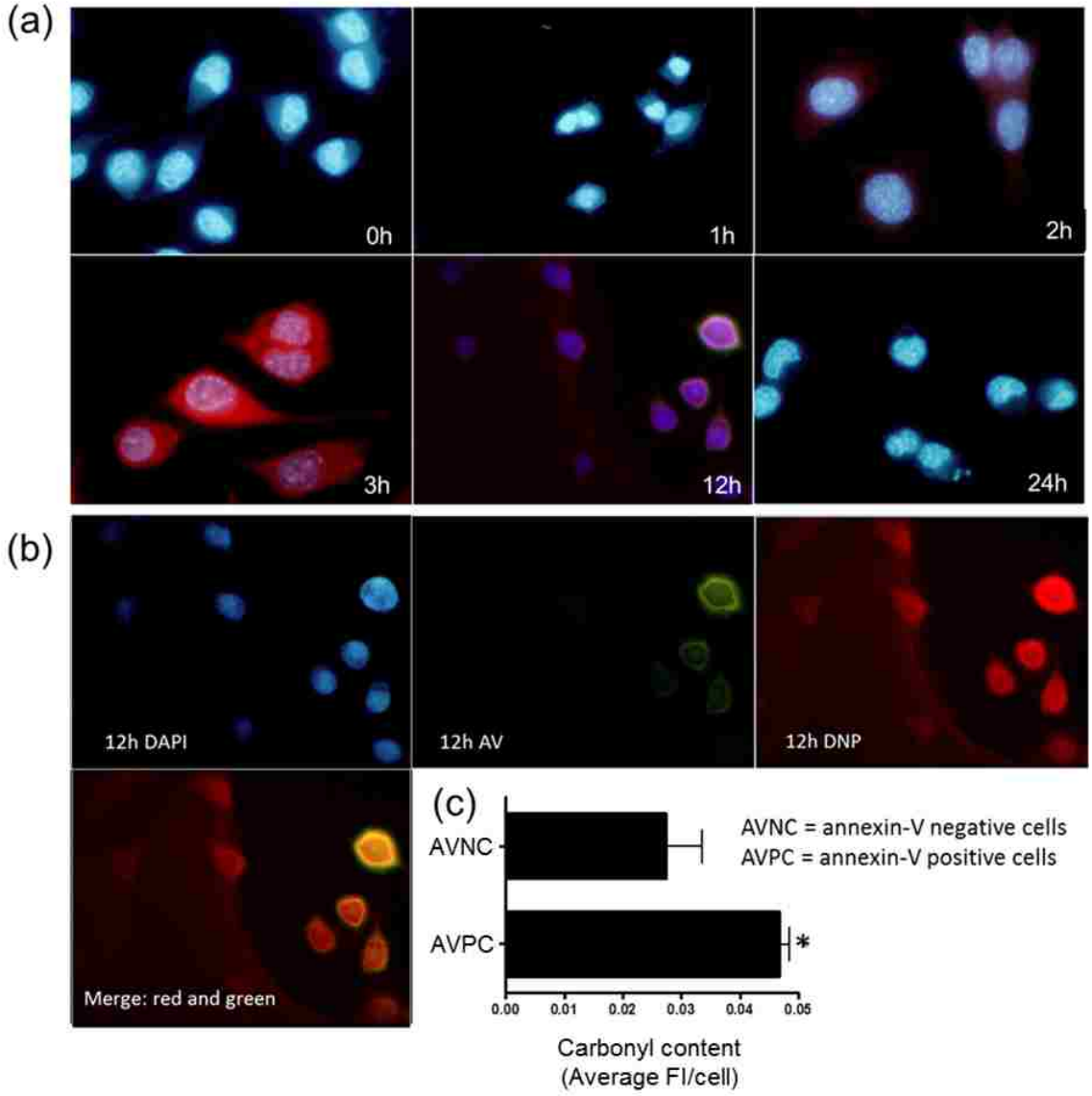

Fig. 6 – Annexin-V positive cells have high carbonyl content. (a) Co-localization of carbonyls and annexin-V in nPC12 cells during GSH depletion. Carbonyls were detected with anti-DNP antibodies after derivatization with DNPH (red). Annexin-V staining for apoptosis and DAPI staining for nuclei are shown in green and blue, respectively. (b) DAPI staining was subtracted from the picture corresponding to 12h-incubation with DEM to better show the co-localization of carbonyls and annexin–V. (c) Carbonyl intensity in annexin-V positive cells (AVPC) and annexin-V negative cells (AVNC) at 12h of treatment with DEM. Values represent the mean ± SEM of 200 cells per experiment; *$p<0.05$.

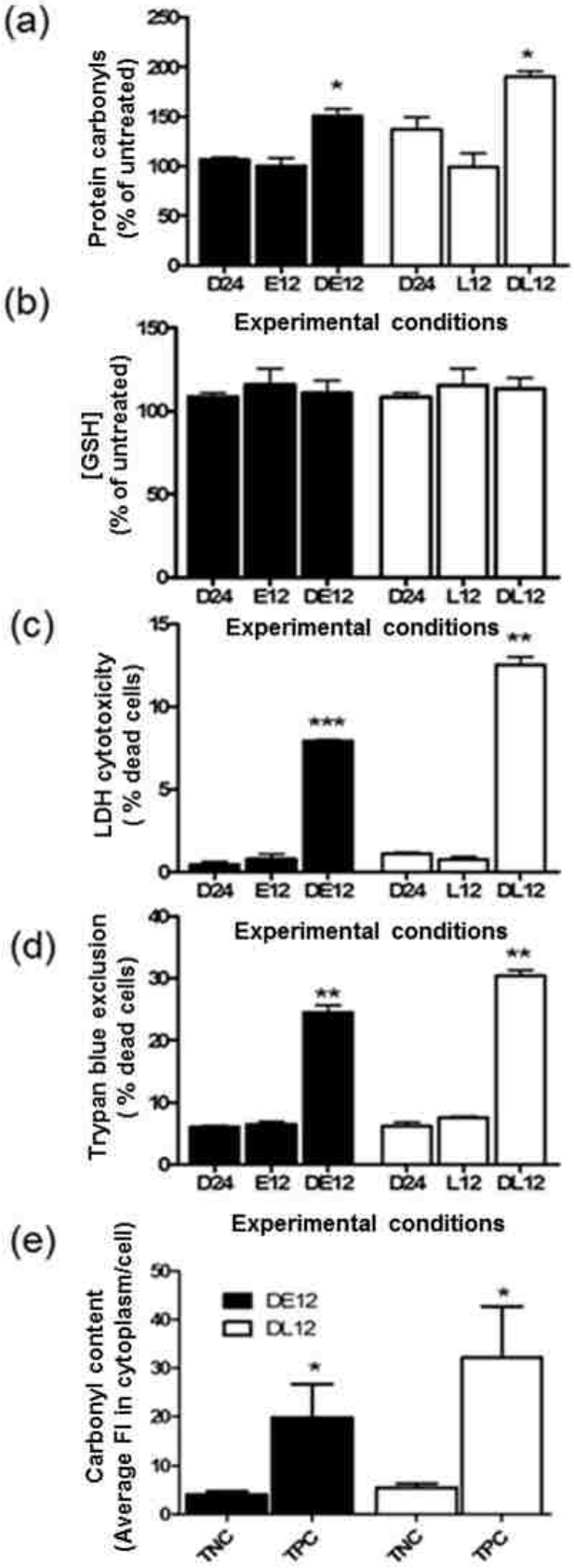

Fig. 7 - Impaired proteasomal activity augments protein carbonylation and apoptosis of DEM-treated nPC12 cells. Cells were incubated with or without 50μM DEM for 12h, after which 1μM epoxomicin (DE12, E12) or 1μM lactacystin (L12, DL12) was added to the medium and incubation continued for another 12h. D24 corresponds to cells incubated with DEM for the entire 24h-period. (a) PCO levels determined by oxyblot. (b) Glutathione assayed by spectrophotometric analysis. (c,d) Cell death quantified using the trypan blue exclusion assay and LDH release. (e) PCO levels in the cytoplasm of TUNEL positive cells (TPC) and TUNEL negative cells (TNC) in DEM-treated cells incubated for 12h with epoxomixin (DE12) or lactacystin (DL12). Values represent the mean ± SEM of 4 experiments. Asterisks denote values that are significantly different from D24; *$p<0.05$, **$p<0.01$, ***$p<0.001$.

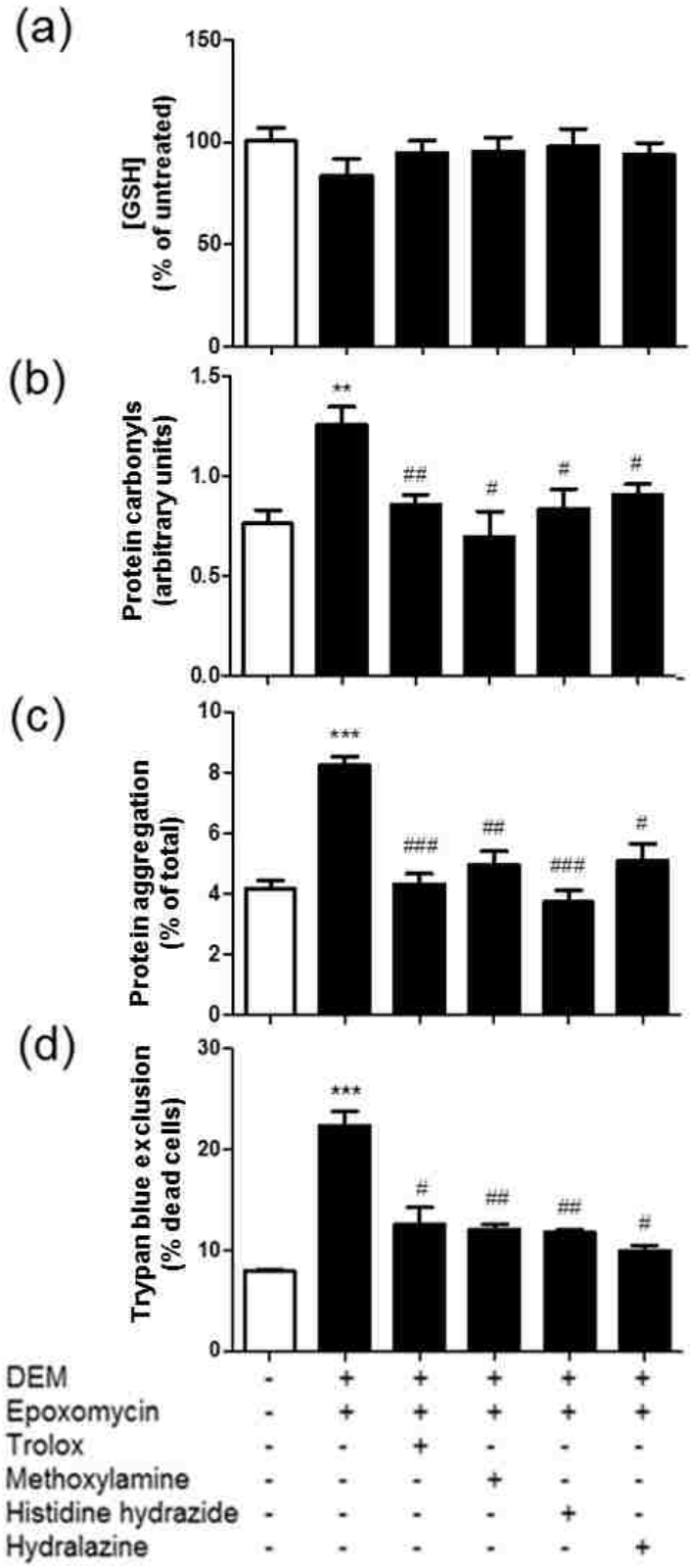

Fig. 8 – Addition of carbonyl scavengers to DEM/epoxomicin-treated nPC12 cells prevents protein aggregation and cell death. Cells were incubated with or without 50μM DEM for 12h, after which epoxomocin (1μM) along with various scavengers (500μM) were added to the medium and incubation continued for another 12h. (a) Glutathione levels assayed by spectrophotometric analysis. (b) PCO levels determined by oxyblot. (c) Protein aggregation measured by differential centrifugation. (d) Cell death quantified using the trypan blue exclusion assay. Values represent the mean ± SEM of 4 experiments. Asterisks denote values that are significantly different (**p<0.01, ***p<0.001) from untreated cells. Pound symbols denote values that are significantly different ($^{\#}$p<0.05, $^{\#\#}$p<0.01, $^{\#\#\#}$p<0.001) from DEM/epoxomicin-treated cells.

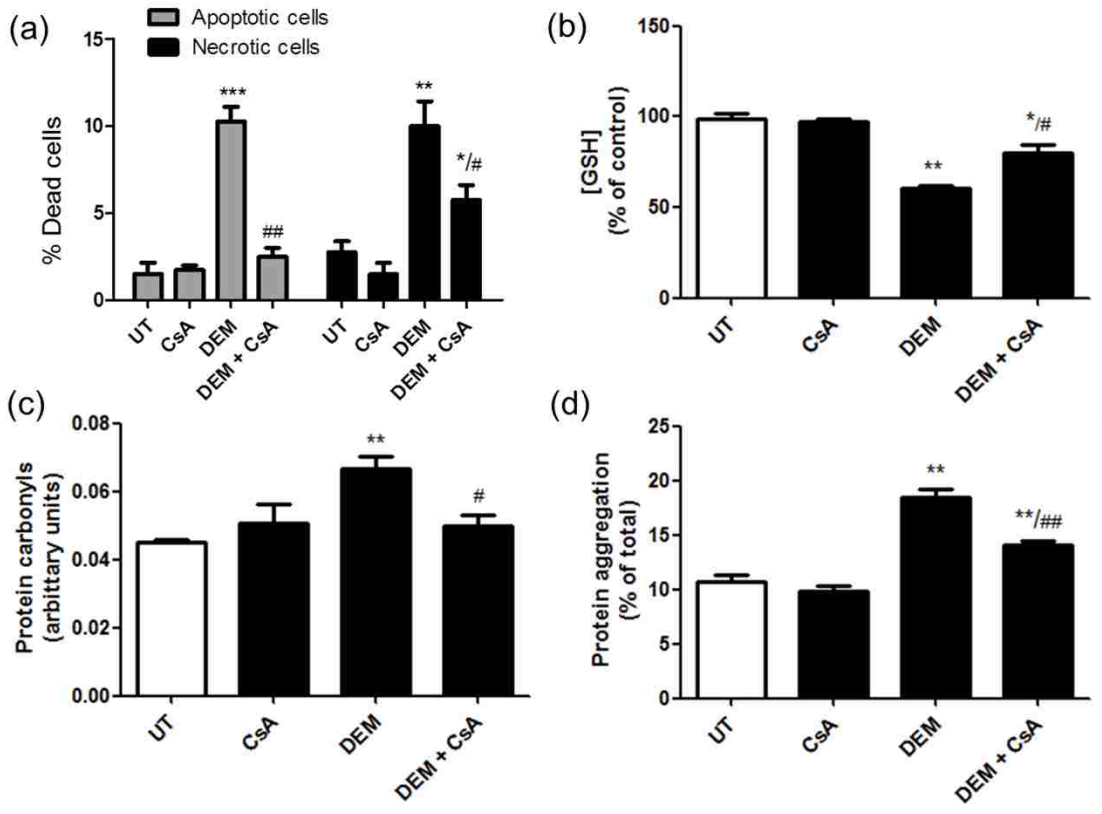

Fig. 9 - Cyclosporin A prevents protein carbonylation, protein aggregation and cell death (both necrosis and apoptosis) induced by partial GSH depletion. nPC12 cells were incubated for 12h with 50µM DEM in the absence or presence of 5µM cyclosporin A (CsA), a classical MPTP inhibitor. (a) The proportion of necrotic and apoptotic cells determined by morphological analysis of 400 cells. (b) GSH levels measured by spectrophotometric analysis. (c) PCO levels measured by oxyblot. (d) Protein aggregation measured by differential centrifugation. Values represent the mean ± SEM of 3 experiments. Asterisks denote values that are significantly different (*p<0.05, **p<0.01, ***p<0.001) from untreated cells. Pound symbols denote values that are significantly different ($^{\#}$p<0.05, $^{\#\#}$p<0.01) from DEM-treated cells.

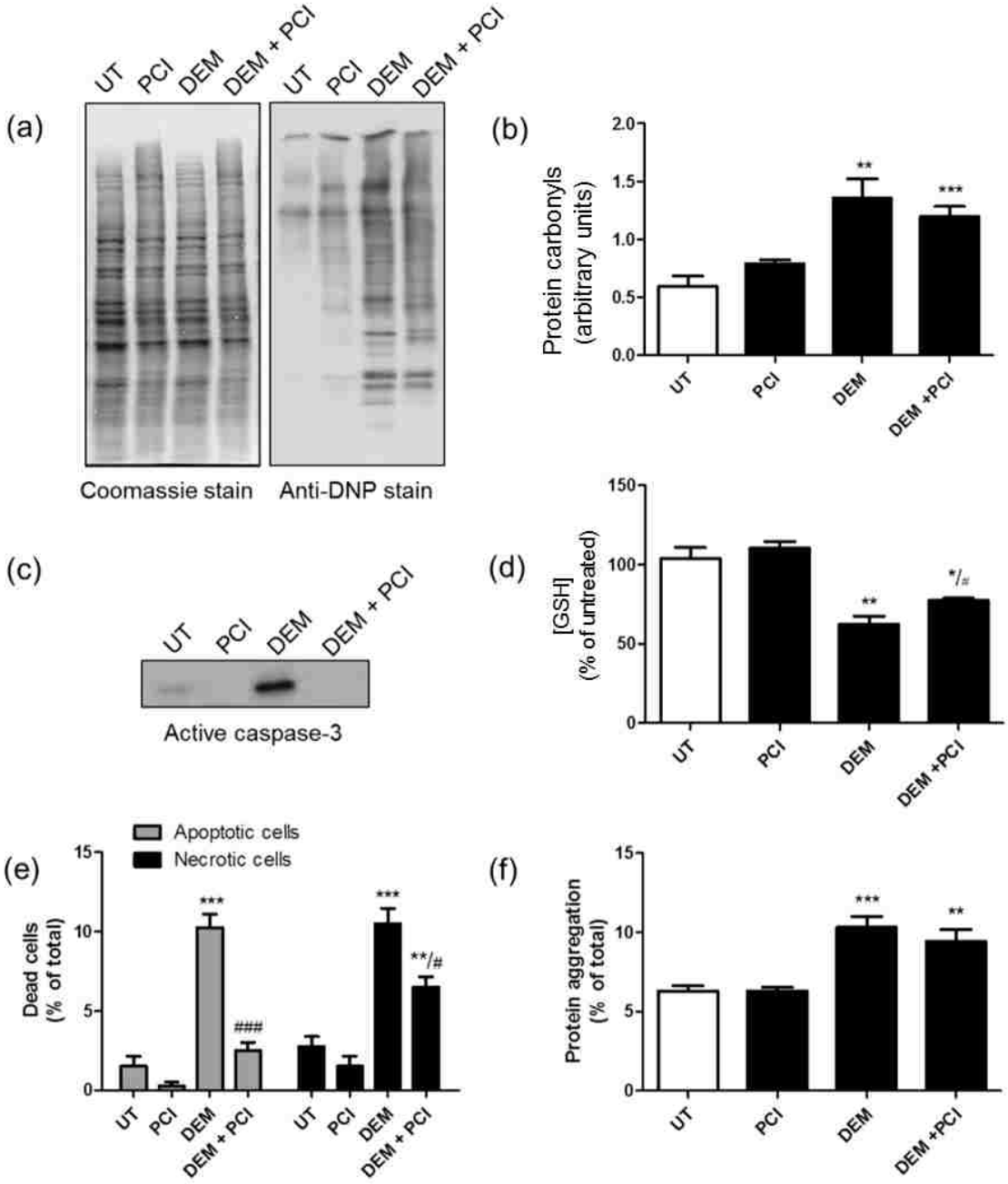

Fig. 10 – Pan-caspase inhibition reduces necrosis and apoptosis of nPC12 cells induced by partial GSH depletion without effecting protein carbonylation or aggregation. nPC12 cells were incubated for 12h with 50μM DEM in the absence or presence of 10μM zVAD-fmk, a classical pan-caspase inhibitor (PCI). (a) Representative oxyblot of total cell proteins. Lane intensities were measured by scanning densitometry and were used to calculate PCO levels (b). (c) Western blot of total cell proteins developed with anti-caspase-3 antibody. (d) GSH levels measured by spectrophotometric analysis. (e) The proportion of necrotic and apoptotic cells determined by morphological analysis of 400 cells. (f) Protein aggregation measured by differential centrifugation. Values represent the mean ± SEM of 5 experiments. Asterisks denote values that are significantly different (*p<0.05, **p<0.01, ***p<0.001) from untreated cells. Pound symbols denote values that are significantly different ($^{\#}$p<0.05, $^{\#\#}$p<0.01) from DEM-treated cells.

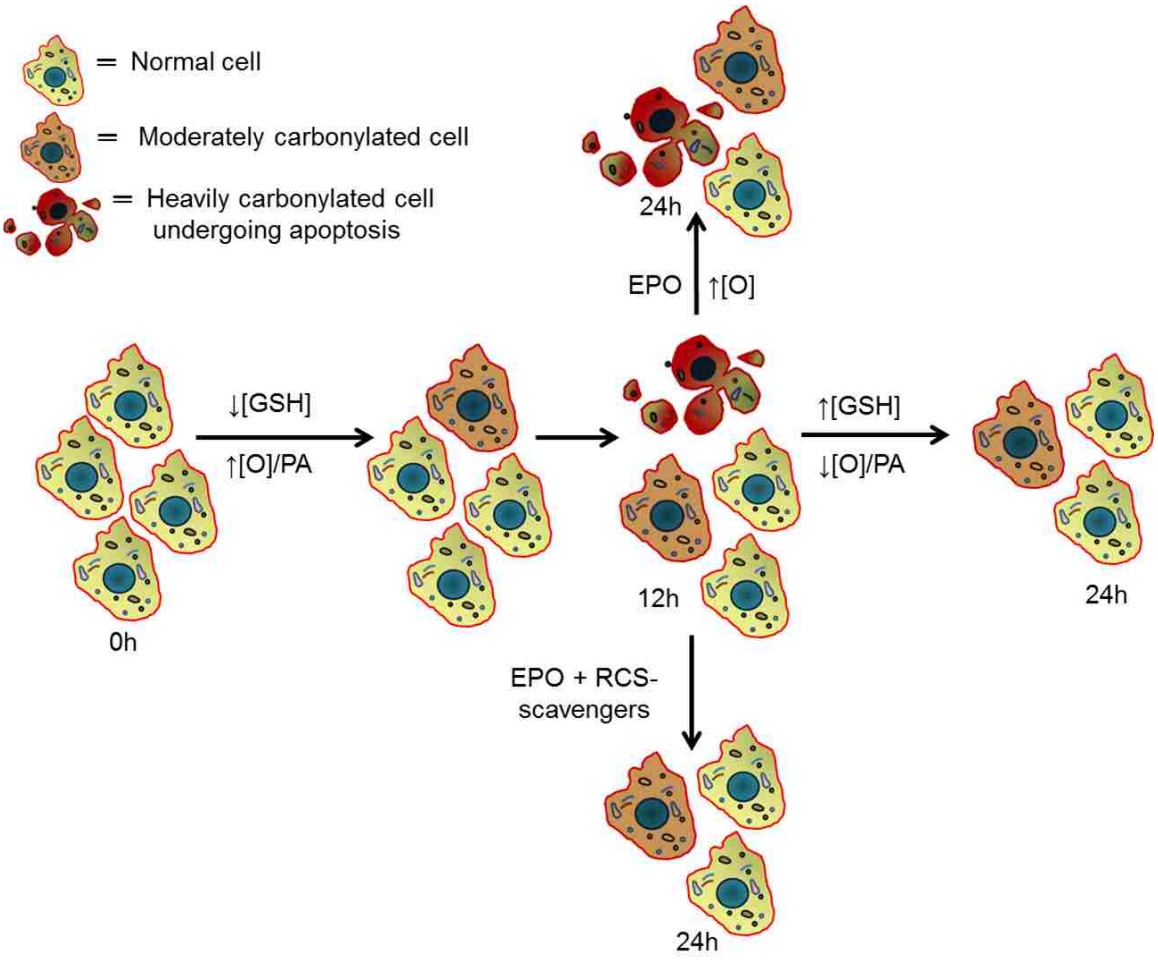

Fig. 11 – Schematic diagram that incorporates the major findings of this study. Partial GSH depletion increases the production of mitochondrial ROS, which are responsible for the incorporation of carbonyl groups into proteins. The rise in proteasomal expression and activity that occurs during the first 12h of incubation is not sufficient to overcome the increase in protein oxidation (indicated as ↑[O]/PA or increased oxidation/protasome activity ratio), leading to the progressive accumulation of PCOs. Some cells accumulate more PCOs than others perhaps reflecting variations in antioxidant defense mechanisms and/or in proteasome expression. When protein oxidation reaches a threshold value (3h-12h of incubation), it triggers apoptosis/necrosis. As incubation progresses, dead cells are removed from the system and the surviving cells slowly replenish their GSH to normal levels, leading to a ↓[O]/PA ratio, a decline in PCO accumulation and reduced cell death. Addition of epoxomicin (EPO) at the beginning of this period prevents the proteasome-mediated removal of damaged proteins causing a build-up of PCOs and loss of cell viability. These effects are prevented by several RCS scavengers, indicating that protein carbonylation is indeed toxic to cells.

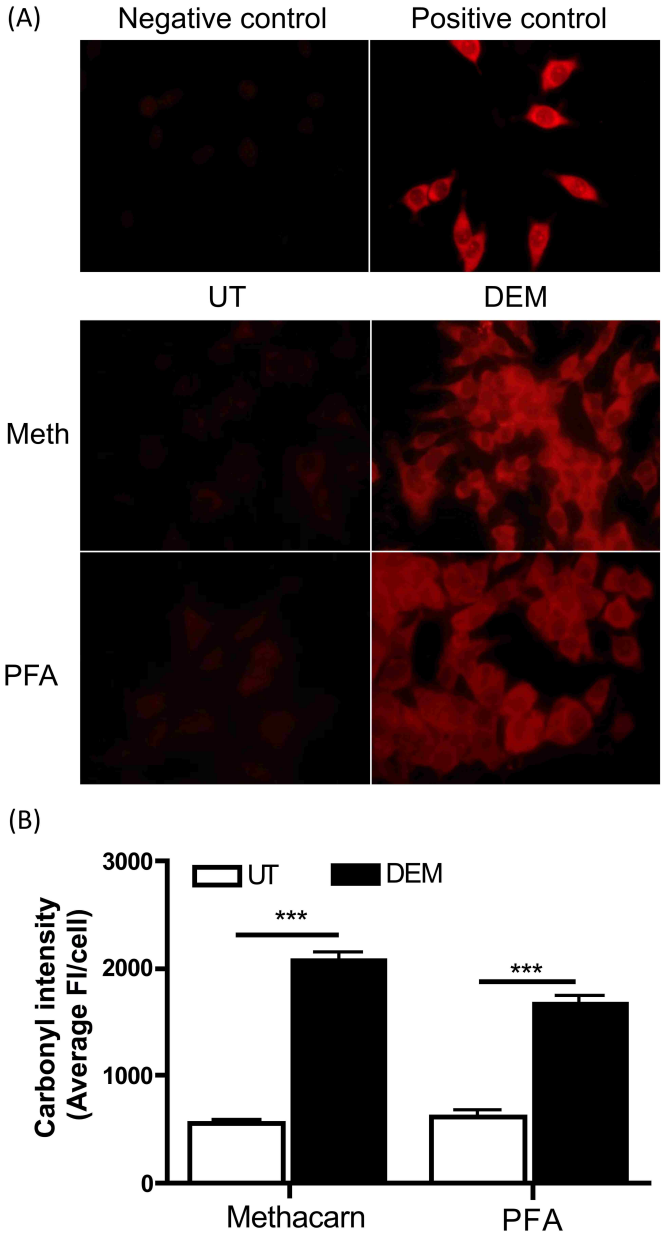

Fig. 1 (supplementary): Methacarn and paraformaldehyde fixatives had similar effect on DNP staining of carbonyls in nPC12 cells. (a) Immunocytochemical detection of carbonyls with anti-DNP after derivatization with DNPH (red) using different fixatives. (b) Quantitative representation of carbonyl levels using different fixatives on nPC12 cells incubated with 50μM DEM for 12h. Values represent the mean ± SEM of 3 experiments. Asterisks denote values that are significantly different (***$p<0.001$) from untreated cells (UT).

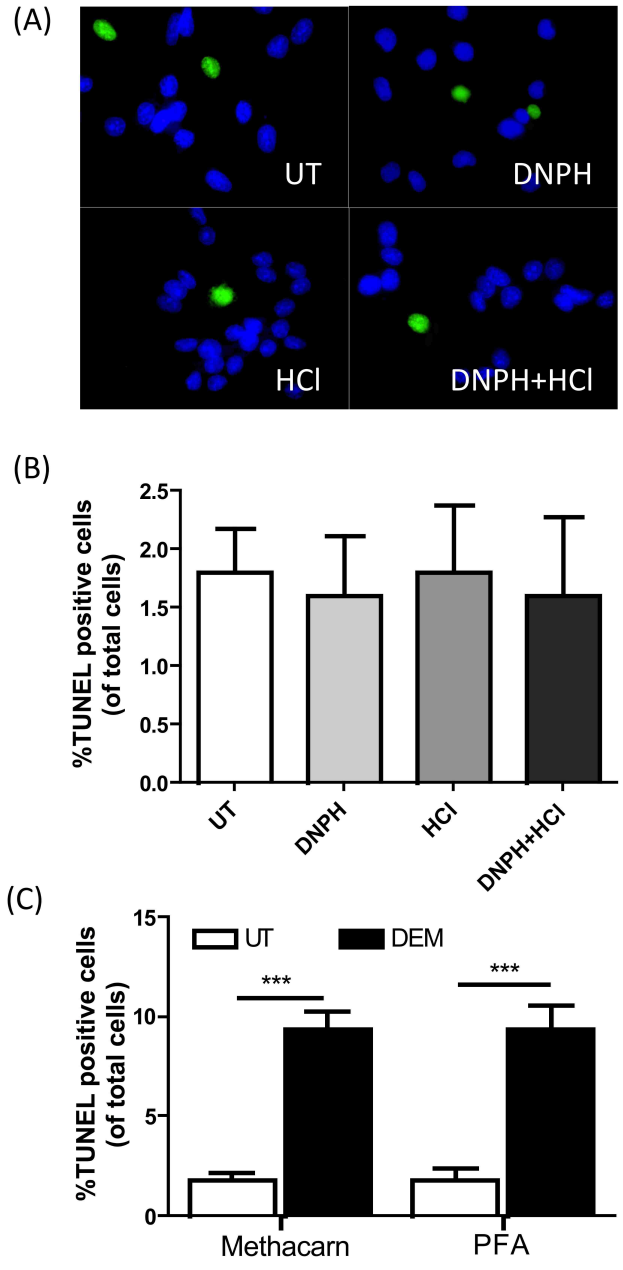

Fig. 2 (supplementary): Incubation with HCl did not affect TUNEL staining in nPC12 cells. (A) Immunocytochemical detection of TUNEL positive cells (green) under different conditions. (B) No changes in the number of TUNEL positive cells upon incubation with DNPH or HCl or both. (C) Increase in TUNEL positive cells to similar extent as compared to its respective untreated controls using different fixatives on nPC12 cells incubated with 50μM DEM for 12h. Values represent the mean ± SEM of 3 experiments. Asterisks denote values that are significantly different (***$p<0.001$) from untreated cells (UT).

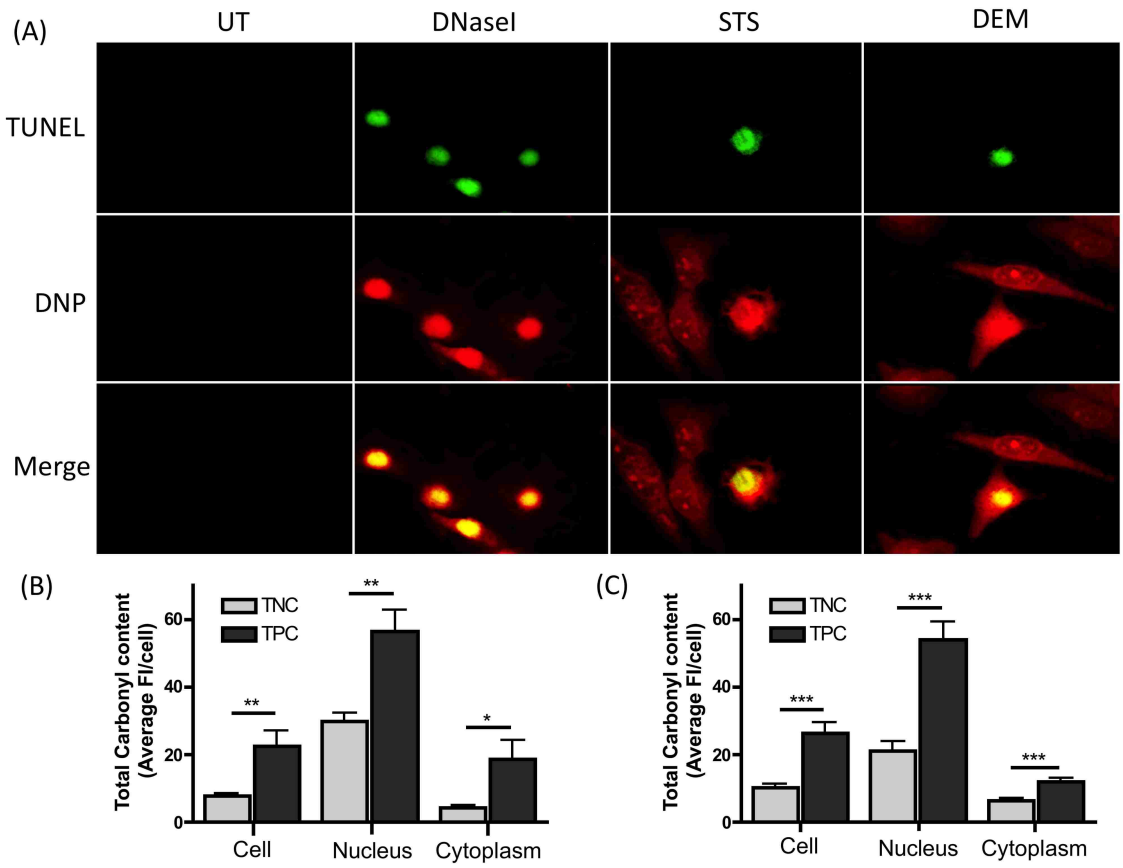

Fig. 3 (supplementary): Damaged-nuclei stains with anti-DNP in nPC12 cells. (A) Immunocytochemical detection of carbonyls with anti-DNP after derivatization with DNPH (red) and TUNEL positive cells (green) under different conditions using paraformaldehyde as a fixative. Majority of nuclei of nPC12 cells incubated with DNase I stained positive for TUNEL and carbonyls. Increase in the number of TUNEL positive cells (TPC) was observed in nPC12 cells incubated either with 5μM of STS for 16 hours or 50μM DEM for 12h. (B) Quantitative representation of carbonyl intensity in the cells, nucleus and cytoplasm of TPC as compared to the TUNEL negative cells (TNC) when incubated with 5μM of STS for 16 hours or (C) with 50μM DEM for 12h. Values represent the mean ± SEM of 3 experiments. Asterisks denote values that are significantly different (*$p<0.05$, **$p<0.01$, ***$p<0.001$) from untreated cells (UT).

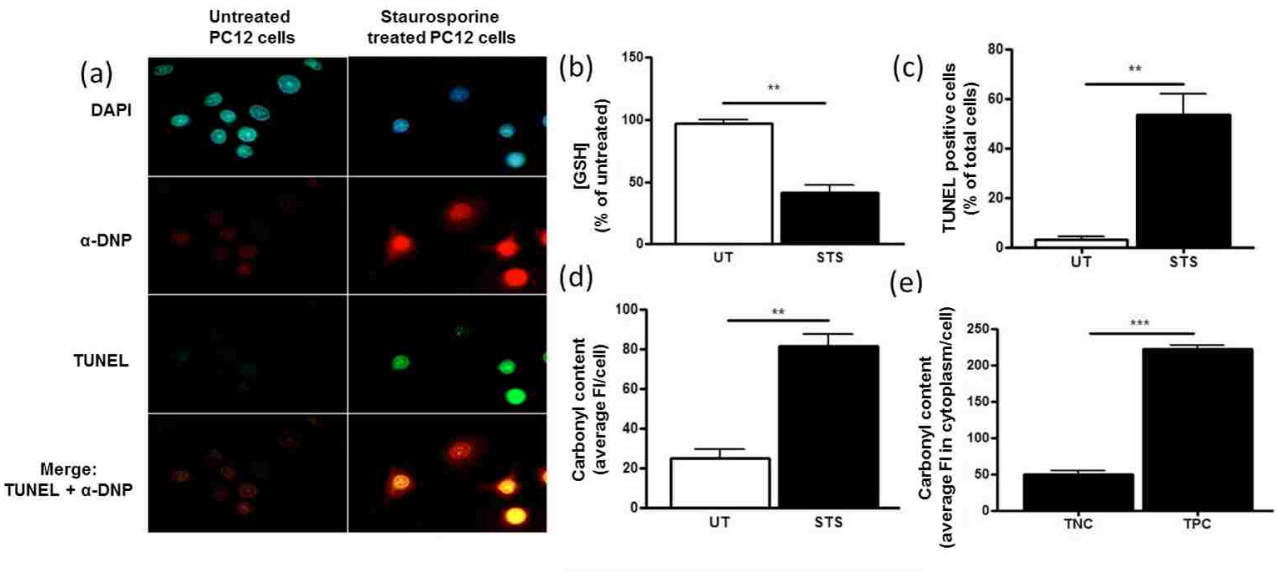

Fig. 4 (supplementary) - Positive relationship between carbonylation andapoptosis in staurosporin-treated nPC12 cells. Cells were incubated with 5μMstaurosporin (STS) for 3h. (a) Immunocytochemical detection with anti-DNPantibodies after derivatization with DNPH (red). TUNEL staining for apoptosis and DAPI staining for nuclei are shown in green and blue, respectively. (b) GSH levels determined by spectrophotometry. (c) Proportion of apoptotic cell determined by TUNEL. (d) Total carbonyl content determined by immunocytochemistry. (e) PCO levels in the cytoplasm of TUNEL positive cells (TPC) and TUNEL negative cells (TNC) at 3h of treatment with staurosporin. Values represent the mean ± SEM of 3 experiments. **p<0.01, ***p<0.001.

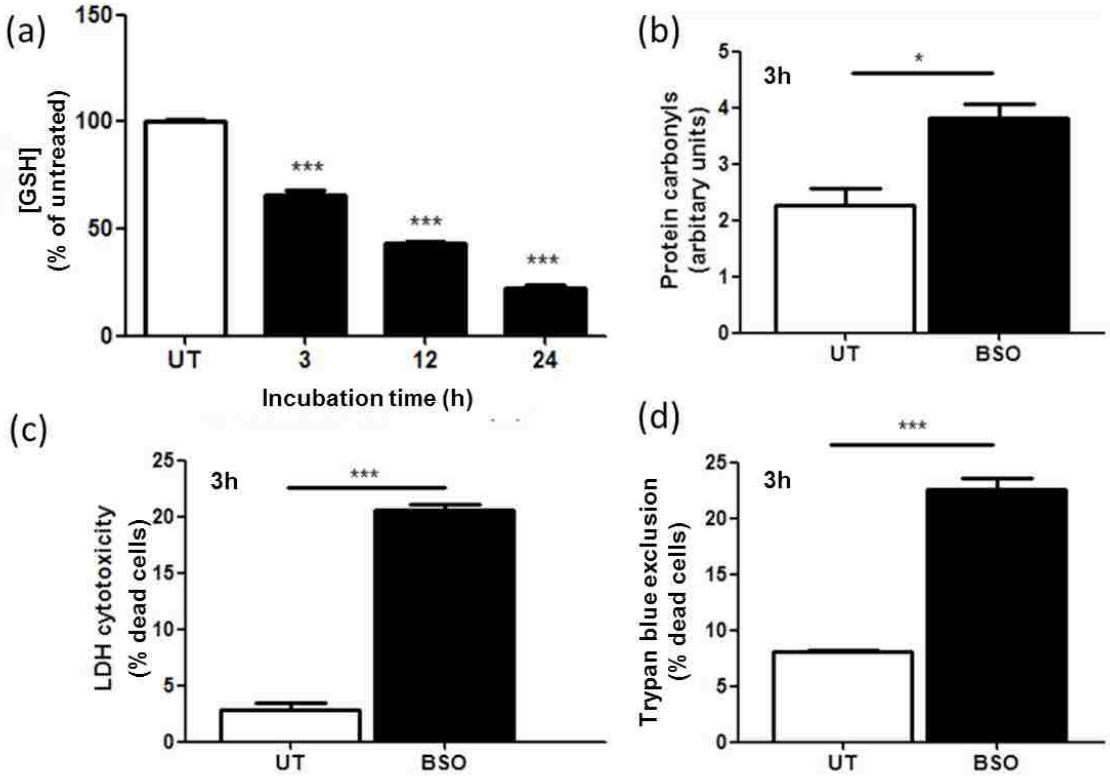

Fig. 5 (supplementary) – BSO-induced GSH depletion also increases carbonylation and cell death. (a) GSH levels in nPC12 cells incubated with 200μM BSO for different time periods. (b) PCO levels in nPC12 cells incubated with 200μM BSO for 3h. (c) Cell death quantified using the LDH release and trypan blue exclusion assay (d) following 3h-incubation with 200μM BSO. Values represent the mean ± SEM of 3 experiments. Asterisks denote values that are significantly different (*$p<0.05$, ***$p<0.001$) from untreated cells (UT).

4. Protein aggregation inhibitors prevent neuronal cell death induced by partial glutathione depletion

Dasgupta A. and Bizzozero O.A.

Department of Cell Biology and Physiology

University of New Mexico School of Medicine

[Manuscript in preparation]

4.1 Abstract

A major consequence of protein carbonylation is the formation of high-molecular weight protein aggregates, which are believed to be cytotoxic. We have previously shown that incubation of neuron-like PC12 cells with 50μM DEM (diethyl maleate) leads to partial depletion of glutathione (GSH) and the ensuing increase in protein carbonyls, protein aggregates and cell death (both by necrosis and apoptosis). In the present study we used the same *in vitro* model of oxidative stress and various carbonyls scavengers and protein aggregation inhibitors in an attempt to strengthen the relationship between protein oxidation, aggregation and apoptosis. The results show that the carbonyl scavengers hydralazine and aminoguanidine (both at 500μM) prevent protein carbonylation, aggregation and cell death caused by GSH depletion. Furthermore, inhibition of protein aggregation with 10μM congo red (CR) or 5μM 2-hydroxypropyl β-cyclodextrin (HPCD) significantly reduced neuronal cell death without affecting the levels of oxidized proteins. Interestingly, we failed to observe the presence of large, juxta-nuclear aggregates (aggresomes) upon GSH depletion, suggesting that the small protein aggregates are the cytotoxic species. Together, these data support our hypothesis that, during severe oxidative stress, carbonylation triggers the formation of small-size protein aggregates to cause neuronal apoptosis

Running Title: Protein aggregation inhibitors prevent neuronal cell death

Key Words: Apoptosis, carbonylation, cell death, glutathione depletion, protein aggregation.

4.2 INTRODUCTION

Many CNS disorders are characterized by oxidative stress induced by overproduction of reactive oxygen species (ROS) and/or failure of the antioxidant defense system. High levels of ROS result in the irreversible, deleterious effects on many cellular components and processes, which trigger cell death (Klein and Ackerman, 2003; Leonardi and Mytilineou, 1998). A major outcome of severe oxidative stress is the formation of protein carbonyls. Increased build-up of oxidized proteins causes substantial alterations in cellular functions that are predominantly cytotoxic (Magi et al., 2004; Curtis et al., 2012; Norberg et al., 2010; Dasgupta et al., 2012). Augmented protein carbonylation and neuronal apoptosis are major features of chronic neurological disorders, including Alzheimer's disease, Parkinson's disease, Huntington's disease and multiple sclerosis (MS) (Bizzozero, 2009).

A rise in the amount of carbonylated proteins is often associated with the formation of protein aggregates (Erjavec et al., 2007; Squier, 2001; Grune et al., 2005). Carbonylation is thought to promote protein aggregation by causing misfolding and exposing hydrophobic regions, which triggers hydrophobic interactions between polypeptides and the formation of supra-molecular assemblies of multiple proteins (Grune *et al.*, 1997). Despite the cytotoxic role of protein aggregates in neurodegeneration is a well established phenomenon (Ross and Poirier, 2004; Lansbury and Lashuel, 2006), the molecular mechanisms for aggregation-associated proteotoxicity is not well understood. Protein aggregates, once formed, can disrupt cellular functions and serve as

nucleation sites for the aggregation of other unrelated proteins, in a manner that further enhances the fraction of misfolded proteins in the cell (Lamark and Johansen, 2012; Wickner *et al*., 1999; Bosshard *et al.,* 2010). It is likely that compartmentalization within the aggregate of proteins that are vital for cell survival leads to cytotoxic responses (Trzesniewska *et al*., 2004; Hachiya *et al.,* 2008; Ross and Poirier*,* 2004; Olzcha *et al.,* 2011). However, it has been argued aggregates may also elicit cytoprotective responses by sequestration of toxic proteins (Dobson, 2003, Zhu *et al.,* 2000).

Recent immunohistochemical studies in the spinal cord of mice with experimental autoimmune encephalomyelitis (EAE), a widely used animal model of MS, revealed that protein carbonylation and protein aggregation have a positive temporal correlation with neuronal/oligodendrocyte apoptosis (Chapter 2). Using a cell culture model of oxidative stress consisting of glutathione-depleted neurons, we recently found that both protein carbonylation and protein aggregation precede apoptosis (Dasgupta *et al.,* 2012; Chapter 3). Moreover, several carbonyl scavengers not only prevented cell death but also reduced the amount of protein aggregates. Yet, the above investigations did not prove conclusively that protein aggregation has a critical role in cell death. The present study was designed to fill this gap by testing the effect of the protein aggregation inhibitors congo red (CR) and 2-hydroxypropyl-β-cyclodextrin (HPCD) on neuronal cell death induced by partial GSH depletion. The results clearly show that both agents not only prevent the formation of protein aggregates but also inhibit cell death without affecting the levels of protein carbonylation. Moreover,

we failed to observe the presence of large, juxta-nuclear aggregates (aggresomes) upon GSH depletion, suggesting that the small protein aggregates are the cytotoxic species.

4.3 MATERIALS AND METHODS

Neuronal cultures and drug treatments

Rat adrenal medullary pheochromocytoma (PC12) cells were cultured on poly-L-lysine-coated 6-well plates (BioCoat™, BD Biosciences, Bedford, MA) in RPMI-1640 media containing 10% serum (7.5% donor horse and 2.5% fetal calf serum; Sigma, St. Louis, MO) and an antibiotic/antimycotic mixture (Invitrogen Corp., Carlsbad, CA). Cells grown at 60-70% confluence were differentiated into a neuronal phenotype by incubation with 100 ng/ml of nerve growth factor (NGF; Sigma) for 24h as described by Harms *et al*. (2010). Cells were incubated for 12 h with the GSH depletor diethylmaleate (DEM, Sigma) in the absence or presence of congo red (Enzo Life Sciences, Plymouth Meeting, PA), 2-hydroxypropyl β-cyclodextrin (Sigma), hydralazine (Sigma), or aminoguanidine (Sigma). Control cells were left untreated after incubation with NGF. After incubation, cells were homogenized in PEN buffer (20 mM sodium phosphate, pH 7.5, 1 mM EDTA, and 0.1 mM neocuproine) containing 1 mM dithiothreitol. For GSH determination, cells were homogenized in PEN buffer without reducing agents and were processed immediately as described below. Protein homogenates were stored at -80°C until use. Protein concentration was

assessed with the Bio-Rad DC™ protein assay (Bio-Rad Laboratories; Hercules, CA) using bovine serum albumin as standard.

Determination of GSH

GSH levels were determined by enzymatic recycling method (Shaik and Mehvar, 2006). Briefly, proteins from cell homogenates were precipitated with 1% sulfosalicylic acid and removed by centrifugation at 10,000g for 15min. Aliquots of the supernatant were then incubated with 0.4U/ml glutathione reductase, 0.2mM NADPH, and 0.2mM 5,5'-dithiobis-(2-nitrobenzoic acid) in 1ml of 0.2M sodium phosphate buffer pH 7.5 containing 5mM EDTA. The rate of appearance of the thionitrobenzoate anion was measured spectrophotometrically at 412 nm. [GSH] was calculated by interpolation on a curve made with increasing concentrations of GSSG (0.1-10nmol).

Oxyblot analysis

Protein carbonyl groups were measured by oxyblot analysis as described earlier (Smerjac and Bizzozero, 2008). In brief, proteins (5µg) were incubated with 2,4-dinitrophenylhydrazine to form the 2,4-dinitrophenyl (DNP) hydrazone derivatives. Proteins were separated by sodium dodecyl sulfate–polyacrylamide gel electrophoresis on 10% gels and blotted to polyvinylidene difluoride membranes. DNP-containing proteins were detected using rabbit anti-DNP antiserum (1:500) and horseradish peroxidase-conjugated goat anti-rabbit IgG antibody (1:2,000). Blots were developed by enhanced chemiluminescence using the Western Lightning ECL™ kit from Perkin-Elmer (Boston, MA). Developed

films were scanned in a Hewlett Packard Scanjet 4890 and the images were quantified using the NIH Image 1.63 imaging analysis program. The intensity of each lane on the film was normalized by the amount of coomassie blue staining in the corresponding lane.

Cell viability assays

Cell death was determined by measuring lactate dehydrogenase (LDH) activity on a 10µl-aliquot from the cell supernatant using the LDH-cytotoxicity assay kit II (ABCAM, Cambridge, MA).

Protein aggregation assay

Cell homogenates prepared in PEN buffer containing 1mM dithiothreitol and 150mM NaCl were centrifuged at 20,000x*g* for 30 min at 4°C. The pellets were then extracted with the same buffer containing 1% triton X-100. Samples were kept on ice for 15 min and were centrifuged at 20,000x*g* for 30 min at 4°C. The final pellet, which contains some cytoskeleton structures but mostly aggregated proteins, was re-suspended in PEN buffer for protein determination. In some cases, samples were analyzed by SDS-PAGE as described above.

Cytochemical detection of aggresomes

Cells, cultured on 12 mm round poly-lysine coated coverslips (BD BioCoat™) were fixed with 4% paraformaldehyde for 20 min. Fixed cells were then incubated for 30 min with ProteoStat® Protein Aggregation Assay solution (Enzo Life Sciences). Cellular nuclei were stained with DAPI (40ng/ml, Sigma). Stained

sections were mounted using 1,4-diazabicyclo[2.2.2]octane in polyvinyl alcohol (Sigma) as antifading agent.

Statistical analysis

Results were analyzed for statistical significance with student *t*-test using GraphPad Prism® program (GraphPad Software incorporation, San Diego, CA).

4.4 RESULTS

Strong correlation between protein carbonylation, aggregation and neuronal cell death. PC12 cell cultures have been widely used as model system for studying apoptosis in neurodegenerative diseases (Kruttgen *et al.*, 1998; Rukenstein *et al.*, 1991; Cheung *et al.,* 2000). These cells differentiate into dopaminergic neurons when treated with low concentrations of nerve growth factor (Das *et al*., 2004; Meakin and Shooter, 1992; Dasgupta *et al*., 2012). As in our previous work (Dasgupta *et al., 2012*), we used diethyl maleate (DEM) to reduce intracellular GSH levels. This electrophilic reagent rapidly conjugates to GSH by a reaction catalyzed by glutathione-S-transferase (Buchmüller-Rouiller *et al.,* 1995), making the tri-peptide unavailable for the reduction of many oxidized metabolites. This leads to mitochondrial production of reactive oxygen species and the development of oxidative stress (Bizzozero *et al.,* 2006). After 12h of incubation with DEM, there is a 30% reduction in GSH levels, followed by GSH replenishment at 24h (Fig. 1a). Concomitant with GSH depletion observed after treatment with DEM for 12h, there is a 50% increase in the amount of protein carbonyls and 300% rise in the amount of aggregated protein, both of which

return back to control values by 24h of incubation (Fig.1b, c). In all experimental conditions approximately one-half of the carbonylated proteins are present in the detergent-insoluble pellets, suggesting that protein carbonyls are integral part of the protein aggregates (Figure 1d). Concurrent with the accumulation of carbonylated proteins and protein aggregates, the extent of cell death, assessed by LDH release into the incubation medium, is also high at 12h of incubation with DEM to decrease thereafter (Fig. 1e). Furthermore, using data points corresponding to incubation periods shorter than 12h, we found that the amount of protein aggregates display a high correlation with both protein carbonylation (Fig. 2a) and cell death (Fig. 2b). These data strongly suggest a possible association between protein carbonylation and protein aggregation in mediating cell death.

Carbonyl scavengers prevent protein aggregation and cell death. As depicted in Fig. 3, the carbonyl scavengers aminoguanidine and hydralazine reduced the amount of carbonylated proteins formed upon GSH depletion for 12h (Fig 3). Furthermore, these agents also prevented the formation of protein aggregates and cell death as compared to the samples incubated with DEM alone. Similar results were found in our previous study using histidine hydrazide and methoxylamine as carbonyls scavengers (Dasgupta *et al.,* 2012; Chapter 3). These data clearly suggest that protein carbonylation causes protein aggregation and neuronal cell death in this *in vitro* system.

Inhibition of protein aggregation prevents cell death without affecting protein oxidation. We next investigated whether protein aggregation plays a

critical role in neuronal cell death induced by GSH depletion. Towards this end, we selected CR and HPCD. Both of these drugs are known protein aggregate inhibitors at low concentrations and do not display any antioxidant properties. As shown in Fig. 4, 5μM HPCD and 10μM of CR inhibited protein aggregation and prevented DEM-induced cell death, without affecting the levels of protein carbonylation. These results demonstrate an ordered mechanistic pathway for mediating neuronal cell death under severe oxidative stress, where carbonylation leads to the formation of protein aggregates to mediate neuronal cell death (Fig. 5).

Large protein aggregates (aggresomes) do not form during GSH depletion. Cytochemical experiments were conducted to determine if DEM-induced neuronal cell death is related to the formation of large juxta-nuclear aggregates (a.k.a. aggresomes). This is important since the protein aggregation assay used until this point measures both small and large aggregates. Aggresomes were detected using the ProteoStat® protein aggregation dye. Surprisingly, the number of large protein aggregates in DEM-treated neurons, even in the presence of the proteasome inhibitor epoxomycin, was very small and indistinguishable from that of control cells (Fig. 6). A positive control made of nPC12 cells treated with the non-specific proteasome inhibitor MG132 led to the formation of aggresomes in most cells, thereby validating this technique for the detection of large protein aggregates. These results suggest that small protein aggregates rather than aggresomes are the inducer of cytotoxicity during partial depletion of GSH.

4.5 DISCUSSION

Accumulation of aggregated proteins is normally considered a cytotoxic process (Estus *et al.,* 1997; Zhu *et al.,* 2000) and has long been associated with neurodegeneration (Lansbury and Lashuel, 2006). The results from the present work are generally in agreement with this notion. Using an *in vitro* model of oxidative stress that mimics the reduction in GSH levels observed in inflammatory demyelinating disorders such as EAE (Chapter 2) and MS (Bizzozero *et al.*, 2005), we showed that (1) there is a positive temporal correlation between protein oxidation, aggregation and neuronal death, (2) carbonyl scavengers prevent both protein aggregation and cytotoxicity, (3) inhibition of protein aggregation significantly reduces cell death without affecting the levels of oxidized proteins, and (4) protein aggregates of large size do not form to any appreciable extent. Together, these data support the hypothesis that carbonylation triggers the formation of small-size protein aggregates to cause neuronal apoptosis (Fig. 5).

Our findings also suggest that, at least in this *in vitro* system, carbonylated proteins are not harmful by themselves but mediate their toxic effects by inducing protein aggregation. Although the mechanism(s) underlying the assembly of protein aggregates during oxidative stress is presently unknown, we have found that carbonylated proteins are not only enriched in the aggregates but also are critical for aggregate formation. It is noteworthy, however, that just a small

fraction (1-2%) of the proteins present in the aggregates are modified by carbonylation. Yet, the incorporation of carbonyl groups (and the ensuing elimination of positive charges) on specific amino acid residues may cause misfolding, thereby exposing hydrophobic surfaces that can mediate aberrant interactions with other (non-oxidized) proteins, as was recently proposed for several cerebral proteopathies (Walker and LeVine, 2012). It is likely that as these abnormal complexes form and grow in size, they may sequester many proteins that are vital for cell survival leading to neurotoxicity and cell death (Trzesniewska *et al.*, 2004; Hachiya *et al.,* 2008; Ross and Poirier*,* 2004; Olzcha *et al.,* 2011).

In chapter 2, I showed that concomitant with increased levels of carbonylated proteins in the spinal cord of EAE mice there is a rise in the amount of cells containing large juxta-nuclear protein aggregates. Thus, it was surprising to discover that GSH-depleted PC12 cells do not contain aggresomes or any other aggregates that are large enough to be detected with the ProteoStat® dye. Moreover, large aggregates were not detected even when DEM-treated cell were incubated in the presence of the proteasome inhibitor epoxomycin (Fig. 6), a condition that further increases cell death, the levels of protein carbonyls and the amount of protein aggregates determined with a biochemical technique (Dasgupta *et al.,* 2012). Based on these findings, it is fair to conclude that small-size protein aggregates are actually neurotoxic. Indeed, a number of recent studies have suggested that aggresomes, in contrast to small protein aggregates, are cytoprotective (Kopito, 2000; Zhang and Qian, 2011; Lamark

and Johansen, 2012). It is noteworthy that incubation of nPC12 cells with the proteasome inhibitor MG132 leads to the formation of aggresomes in most cells. However, this is likely due to the fact that MG132, in contrast to epoxomycin, is not a very specific and can also inhibit the lysosomal-cathepsins (Kadlčíková *et al.,* 2004), thereby interfering with the autophagy process and the removal of larger aggregates. This suggests that the decreased autophagy index, rather than augmented carbonylation, is perhaps the major factor triggering the formation of aggresomes in acute and chronic EAE (Chapter 2).

We have shown for the first time that CR and HPCD inhibit carbonylation-triggered protein aggregation and the ensuing neuronal cell death. Their inhibitory activities can be attributed to their hydrophobicity, which possibly functions to prevent the assembly of aggregated proteins or to facilitate their disassembly. CR is known to interfere with polypeptide misfolding and to stabilize native protein monomers or partially misfolded intermediates (Podlisny *et al.,* 1995) whereas HPCD has a detergent-like activity that can help in the refolding process, thereby preventing the protein association (Wang, 2005). Yet, regardless of their mechanism of action, agents like CR and HPCD may become in the future important tools to evaluate the causative and consequential role of protein aggregation in the pathogenesis and progression of EAE. Indeed, CR has already been shown to have an ameliorative effect in cell and animal models of other neurological disorders, including Alzheimer's, Parkinson's, Huntington's and prion diseases (Frid *et al.*, 2007).

4.6 REFERENCES

Bizzozero OA. 2009. Protein carbonylation in neurodegenerative and demyelinating CNS diseases. In “Handbook of Neurochemistry and Molecular Neurobiology” (Lajtha A, Banik N, Ray S, eds) Springer, pp. 543-562.

Bizzozero OA, DeJesus G, Callahan K, Pastuszyn A. 2005. Elevated protein carbonylation in the brain white matter and gray matter of patients with multiple sclerosis. J Neurosci Res 81: 687–695.

Bizzozero OA, Ziegler JL, De Jesus G, Bolognani F. 2006. Acute depletion of reduced glutathione causes extensive carbonylation of rat brain proteins. J Neurosci Res 83: 656-667.

Bosshard F, Riedel K, Schneider T, Geiser C., Bucheli M, Egli T. 2010. Protein oxidation and aggregation in UVA-irradiated Escherichia coli cells as signs of accelerated cellular senescence. Environ Microbiol 10.1111/j.1462-2920.2010.02268.x

Buchmuller-Rouiller Y, Corrandin SB, Smith J, Schneider P, Ransijn A, Jongeneel CV, Mauel J. 1995. Role of glutathione in macrophage activation: effect of cellular glutathione depletion on nitrite production and leishmanicidal activity. Cell Immunol 164: 73-80.

Cheung WM, Hui WS, Chu PW, Chiu SW, Ip NY. 2000. Ganoderma extract activates MAP kinases and induces the neuronal differentiation of rat pheochromocytoma PC12 cells. FEBS Lett 486: 291–296.

Curtis JM, Hahn WS, Long EK, Burrill JS, Arriaga EA, Bernlohr DA. 2012. Protein carbonylation and metabolic control systems. TEM 23: 399-406.

Das KP, Freudenrichb TM, William R. 2004. Assessment of PC12 cell differentiation and neurite growth: a comparison of morphological and neurochemical measures. Neurotoxicol Teratol 26: 397–406.

Dasgupta A, Zheng J, Bizzozero OA. 2012. Protein carbonylation and aggregation precede neuronal apoptosis induced by partial glutathione depletion. ASN neuro 10.1042/AN20110064.

Dobson CM. 2003. Protein folding and misfolding. Nature 426: 884–890.

Erjavec N, Larsson L., Grantham J, Nyström T. 2007. Accelerated aging and failure to segregate damaged proteins in Sir2 mutants can be suppressed by overproducing the protein aggregation-remodeling factor Hsp104p. Genes & Develop 21: 2410-2421.

Estus S, Tucker HM, Van Rooyen C, Wright S, Brigham EF, Wogulis M, Rydel RE. 1997. Aggregated amyloid-β protein induces cortical neuronal apoptosis and concomitant “apoptotic” pattern of gene induction. J Neurosci 17: 7736–7745.

Frid P, Anisimov SV, Popovic N. 2007. Congo Red and protein aggregation in neurodegenerative diseases. Brain Res Rev 53:135–160.

Grune T, Davies KJ. 1997. Breakdown of oxidized proteins as a part of secondary antioxidant defenses in mammalian cells. Biofactors 6: 165–172.

Grune T, Merker K, Jung T, Sitte N, Davies KJ. 2005. Protein oxidation and degradation during postmitotic senescence. Free Radic Biol Med 39: 1208-15.

Hachiya NS, Kozuka Y, Kaneko K. 2008. Mechanical stress and formation of protein aggregates in neurodegenerative disorders. Medical Hypotheses 70: 1034-1037.

Harms KM, Li L, Cunningham LA. 2010. Murine neural stem/progenitor cells protect neurons against ischemia by HIF-1a-Regulated VEGF signaling. PLoS ONE 5: e9767.

Kadlčíková J, Holeček M, Šafránek R, Tilšer I, Kessler BM. 2004. Effects of proteasome inhibitors MG132, ZL3VS and AdaAhx3L3VS on protein metabolism in septic rats. Int J Exp Pathol 85: 365–371.

Klein JA, Ackerman SL. 2003. Oxidative stress, cell cycle, and neurodegeneration. J Clin Invest 111: 785–793.

Kopito RR. 2000. Aggresomes, inclusion bodies and protein aggregation. TICB10: 524–530.

Kruttgen A, Moller JC, Heymach JV, Shooter EM. 1998. Neurotrophins induce release of neurotrophins by the regulated secretory pathway. Proc Natl Acad Sci 95: 9614–9619.

Lamark T, Johansen T. 2012. Aggrephagy: selective disposal of protein aggregates by macroautophagy. Int J. Celll Biol e736905.

Lansbury PT and Lashuel HA (2006), A century-old debate on protein aggregation and neurodegeneration enters the clinic. Nature 443: 774–779.

Leonardi, ET, Mytilineou C. 1998. Cell culture models of neuronal degeneration and neuroprotection. Implications for Parkinson's disease. Adv Exp Med Biol 446: 203-222.

Magi B, Ettorre A, Liberatori S, Bini L, Andreassi M, Frosali S, Neri P, Pallini V, Di-Stefano A. 2004. Selectivity of protein carbonylation in the apoptotic response to oxidative stress associated with photodynamic therapy: a cell biochemical and proteomic investigation. Cell Death Differ 11: 842–852.

Meakin SO, Shooter EM. 1992. The nerve growth factor receptors. TINS 15: 323–331.

Norberg E, Orrenius S, Zhivotovsky B. 2010. Mitochondrial regulation of cell death: Processing of apoptosis-inducing factor (AIF). Biochem Biophys Res Commun 396: 95–100.

Olzscha H, Schermann SM, Woerner AC, Pinket S, Hecht MH, Tartaglia GG, Vendruscolo M, Hayer-Hartl M, Hartl FU, Vabulas RM. 2011. Amyloid-like aggregates sequester numerous metastable proteins with essential cellular functions. Cell 144: 67–78.

Podlisny MB, Ostaszewski BL, Squazzo SL, Koo EH, Rydel RE, Teplow DB, Selkoe DJ. 1995. Aggregation of secreted amyloid β-protein into SDS-stable oligomers in cell culture. J Biol Chem 270: 9564–9570.

Ross CA, Poirier MA. 2004. Protein aggregation and neurodegenerative disease. Nature Med 10: S10-17.

Rukenstein A, Rydel RE, Greene LA. 1991. Multiple agents rescue PC12 cells from serum-free cell death by translation-and transcription-independent mechanisms. J Neurosci 11: 2552–2563.

Shaik IH, Mehvar R. 2006. Rapid determination of reduced and oxidized glutathione levels using a new thiol-masking reagent and the enzymatic recycling method: Application to the rat liver and bile samples. Anal Bioanal Chem 385: 105–113.

Smerjac SM, Bizzozero OA. 2008. Cytoskeletal protein carbonylation and degradation in experimental autoimmune encephalomyelitis. J Neurochem 105: 763-772.

Squier TC. 2001. Oxidative stress and protein aggregation during biological aging. Exp Gerontol 36: 1539–1550.

Trześniewska K, Brzyska M, Elbaum D. 2004. Neurodegenerative aspects of protein aggregation. Acta Neurobiol Exp 64: 41-52.

Walker LC, LeVine H. 2012. Corruption and spread of pathogenic proteins in neurodegenerative diseases. J Biol Chem 287: 33109-33115.

Wang W. 2005. Protein aggregation and its inhibition in biopharmaceutics. Int J Pharmaceu 289: 1-30.

Wickner S, Maurizi MR, Gottesman S. 1999. Posttranslational quality control: folding, refolding, and degrading proteins. Science 286: 1888–1893.

Zhang X, Qian SB. 2011. Chaperone-mediated hierarchical control in targeting misfolded proteins to aggresomes. Mol Biol Cell 22: 3277–3288.

Zhu YJ, Lin H, Lal R. 2000. Fresh and nonfibrillar amyloid beta protein(1-40) induces rapid cellular degeneration in aged human fibroblasts: evidence for AbetaP-channel-mediated cellular toxicity. FASEB J 14: 1244–54.

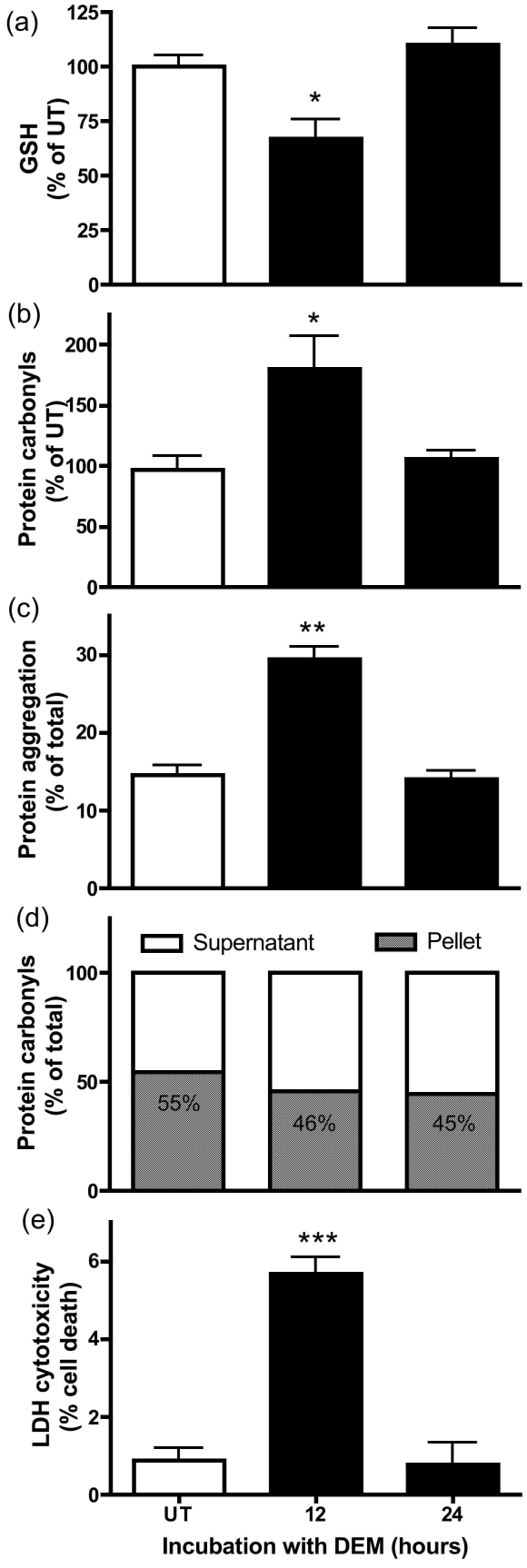

Fig. 1 – Time-course changes in protein carbonylation, protein aggregation and cell death in DEM-treated nPC12 cells. (a) Effect of 50μM DEM on GSH levels, (b) Levels of protein carbonyls measured by oxyblot analysis, (c) Protein aggregates determined by calculating the protein concentration in the triton insoluble pellets, (d) percentage of protein carbonyls partitioning into the protein aggregates, and (e) cell death assayed by LDH release at 12h and 24h of incubation with DEM. Values represent the mean ± SEM of 4 experiments. Asterisks denote values that are significantly different from those obtained in untreated (UT) cells; *p<0.05, **p<0.01, ***p<0.001.

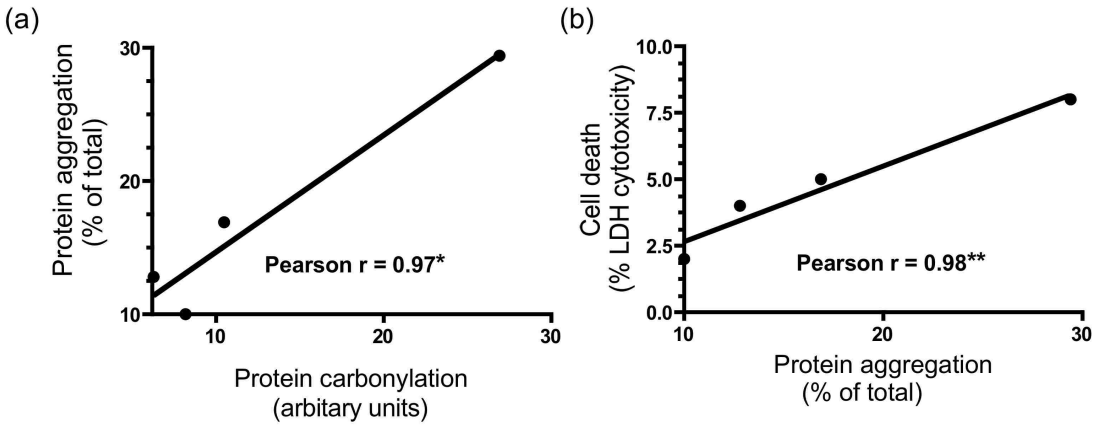

Fig. 2 – Positive correlation exists between protein carbonylation, protein aggregation and cell death. Correlation curves showing strong positive correlation (a) between protein aggregation and protein carbonylation (r=0.97) and (b) between cell death and protein aggregation (r=0.98) in GSH-depleted nPC12 cultures. Each point represents the average values from 3 experiments. Asterisks denote the significance of Pearson correlation coefficient (r); *p<0.05, **p<0.01.

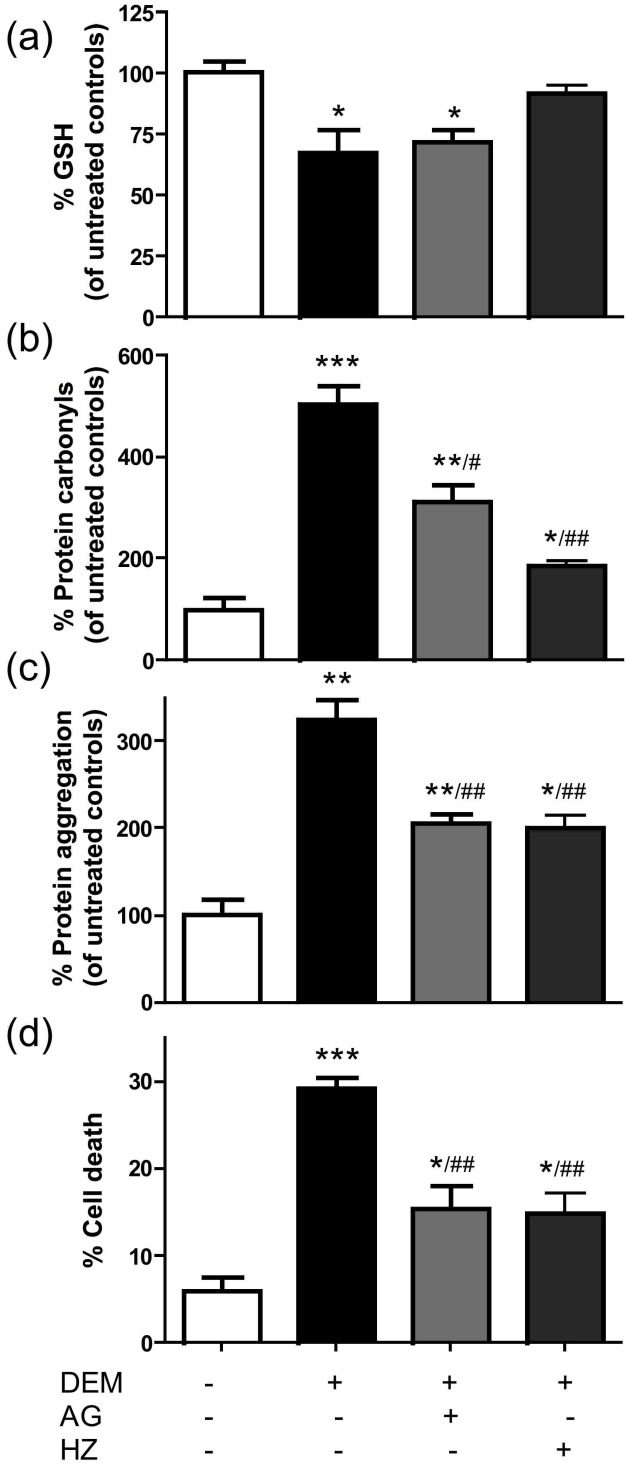

Fig. 3 – Carbonyl scavengers prevent protein aggregation and cell death in DEM-treated nPC12 cells. Cells were incubated with 50μM DEM for 12h along with either 500μM of aminoguanidine (AG) or hydralazine (HZ) (a) [GSH] was measured by spectrophoto-metric analysis. (b) Protein carbonyls were measured by oxyblot analysis. (c) Protein aggregation was assayed by differential centrifugation. (d) Cell death was quantified using LDH release. Values represent the mean ± SEM of 4 experiments. Asterisks denote values that are significantly different (**p<0.01, ***p<0.001) from untreated cells (UT). Pound symbols denote values that are significantly different ($^{\#}$p<0.05, $^{\#\#}$p<0.01, $^{\#\#\#}$p<0.001) from DEM-treated cells.

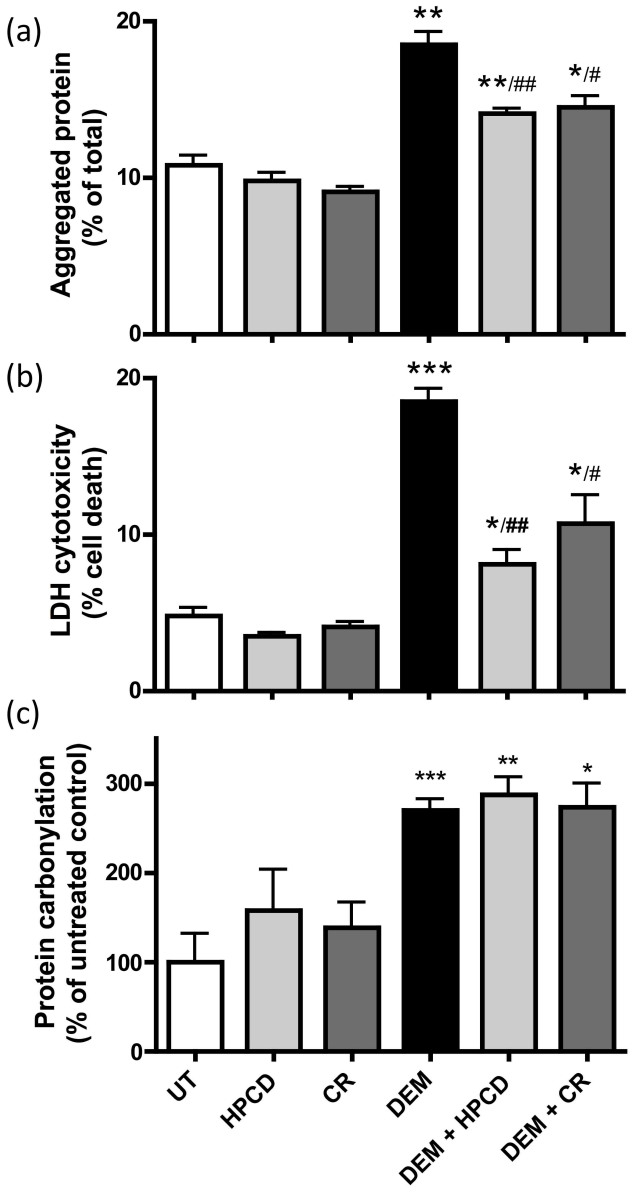

Fig. 4 – Inhibition of protein aggregation blocks DEM-induced nPC12 cell death without affecting protein oxidation. Cells were incubated with or without 50μM DEM along with either 10μM of congo red (CR) or 2-hydroxypropyl β-cyclodextrin (HPCD) for 12h. (a) Protein aggregation levels were measured by differential centrifugation. (b) Cell death was determined by LDH release (c) Protein carbonyl levels were quantified by oxyblot analysis. Values represent the mean ± SEM of 3 experiments. Asterisks denote values that are significantly different (**$p<0.01$, ***$p<0.001$) from untreated cells (UT). Pound symbols denote values that are significantly different ($^{\#}p<0.05$, $^{\#\#}p<0.01$, $^{\#\#\#}p<0.001$) from DEM-treated cells.

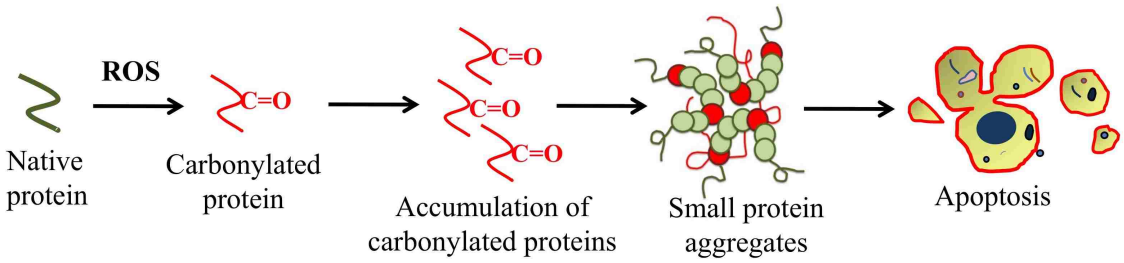

Fig. 5 – Schematic diagram representing the key findings of this study. Partial GSH depletion increases ROS levels in the nPC12 cells. Excessive ROS leads to the progressive accumulation of carbonylated proteins, which causes protein misfolding and triggers the formation of small-size protein aggregates. These cytotoxic aggregates ultimately cause neuronal death by apoptosis or necrosis.

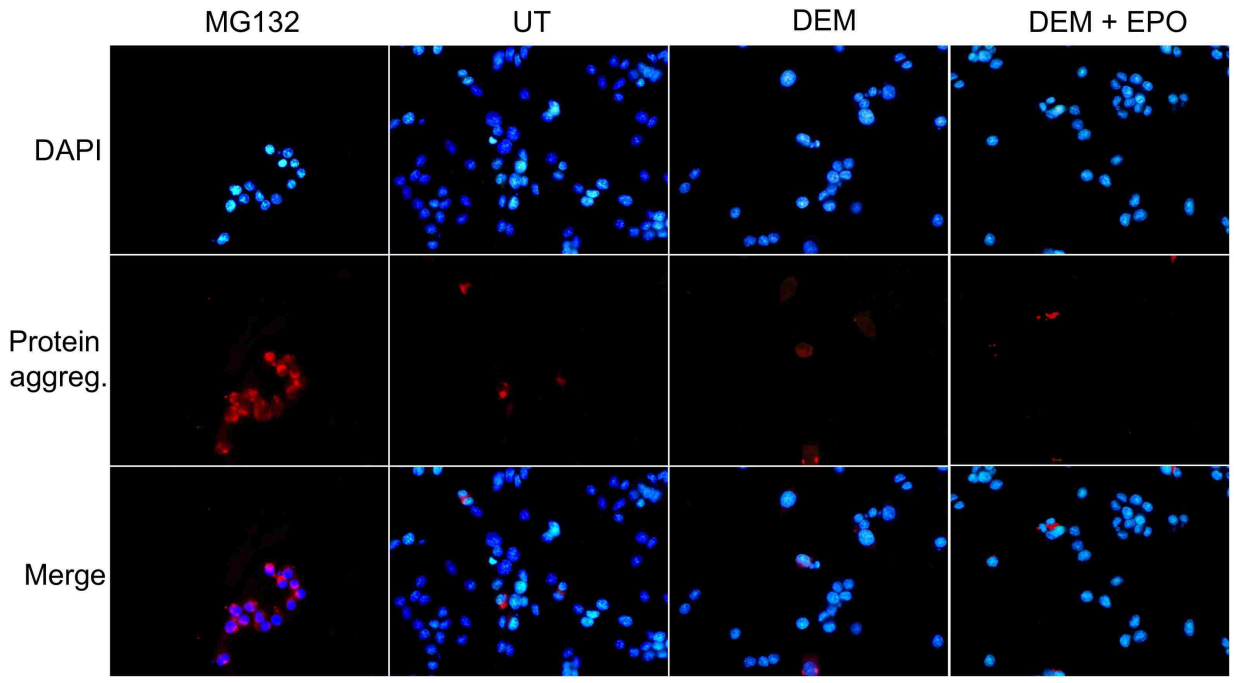

Fig. 6 – Partial GSH depletion does not induce additional large-size protein aggregates (aggresomes) in nPC12 cells. Cells were incubated with MG132, 50μM DEM or 50μM DEM + epoxomycin (EPO) for 12h. Protein aggregation was detected with the Proteostat® detection kit. UT, untreated cells.

5. Discussion

5.1 Oxidative stress and cell death

Acute oxidative stress may result in cell death via apoptosis or necrosis (England and Cotter, 2004). Due to the critical role of cell death in the pathophysiology of inflammatory demyelination, the identification of the processes responsible for apoptosis/necrosis have become the subject of intense study. Proteases like calpain and caspases play a central role in cell death. Elevation of calpain (marker of apoptosis and necrosis) and caspases (marker of apoptosis) in EAE and neuronal cells in culture (this study) indicates that both apoptosis and necrosis may take place simultaneously. Further, inhibition of calpain prevents cell death in EAE rats (Das et al., 2008). Since increased calpain activity is also found in the CNS of MS patients (Imam, 2007), it is possible that calpain-regulated mechanism of cell death, with both apoptosis and necrosis, might be happening at the same time in the CNS of these patients.

Multiple mechanisms have been proposed to explain how oxidative stress triggers cell death. One of these processes involves reduced glucose utilization during oxidative stress. It is believed that protein oxidation can inhibit glycolytic enzymes resulting in reduced glucose utilization and ATP production (England et al., 2004). When ATP levels reach a lower threshold, cells switch from apoptosis to necrosis because apoptosis is an energy dependent process (England et al., 2004; Troyano et al., 2001). The ultimate fate of a dead cell regardless of the type of cell death is its removal via phagocytosis (Krysko et al., 2006). Necrotic

cells are notorious for the release of their intracellular contents, which may elicit the production of inflammatory cytokines and the activation of immune system (Iyer et al., 2009). Both of these processes have a detrimental effect on neighboring cells further promoting tissue injury. It is generally accepted that apoptosis, in contrast to necrosis, does not lead to an inflammatory response. Yet, when there is massive apoptosis such that phagocytic activity is not sufficient to remove the dying cells, inflammation, oxidative stress and subsequent increase in cell death become apparent leading to a vicious detrimental cycle (Denecker et al., 2001).

Autophagic cell death under oxidative stress conditions is an important mechanism for elimination of cancer cells (Chen and Kilonsky, 2011), while in normal cells autophagy is mostly cytoprotective. For example nutrient deprivation (including glucose, lipids and amino acids) and starvation (Chen and Kilonsky, 2011) induces autophagy (Levine and Yuan, 2005) to recycle intracellular cytoplasmic components. This, in turn, supports mitochondrial energy production needed for cell survival (Levine and Yuan, 2005). Excessive autophagy, however, may be lethal as most of the cytoplasm is consumed due to its excessive digestion (Zhao et al., 2008). Yet, direct cell death by autophagy is relatively uncommon and applicable only under specific scenarios (Denton et al., 2011).

Oxidative damage-associated mitochondrial dysfunction results in energy depletion and cell death (Ryter et al., 2007). Recently, mitochondrial dysfunction with subsequent energy failure has been postulated to contribute to MS

pathogenesis (Witte et al., 2009) by promoting neurodegeneration during the onset and progression of the disease (Lee et al., 2012). Moreover, low levels of ATP and high levels of ATP-derived metabolites are found in the cerebro spinal fluid of MS patients (Tavazzi et al., 2011). Thus, the demise of CNS cells in MS patients may be partly due to oxidative stress and ATP depletion that take place in both neurons and glial cells (Figure 1). Oxidative stress is a major inducer of neuronal cell death (Schmuck et al., 2002; Watts et al., 2005, Harrison et al., 2005) and my observation of a 30% decrease in the number of neurons in the spinal cord of mice with acute EAE concomitant with the decrease in GSH levels strongly suggest that oxidative stress is an important cytotoxic mechanism.

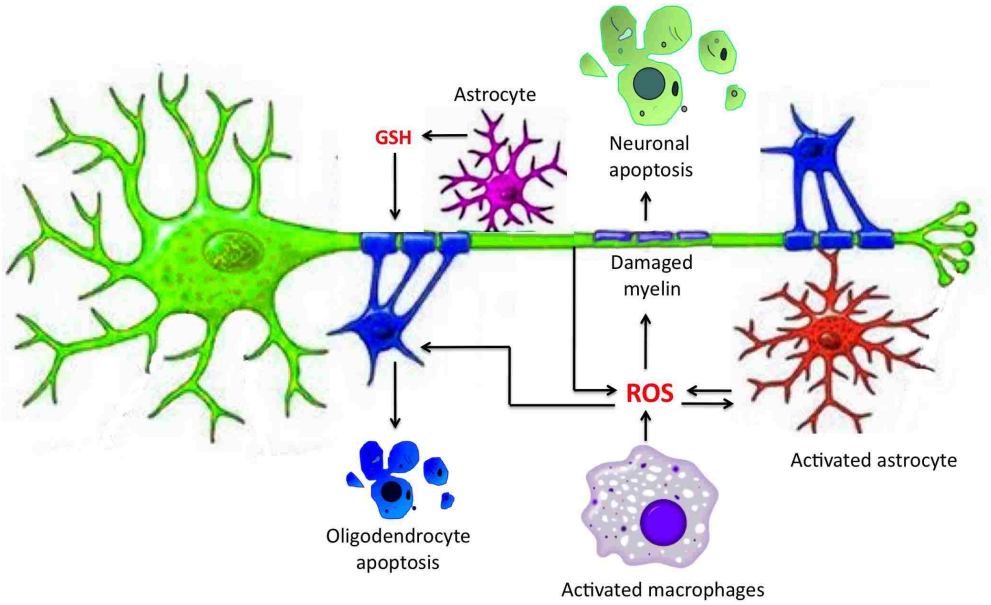

Figure 1: Cellular communication has additive impact of oxidative stress. Normally astrocytes protect neurons from oxidative stress by releasing glutathione (GSH) for its direct uptake by neurons. However, when astrocytes are activated they start generating ROS along with other cells (activated macrophages, damaged neurons, oligodendrocytes etc), accumulate and release ROS in excess that result in the ultimate demise of neurons and oligodendrocytes.

5.2 Differential cellular response to oxidative stress and accumulation of protein carbonyls

Severe oxidative stress can modify proteins leading to neuronal damage (Bharath and Anderson, 2005). One of the major protein modifications during oxidative stress is the formation of protein carbonyls. Inflammatory disorders such as MS and EAE are often associated with sustained periods of severe oxidative stress resulting in the accumulation of oxidized proteins (Smerjac and Bizzozero, 2008; Zheng and Bizzozero, 2010). However, my study revealed that carbonylated proteins accumulate in acute EAE (where oxidative stress is high) as well as in chronic EAE (where GSH and TBARS levels are normal). The latter is due to decreased proteasomal activity in chronic EAE. Thus, apoptosis correlates better with the build-up of protein carbonyls that with oxidative stress.

Due to a number of reasons described in the introduction to this dissertation, CNS cells are more susceptible to oxidative damage than those from other tissues. Additionally, different CNS cells have unique responses to oxidative stress and display variable build-up of protein carbonyls. In fact, I have observed that different CNS cell types (astrocytes, oligodendrocytes and neurons) vary in their sensitivity to oxidative stress and that nPC12 cells accumulate different levels of protein carbonyls when subjected to similar oxidative stress conditions. As shown in Chapter 2, astrocytes contain the highest levels of carbonyls in both control and EAE spinal cord, followed by oligodendrocytes and neurons. This is perhaps due to the large amounts of ROS produced by astrocytes and microglial cells (Keller et al., 1999), which could oxidize endogenous proteins. Yet, it was

somewhat surprising to discover that the basal carbonyl staining in neurons and oligodendrocytes are significantly lower, particularly when these two cell types are considered to be highly susceptible to oxidative damage (Halliwell, 2006; Benarroch, 2009). Interestingly, the notion that astrocytes are less sensitive to oxidative damage than other CNS cells has been recently challenged, as they were found to contain significantly lower GSH levels *in vivo* than neurons and oligodendrocytes (Miller et al., 2009). Another possibility is that oligodendrocytes and neurons may have a more efficient proteolytic machinery to remove oxidized proteins thus reducing the build up of carbonylated proteins in these cells.

5.3 Carbonylated proteins are cytotoxic

My data also suggest that shortly after the cells reach a threshold level of protein carbonyls, the plasma membrane becomes leaky (as evident from LDH release in DEM-treated nPC12 cells) and the cells rapidly die either by necrosis or apoptosis. Most likely, cells initially marked for apoptosis switched to necrosis as ATP became limiting. It is noteworthy that the subpopulation of glutathione depleted nPC12 cells that selectively accumulated the highest amount of protein carbonyls was also TUNEL positive. I also detected an equal number (~10-11%) of apoptotic and necrotic cells. Further, scavenging protein carbonyls prevented both type of cell death. Increased carbonylation of TUNEL positive cells was also observed in the spinal cord of EAE mice. These data suggest a critical role of protein carbonylation in both nPC12 cell death and in inflammatory demyelinating disorders. In the future, it will be important to develop and test specific carbonyl scavengers to determine whether or not this oxidative protein modification

significantly contributes to the pathophysiology of EAE. This approach is not without challenges since many carbonyl scavengers have anti-inflammatory properties, and inactivation of the immune system will undoubtedly ameliorate EAE. Thus, these drugs will have to be administered later in the disease course where inflammation in minimal.

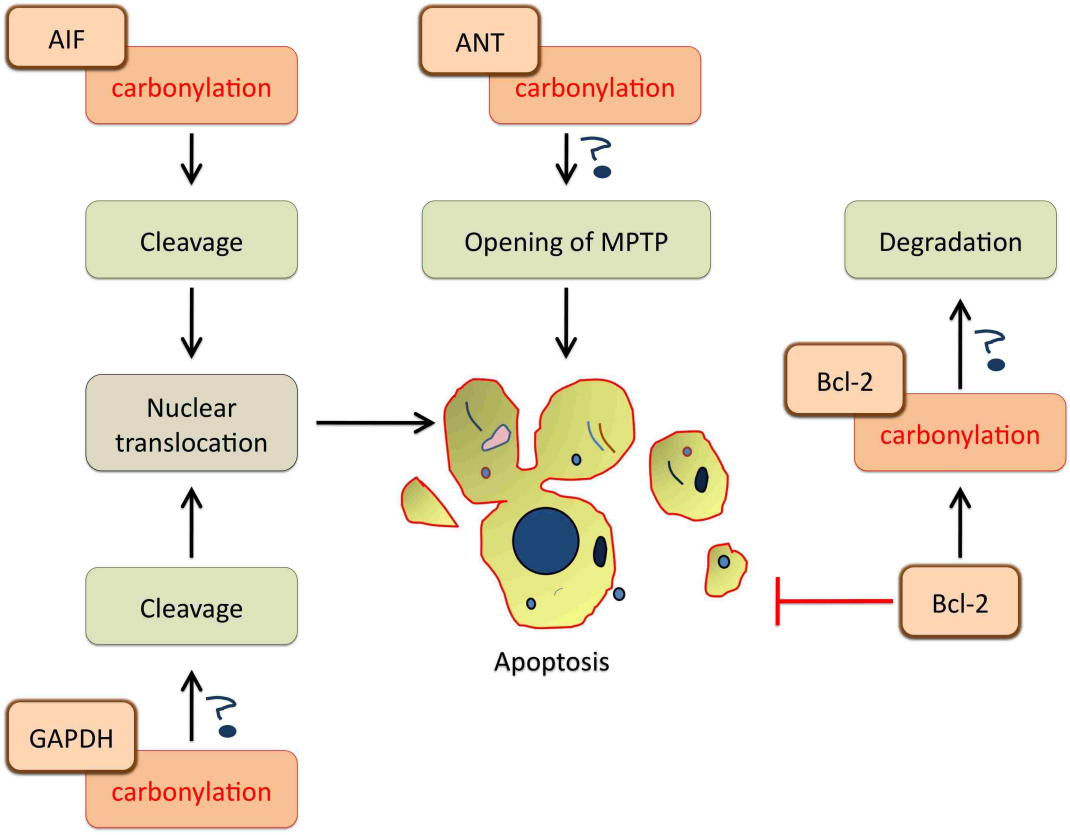

Figure 2: Possible mechanisms suggested for induction of apoptosis by protein carbonyls. Apoptosis inducing factor (AIF), adenine nucleotide protein (ANT) and B-cell lymphoma 2 (Bcl-2) are mitochondrial membrane proteins. Carbonylation of AIF has been shown to signal for apoptosis. ANT carbonylation precedes opening of MPTP that causes apoptosis. Degradation of anti-apoptotic protein, Bcl-2 occurs subsequent to its carbonylation followed by cellular apoptosis. Carbonylation of glycolytic protein glyceraldehyde-3-phosphate dehydrogenase (GAPDH) takes place before its nuclear translocation for apoptotic signaling.

There is evidence suggesting that after incorporation of carbonyl groups into specific proteins there are alterations in signaling leading to apoptosis (Cahuana

et al., 2004; Norberg et al., 2010). For example, carbonylation of B-cell lymphoma-2 (Bcl-2, anti-apoptotic protein) precedes its downregulation (Cahuana et al., 2004) and decreased Bcl-2 levels is a feature that happens prior to apoptosis (Xie et al., 1997; Krisch et al., 1999). Bcl-2 and antioxidants can prevent adenine nucleotide protein (ANT) dependent opening mitochondrial permeability transitional pore (MPTP) (Vieira et al., 2001), a critical for apoptosis (Kroemer et al, 2007; Dasgupta et al., 2012). ANT, a component of MPTP, is carbonylated during oxidative stress (Giron-Calle et al., 1994; Cahuana et al, 2004) but is unclear if this causes MPTP-mediated apoptosis. Another example is the glycolytic enzyme glyceraldehyde-3-phosphate dehydrogenase (GAPDH), which when carbonylated not only decreases its specific activity (Gomez-Pator et al., 2012) but also increases its translocation from cytoplasm to nucleus (Cahuana et al., 2004). However, while nuclear translocation of GAPDH is known to induce apoptosis (Tajima et al., 1999) direct evidence linking the specific carbonylation of GAPDH to apoptosis is still lacking. The only molecular event that documents apoptotic signaling by a carbonylated protein is through apoptosis inducing factor (AIF). AIF is a mitochondrial protein, whose susceptibility to calpain-mediated cleavage augments significantly after its carbonylation. Cleaved AIF migrates to the nucleus to induce apoptosis (Norberg et al., 2010). All of these molecular mechanisms have been integrated to show the possible induction of apoptosis via carbonylation of specific proteins (Figure 2). This picture, however, does not include another major consequence of protein oxidation, namely the formation of toxic protein aggregates.

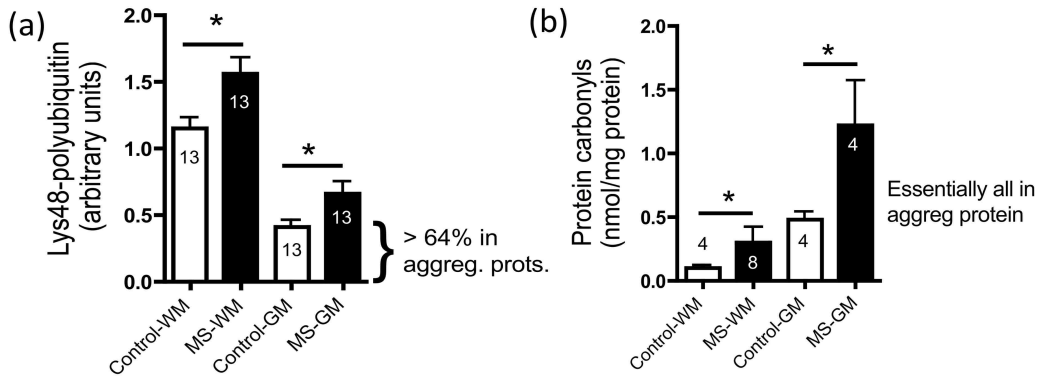

Figure 3: **Most carbonylated and poly-ubiquitinated proteins in MS partition into the fraction containing aggregated proteins. Levels of carbonylated proteins and Lys-48 poly-ubiquitinated were determined by western blot**. (a) Levels of poly-ubiquitinated proteins are increased in MS white matter (WM) and gray matter (GM), and 64% of the latter is present in protein aggregates. (b) The amount of carbonylated proteins is elevated in MS WM and GM and essentially all of them partition into the protein aggregate fraction. Values represent the mean ± SEM of the number of experiments shown inside the bars. *p<0.05.

5.4 Protein aggregation and its potential role in demyelinating disorders

In recent years, the study of intracellular protein aggregation has received extraordinary impetus in most fields of biomedical sciences, particularly in neurodegenerative diseases. The amount of protein aggregates (this study) and carbonylated proteins (Zheng and Bizzozero, 2010) have been found to increase with the progression of inflammatory demyelination. Carbonylation causes protein misfolding, thereby exposing hydrophobic regions that promote aggregation (Grune et al., 2005). Preliminary experiments from our laboratory using post-mortem human tissues have shown that Lys-48 poly-ubiquitinated proteins and carbonylated proteins are enriched in the detergent-insoluble fraction of brain white and gray matter, suggesting the occurrence of protein aggregation in MS (Figure 3). Furthermore, I also observed that an elevated proportion of carbonylated proteins in EAE partitions into the fraction containing

aggregated proteins (Figure 4). These data, along with those presented in chapter 2, demonstrate for the first time the presence of aggregates in demyelinating disorders.

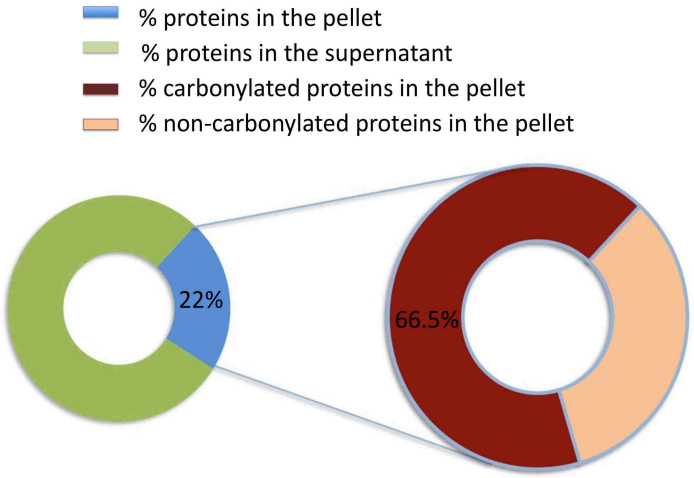

Figure 4: Levels of carbonylated proteins are elevated in the spinal cord of EAE mice, and approximately 67% of these oxidized proteins are present within aggregates.

In general, the accumulation of protein aggregates occurs in parallel with cell damage. However, it could be argued that formation of protein aggregates is a consequence of a primary neurotoxic event, thus representing a marker for neurodegeneration. Alternatively, aggregation may constitute a cellular defense mechanism that attempts to reduce the levels of toxic free proteins (Cleveland, 1999; Tran et al., 1999). One report, however, suggests that protein aggregation may contribute to motor neuron degeneration (Wood et al., 2003). Supporting this idea, my own study (chapter 4) clearly shows the neurotoxic role of protein aggregates in glutathione-depleted nPC12 cells. I believe that the discrepancy between the various studies on whether or not protein aggregates are toxic lies

on the type of protein aggregate. Not only aggregates can be made of different proteins but they may also differ significantly in size (from microaggregates to aggresomes).

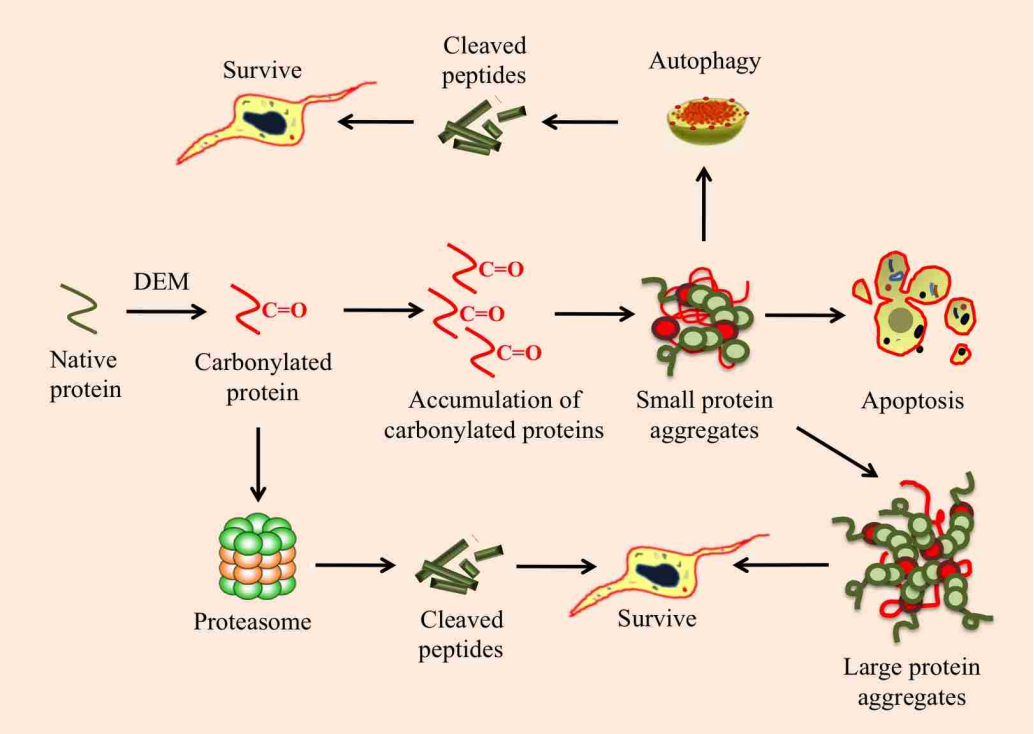

Figure 5: **Mechanistic model depicting how protein carbonylation may cause protein aggregation to mediate apoptosis.** Protein carbonyls are formed by oxidation of specific amino acid residues. Moderate levels of carbonylated proteins are maintained by an efficient removal via the proteasome. Increased rate of oxidation and/or defective proteasomal degradation cause a large accumulation of carbonylated proteins, followed by augmented protein aggregation and cell death. Active autophagy removes cytoprotective aggresomes but most importantly the cytotoxic small protein aggregates, whose build-up ultimate kills the cells.

The presence in EAE tissues of a significant number of cells containing large protein aggregates is likely due to an increase in the amount of carbonylated proteins along with a deficient removal. In this regard, we found that autophagy, the major mechanism for protein aggregate clearance (Son et al., 2012), is significantly reduced in both acute and chronic EAE, which explains the

occurrence of juxta-nuclear protein aggregates throughout the disease. As indicated above, while these large inclusion bodies may contribute significantly to cell death, there is some evidence suggesting aggresomes may be cytoprotective by sequestering the toxic, aggregated proteins (Tyedmers et al., 2010). Also, some of the same studies propose that the smaller protein aggregates are the cytotoxic species. Indeed, *in vitro* studies presented in chapter 4 showed that during GSH depletion aggresomes do not form despite the presence of cell death and protein aggregates determined by differential centrifugation. Thus, it fair to speculate that the overproduction and/or failure to clear small protein deposits is a likely contributor to neuronal damage. It will be very important to determine the size-distribution of protein aggregates during the course of the disease as we may find that the presence of small rather than large aggregates correlates better with the changes in pathology and disease activity.

Multiple studies suggest that protein carbonyls promote the formation of protein aggregates (Maisonneuve et al., 2008; Erjavec et al., 2007; Szokalska et al., 2009; Squier, 2001; Boshard et al., 2010). Yet until now no studies have directly established a link between protein carbonylation and protein aggregation. In this dissertation I attempted to elucidate whether protein carbonylation precedes protein aggregation to cause neuronal death triggered by partial glutathione depletion. To that end, I showed (1) that scavenging protein carbonyls prevents protein aggregation and neuronal death, and (2) that inhibiting protein aggregation reduces cell death without affecting the levels of protein carbonyls. This clearly demonstrates that protein oxidation is required for protein

aggregation to mediate neural apoptosis in our model of oxidative stress. Further, clearance of protein carbonyls by proteasomes helps in cell survival. Active autophagy may remove both small (potentially cytotoxic) and large (potentially cytoprotective). A mechanistic model representing my findings is shown in Figure 5.

5.5 Significance

In recent years there has been significant progress towards establishing the role of protein aggregation in neurological disorders but little research has been conducted to explore the possibility that protein carbonylation is the major triggering factor in aggregate formation. The work in this dissertation provides some answers to that possibility. My study is the first to (1) characterize cell death in the spinal cord of EAE mice at different disease stages, (2) show correlation between protein carbonylation, protein aggregation and cell death, and also their correlation to clinical disability in EAE, (3) report a decrease in autophagy in the acute and chronic phase of EAE, (4) demonstrate that protein carbonylation causes protein aggregation to mediate neural apoptosis.

Ultimately, understanding the role of protein carbonylation and protein aggregation in the development of CNS lesions in EAE/MS may help develop new therapeutic approaches to treat these disorders. Furthermore, I have obtained encouraging results using protein aggregate inhibitors to reduce cell death *in vitro* and future studies will attempt to prevent cellular apoptosis in EAE by using similar agents (see below). This strategy will serve both as a proof-of-

principle to demonstrate the role of aggregation in demyelinating disease and as basis for translational studies.

5.6 Future studies

Preliminary results show that protein aggregates containing poly-ubiquitinated and carbonylated proteins are present in MS brains. I have also obtained biochemical and histochemical evidence demonstrating the occurrence of intracellular protein aggregates in the spinal cord of mice with MOG peptide-induced EAE. Furthermore, at least in acute EAE, the amount of protein carbonyls, the number of protein aggregates and the extent of cell death all show a positive correlation with the clinical symptoms. Using neuronal cultures, I demonstrated that a moderate depletion of glutathione (GSH) (similar to that observed in EAE) leads to increased protein oxidation, aggregation and cell death, all of which are temporally correlated. Furthermore, inhibition of protein aggregation with Congo Red (CR) and 2-hydroxypropyl-β-cyclodextrin (HPCD) reduce neuronal cell death induced by partial glutathione depletion without affecting oxidative stress or protein carbonylation, suggesting a direct link between protein oxidation, protein aggregation and cell death. Considering these *in vitro* and *in vivo* findings, the obvious next step is to determine whether or not protein aggregation is pathogenic in EAE. I plan to address this issue by testing the effectiveness of protein aggregation inhibitors at reducing neuronal and glial cell death, tissue pathology and neurological symptoms in EAE mice.

Protein aggregate inhibitors are agents of diverse chemical nature that have in common the ability to aid in the refolding of proteins or to interfere with the assembly of larger protein structures. Some of them display specificity for a particular type of aggregates (e.g. rhodamine derivatives and anthraquinones for tau aggregates) while others are generally nonspecific (e.g. CR, lacmoid, cyclodextrin) (Lendel et al., 2009; Bulic et al., 2010). Based on the results shown in chapter 4, the bioavailability of the drugs and the lack of information regarding the type of protein aggregates present in EAE tissues, I will select two nonspecific inhibitors: CR and the cyclodextrin derivative HPCD. I believe that these are ideal agents to test our hypothesis since neither compound has antioxidant properties and have been already used *in vivo* (Frid et al., 2007; Burgevin et al., 1994; Gould and Scott, 2005). In fact, CR has an ameliorative effect in cell and animal models of neurodegenerative disorders, such as Alzheimer's, Parkinson's, Huntington's and prion diseases (Frid et al., 2006). There are several CR analogues with increased bioavailability and blood-brain barrier permeability that can be also tested in EAE.

I also need to identify the type of cell(s) in the EAE spinal cord where protein aggregates accumulate, their link to cell death, and if there is any spatial relationship between the presence of aggregates and the site of the inflammatory lesion. Finally, I would like to develop biochemical and histochemical techniques to characterize the size of the aggregates formed during the course of EAE. This is an important objective since we believe that cytotoxicity is mediated by the small-size protein aggregates. In sum, a number of novel and exciting studies

await to be carried out to elucidate the contribution of oxidative stress and altered proteostasis to the development of inflammatory demyelination.

References

Aktas O, Ullrich O, Infante-Duarte C, Nitsch R, Zipp F (2007), Neuronal damage in brain inflammation. Arch. Neurol. 64: 185–189.

Alonso A , Hernan MA (2008), Temporal trends in the incidence of multiple sclerosis: a systematic review. Neurology 71:129.

Arrasate M, Mitra S, Schweitzer ES, Segal MR, Finkbeiner S (2004), Inclusion body formation reduces levels of mutant huntingtin and the risk of neuronal death. Nature, 431(7010): 805–810.

Bast A, Haenen GRMM, Doelman CJA (1991), Oxidants and antioxidants: state of the art. Amer J Med 91(3C): 2S–13S.

Benarroch EE, Schmeichel AM, Dugger BN, Sandroni P, Parisi JE, Low PA (2009), Dopamine cell loss in the periaqueductal gray in multiple system atrophy and Lewy body dementia. Neurology. 73(2):106-12

Berlett BS , Stadtman ER (1997), Protein Oxidation in Aging, Disease, and Oxidative Stress. J of Bio. Chem 272: 20313-20316.

Bharath S, Anderson JK (2005), Glutathione depletion in a midbrain-derived immortalized dopaminergic cell line results in limited tyrosine nitration of mitochondrial complex I subunits: implications for Parkinson's disease. Antioxid Redox Signal. 7:900–10.

Bizzozero OA (2009), Protein Carbonylation in Neurodegenerative and Demyelinating CNS Diseases. Handbook of Neurochemistry and Molecular Neurobiology 543-562.

Bizzozero OA, DeJesus G, Callahan K, Pastuszyn A (2005), Elevated protein carbonylation in the brain white matter and gray matter of patients with multiple sclerosis. J. Neurosci. Res. 81: 687-695.

Bosshard F, Riedel K, Schneider T, Geiser C, Bucheli M, Egli T (2010), Protein oxidation and aggregation in UVA-irradiated Escherichia coli cells as signs of accelerated cellular senescence. Environ Microbiol. 10.1111/j.1462-2920.2010.02268.x.

Bulic B, Pickhardt M, Mandelkow EM, Mandelkowb E (2010), Tau protein and tau aggregation inhibitors. Neuropharmacology 59:276-289

Burcham PC, Fontaine F (2001), Extensive protein carbonylation precedes acrolein-mediated cell death in mouse hepatocytes. J. Biochem. and Mol. Toxicology 15(6): 309-316.

Burgevin MC, Passat M, Daniel N, Capet M, Doble A (1994), Congo red protects against toxicity of β-amyloid peptides on rat hippocampal neurons. NeuroReport, 5: 2429–2432.

Cahuana GM, Tejedo JR, Jiménez J, Ramírez R, Sobrino F, Bedoya FJ (2004), Nitric oxide-induced carbonylation of Bcl-2, GAPDH and ANT precedes apoptotic events in insulin-secreting RINm5F cells. Exp Cell Res 293:22-30.

Chandra J (2009), Oxidative Stress by Targeted Agents Promotes Cytotoxicity in Hematologic Malignancies. Antioxid. Redox Signal. 11: 1123–1137.

Chen Y, Klionsky DJ (2011. The regulation of autophagy – unanswered questions. J Cell Sci 2011; 124: 161–170.

Cleveland DW (1999), From Charcot to SOD1: mechanisms of selective motor neuron death in ALS. Neuron 24: 515–20.

Constantinescu CS, Farooqi N, O'Brien K, Gran B (2011), Experimental autoimmune encephalomyelitis (EAE) as a model for multiple sclerosis (MS). Br J Pharmacol. 164:1079–106.

Das A, Guyton MK, Matzelle DD, Ray SK, Banik NL (2008), Time-dependent increases in protease activities for neuronal apoptosis in spinal cords of Lewis rats during development of acute experimental autoimmune encephalomyelitis. J of Neurosci Res. 86(13): 2992-3001.

Dasgupta A, Bizzozero OA (2011), Positive correlation between protein carbonylation and apoptosis in EAE. Trans Am Soc Neurochem. 42:PSM08-01.

Dasgupta A, Zheng J, Bizzozero OA (2012), Protein carbonylation and aggregation precede neuronal apoptosis induced by partial glutathione depletion. ASN neuro 10.1042/AN20110064.

Denecker G, Vercammen D, Steemans M, Vanden-Berghe T, Brouckaert G, Van-Loo G, Zhivotovsky B, Fiers W, Grooten J, Declercq W, Vandenabeele P (2001), Death receptor-induced apoptotic and necrotic cell death: differential role of caspases and mitochondria. Cell Death Differ. 8, 829–840.

Denton D, Nicolson S, Kumar S (2011), Cell death by autophagy: facts and apparent artefacts. Cell Death & Differentiation 19(1): 87-95.

Divald A, Powell SR (2006), Proteasome mediates removal of proteins oxidized during myocardial ischemia. Free Radic. Biol. Med. 40: 156-164.

England K, O'Driscoll C, Cotter TG (2004), Carbonylation of glycolytic proteins is a key response to drug-induced oxidative stress and apoptosis. Cell Death and Differentiation 11:252–260.

Erjavec N, Larsson L, Grantham J, Nyström T (2007). Accelerated aging and failure to segregate damaged proteins in Sir2 mutants can be suppressed by overproducing the protein aggregation-remodeling factor Hsp104p. Genes & development, 21(19): 2410-2421.

Estus S, Tucker HM, Van-Rooyen C, Wright S, Brigham EF, Wogulis M, Rydel R E (1997), Aggregated amyloid-β protein induces cortical neuronal apoptosis and concomitant "apoptotic" pattern of gene induction. J. Neurosci. 17: 7736–7745.

Etienne MA, Edwin NJ, Aucoin JP, Russo PS, McCarley RL, Hammer RP (2007), Beta-amyloid protein aggregation. Methods Mol Biol. 386: 203-25.

Fox RJ (2010), Primary neuroprotection: the Holy Grail of multiple sclerosis therapy. Neurol. 74(13): 1018-9.

Frid P, Anisimov SV, Popovic N (2007), Congo red and protein aggregation in neurodegenerative diseases. Brain research reviews 53(1): 135-160.

Giron-Calle J, Zwizinski CW, Schmid HO (1994), Peroxidative damage to cardiac mitochondria: II. Immunological analysis of modified adenine nucleotide translocase. Arch. Biochem. Biophys. 315: 1–7.

Gold R, Hartung HP, Toyka KV, (2000), Animal models for autoimmune demyelinating disorders of the nervous system, Mol Med Today, 6: 88-91.

Gómez-Pastor R, Pérez-Torrado R, Cabiscol E, Ros J, Matallana E (2012), Engineered Trx2p industrial yeast strain protects glycolysis and fermentation proteins from oxidative carbonylation during biomass propagation. Microb Cell Fact. 11: 4.

Gould S, Scott RC (2005), 2-Hydroxypropyl-beta-cyclodextrin (HP-beta-CD): a toxicology review. Food Chem Toxicol. 43(10):1451-9.

Grune T, Davies KJ (1997), Breakdown of oxidized proteins as a part of secondary antioxidant defenses in mammalian cells. Biofactors, 6: 165–172.

Grune T, Klotz LO, Gieche J, Rudeck M, Sies H (2001), Protein oxidation and proteolysis by the nonradical oxidants singlet oxygen or peroxynitrite. Free Radic. Biol. Med. 30: 1243–1253.

Grune T, Merker K, Jung T, Sitte N, Davies KJ (2005), Protein oxidation and degradation during postmitotic senescence. Free Radic Biol Med. 39(9): 1208-15.

Hachiya NS, Kozuka Y, Kaneko K (2008), Mechanical stress and formation of protein aggregates in neurodegenerative disorders. Medical Hypotheses 70(5): 1034-7.

Halliwell B (2006), Oxidative stress and neurodegeneration: where are we now? J Neurochem. 97(6):1634-58.

Harrison JF, Hollensworth SB, Spitz DR, Copeland WC, Wilson GL, LeDoux SP (2005), Oxidative stress-induced apoptosis in neurons correlates with mitochondrial DNA base excision repair pathway imbalance. Nucleic Acids Res. 33 (14): 4660-4671.

Henderson AP, Barnett MH, Parratt JD, Prineas JW (2009), Multiple sclerosis: distribution of inflammatory cells in newly forming lesions. Ann Neurol, 66(6): 739-53.

Imam SA (2007), Increased calpain correlates with Th1 cytokine profile in PBMCs from MS patients. J Neuroimmunol. 190: 139–145.

Iyer SS, Pulskens WP, Sadler JJ, Butter LM, Teske GJ, Ulland TK, Eisenbarth TC, Florquin S, Flavell RA, Leemans JC, and Sutterwala SF (2009), Necrotic cells trigger a sterile inflammatory response through the Nlrp3 inflammasome. PNAS 106 (48): 20388-20393.

Johansson A, Vestling M, Zetterström P, Lang L, Leinartaitė L, Karlström M, Danielsson J, Marklund SL, Oliveberg M (2012), Cytotoxicity of Superoxide Dismutase 1 in Cultured Cells Is Linked to Zn2+ Chelation. PLoS ONE 7(4): e36104.

Keegan BM, Noseworthy JH (2002), Multiple sclerosis. Annu Rev Med. 53:285-302.

Kirsch DG, Doseff A, Nelson-Chau B, Lim DS, de Souza-Pinto NC, Hansford R, Kastan MB, Lazebnik YA, Hardwick JM (1999), Caspase-3-dependent cleavage of Bcl-2 promotes release of cytochrome c. J. Biol. Chem.274: 21155–212161.

Kopito RR (2000), Aggresomes, inclusion bodies and protein aggregation. Trends in Cell Biology 10(12) 524–530.

Kroemer G, Galluzzi L, Brenner C (2007), Mitochondrial membrane permeabilization in cell death. Physiol Rev. 87: 99–16.

Krysko DV, D':Herde K, Vandenabeele P. 2006. Clearance of apoptotic and necrotic cells and its immunological consequences. Apoptosis 11:1709–1726.

Lamark T, Johansen T (2012), Aggrephagy: Selective Disposal of Protein Aggregates by Macroautophagy. Int. J. Cell Bio. Article ID 736905, 21 pages, doi:10.1155/2012/736905.

Lee DH, Gold R, Linker RA (2012), Mechanisms of Oxidative Damage in Multiple Sclerosis and Neurodegenerative Diseases: Therapeutic Modulation via Fumaric Acid Esters. Int J Mol Sci. 13(9): 11783-803.

Lendel C, Bertoncini CW, Toth G (2009), On the mechanism of nonspecific inhibitors of protein aggregation: dissecting the interactions of α-synuclein with Congo red and Lacmoid. Biochemistry 48:8322–8334.

Levine, B. and Yuan, J. (2005). Autophagy in cell death: an innocent convict? J. Clin. Invest. 115, 2679-2688.

Maisonneuve E, Fraysse L, Moinier D, Dukan S (2008), Existence of abnormal protein aggregates in healthy Escherichia coli cells. J. Bacteriol. 190: 887–89.

Majno G , Joris I (1995), Apoptosis, oncosis, and necrosis. An overview of cell death. Am. J. Pathol. 146: 3–15.

McDonnell GV, Hawkins SA (1996), Primary progressive multiplesclerosis: a distinct syndrome?. Mult Scler. 2: 137–141.

Meyer R, Weissert R, Diem R, Storch M K, de Graaf K L, Kramer B and Bahr M (2001), Acute Neuronal Apoptosis in a Rat Model of Multiple Sclerosis. J. Neurosc. 21(16): 6214–6220.

Miller VM, Lawrence DA, Mondal TK, Seegal RF (2009), Reduced glutathione is highly expressed in white matter and neurons in the unperturbed mouse brain—implications for oxidative stress associated with neurodegeneration. Brain Res. 1276:22–30.

Mirzaei H, Regnier F, (2008), Protein:protein aggregation induced by protein oxidation, J Chromatogr B Analyt Technol Biomed Life Sci., 873(1): 8-14

MMaisonneuve E, Fraysse L, Lignon S, Capron L, Dukan S (2008), Carbonylated proteins are detectable only in a degradation-resistant aggregate state in Escherichia coli. Journal of bacteriology 190(20): 6609-6614.

Nilsberth C, Westlind-Danielsson A, Eckman CB, Condron MM, Axelman K, Forsell C, Stenh C, Luthman J, Teplow DB, Younkin SG, Näslund J, Lannfelt L (2001), The 'Arctic' APP mutation (E693G) causes Alzheimer's disease by enhanced Abeta protofibril formation. Nat Neurosci. 4(9): 887–93.

Norberg E, Orrenius S, Zhivotovsky B (2010), Mitochondrial regulation of cell death: Processing of apoptosis-inducing factor (AIF), Biochemical and Biophysical Research Communications 396: 95–100.

Pender MP, Nguyen KB, McCombe PA, Kerr J F (1991). Apoptosis in the nervous system in experimental allergic encephalomyelitis. J Neurol Sci. 104 (1): 81-7.

Ross CA, Poirier MA (2004), Protein aggregation and neurodegenerative disease. Nat Me. 10: S10-7.

Ryter SW, Kim HP, Hoetzel A, Park JW, Nakahira K, Wang X, Choi AM (2007), Mechanisms of cell death in oxidative stress. Antioxid Redox Signal. 9(1): 49-89.

Schmuck G, Rohrdanz E, Tran-Thi QH, Kahl R, Schluter G (2002), Oxidative stress in rat cortical neurons and astrocytes induced by paraquat in vitro. Neurotox Res. 4:1–13.

Schulz JB, Lindenau J, Seyfried J, Dichgans J (2000), Glutathione, oxidative stress and neurodegeneration., Eur J Biochem. 267(16): 4904-11.

Shacter E (2000), Quantification and significance of protein oxidation in biological samples, Drug Metabolism Reviews. 32 (3&4): 307–326.

Smerjac S, Bizzozero OA (2008), Cytoskeletal protein carbonylation and degradation in experimental autoimmune encephalomyelitis. J. Neurochem.105: 763-772.

Smith KJ, Kapoor R, Felts PA (1999), Demyelination: the role of reactive oxygen and nitrogen species. Brain Pathol. 9:69–92.

Son JH, Shim JH, Kim KH, Ha JY, Han, JY (2012), Neuronal autophagy and neurodegenerative diseases. Experimental & Molecular Medicine, 44(2): 89-98.

Squier TC (2001), Oxidative stress and protein aggregation during biological aging. Exp Gerontol 36:1539–1550.

Szokalska, A, Makowski M, Nowis D, Wilczyński GM, Kujawa M, Wójcik, C, Izabela Młynarczuk-Biały I, Salwa P, Bil J, Janowska S, Agostinis P, Verfaillie T, Bugajsk M, Gietka J, Issat T, Glodkowska E, Mrowka P,Stoklosa T, Hamblin MR, Miroz P, Jakobisiak M, Golab J (2009), Proteasome inhibition potentiates antitumor effects of photodynamic therapy in mice through induction of endoplasmic reticulum stress and unfolded protein response. Cancer research 69(10): 4235-4243.

Tajima H, Tsuchiya K, Yamada M, Kondo K, Katsube N, Ishitani R (1999), Overexpression of GAPDH induces apoptosis in COS-7 cells transfected with cloned GAPDH cDNAs. Neuroreport 10: 2029–2033.

Tavazzi B, Batocchi AP, Amorini AM, Nociti V, D'Urso S, Longo S, Gullotta S, Picardi M, Lazzarino G (2011), Serum metabolic profile in multiple sclerosis patients. Mult Scler Int.167156.

Tran PB, Miller RJ (1999), Aggregates in neurodegenerative disease: crowds and power? Trends Neurosci. 22: 194–7.

Troncoso JC, Costello AC, Kim JH, Johnson GV (1995), Metal-catalyzed oxidation of bovine neurofilaments in vitro. Free Radic. Biol. Med.18: 891–899.

Troyano A, Fernández C, Sancho P, de-Blas E, Aller P (2001), Effect of glutathione depletion on antitumor drug toxicity (apoptosis and necrosis) in U-937 human promonocytic cells. The role of intracellular oxidation, J. Biol. Chem., 276: 47107-47115.

Trześniewska K, Brzyska M, Elbaum D (2004), Neurodegenerative aspects of protein aggregation., Acta Neurobiol Exp (Wars) 64(1): 41-52.

Tyedmers J, Mogk A, Bukau B (2010), Cellular strategies for controlling protein aggregation. Nat Rev Mol Cell Biol. 11(11):777-88

Uttara B, Singh AV, Zamboni P, Mahajan RT (2009), Oxidative Stress and Neurodegenerative Diseases: A Review of Upstream and Downstream Antioxidant Therapeutic Options Curr Neuropharmacol, 7(1): 65–74.

Vercellino M, Masera S, Lorenzatti M, Condello C, Merola A, Mattioda A, Tribolo A, Capello E, Mancardi GL, Mutani R, Giordana MT, Cavalla P (2009), Demyelination, Inflammation, and Neurodegeneration in Multiple Sclerosis Deep Gray Matter. J Neuropathol Exp Neurol. 68(5): 489-502.

Vieira HL, Belzacq AS, Haouzi D, Bernassola F, Cohen I, Jacotot E, Ferri KF, El Hamel C, Bartle LM, Melino G, Brenner C, Goldmacher V, Kroemer G (2001), The adenine nucleotide translocator: a target of nitric oxide, peroxynitrite, and 4-hydroxynonenal. Oncogene 20(32):4305-16.

Watts LT, Rathinam ML, Schenker S, Henderson GI (2005), Astrocytes protect neurons from ethanol-induced oxidative stress and apoptotic death. J. Neurosci. Res. 80: 655–666.

Witherick J, Wilkins A, Scolding N, Kemp K (2011), Mechanisms of Oxidative damage in multiple sclerosis and a cell therapy approach to treatment, Autoimmune Diseases 608 - 619.

Witte M.E., Bo L., Rodenburg R.J., Belien J.A., Musters R., Hazes T., Wintjes L.T., Smeitink J.A., Geurts J.J., de Vries H.E., et al. Enhanced number and activity of mitochondria in multiple sclerosis lesions. J. Pathol. 2009;219:193–204

Wood JD, Beaujeux TP, Shaw PJ (2003), Protein aggregation in motor neurone disorders. Neuropathol. Appl. Neurobiol. 29:529–545.

Xie K, Wang , Huang S, Xu L, Bielenberg D, Salas T, McConkey DJ, Jiang W, Fidler IJ (1997), Nitric oxide mediated apoptosis of K-1735 melanoma cells is associated with downregulation of Bcl-2. Oncogene 15: 771–779.

Zhao, Wieman HL, Jacobs SR, Rathmell JC (2008), Mechanisms and Methods in Glucose Metabolism and Cell Death. Methods Enzymol. 442: 439–457.

Zheng J, Bizzozero OA (2010a) Traditional reactive carbonyl scavengers do not prevent the carbonylation of brain proteins induced by acute glutathione depletion. Free Radic Res 44:258-266.

Zheng J, Bizzozero OA (2010b) Accumulation of protein carbonyls within cerebellar astrocytes in murine experimental autoimmune encephalomyelitis. J Neurosci Res 88:3376-3385.

Zheng J, Bizzozero OA (2011), Decreased activity of the 20S proteasome in the brain white matter and gray matter of patients with multiple sclerosis. J Neurochem. 117(1): 143-53.

Zhu YJ, Lin H, Lal R, (2000), Fresh and nonfibrillar amyloid beta protein(1-40) induces rapid cellular degeneration in aged human fibroblasts: evidence for AbetaP-channel-mediated cellular toxicity. FASEB J. 14(9): 1244–54.

List of abbreviations

- ACR: acrolein
- AD: Alzheimer's disease
- AIF: Apoptosis inducing factor
- ALS: Amoyotrophic lateral sclerosis
- ANT: Adenine nucleotide protein
- APC: adenomatous polyposis coli protein
- ATP: Adenosine triphosphate
- AVNC: annexin-V negative cells
- AVPC: annexin-V positive cells
- Bcl-2: B-cell lymphoma -2
- BSO, buthionine sulfoximine
- $CaCl_2$: Calcium Chloride
- CFA: Complete Freund's adjuvant
- CNS: Central nervous system
- CR: Congo red
- CsA: Cyclosporin A
- CSF: Cerebro spinal fluid
- DAPI: 4',6-diamidino-2-phenylindole
- DE: DEM+ epoxomicin
- DEM: diethyl maleate
- DL: DEM+lactacystin
- DNA: Deoxyribonucleic acid
- DNP: 2,4-dinitrophenyl
- DNPH: 2,4-dinitrophenylhydrazine
- DPI: days post immunization
- EAE: experimental autoimmune encephalomyelitis
- EDTA: Ethylenediamine-tetraacetic Acid
- EPO: Epoxomicin
- FI: Fluorescence intensity
- FU: Fluorescence units
- GAP-43: Growth Associated Protein 43
- GAPDH: glyceraldehyde-3-phosphate dehydrogenase
- GFAP: glial fibrillary associated protein
- GM: Gray matter
- GSH: reduced glutathione
- GSSG: glutathione disulfide
- HCl: Hydrogen Chloride
- HD: Huntington's disease
- HL60: Human promyelocytic leukemia cells
- HNE: hydroxynonenal
- HPCD: 2-hydroxypropyl β-cyclodextrin
- HRP: Horseradish peroxidase
- HZ: Hydralazine
- KCl: Potassium Chloride
- LC3: Microtubule-associated protein light chain 3
- LDH: Lactate dehydrogenase
- mAb: Monoclonal antibody
- MDA: malondialdehyde
- MOG: Myelin oligodendrocyte glycoprotein
- MOG: myelin-oligodendrocyte glycoprotein
- MPTP: mitochondrial permeability transition pore
- MS: Multiple sclerosis
- NaCl: Sodium Chloride
- NADH: Nicotinamide adenine dinucleotide hydride
- NADPH: nicotinamide adenine dinucleotide phosphate-oxidase
- NeuN: neuronal nuclear antigen
- NFH: Neurofilament heavy chain
- NGF: nerve growth factor
- NIH: National institute of health

- nPC12 cells: NGF-treated rat adrenal medullary pheochromocytoma cells
- OS: Oxidative stress
- PA: Proteasome activity
- pAb: Polyclonal antibody
- PBS: phosphate-buffered saline
- PC12: rat adrenal medullary pheochromocytoma cells
- PCD: Programmed cell death
- PCI: Pancaspase inhibitor
- PCO: protein carbonyl
- PD: Parkinson's disease
- PFA: Paraformaldehyde
- RCS: reactive carbonyl species
- SDS-PAGE: Sodium dodecyl sulfate polyacrylamide gel electrophoresis
- SEM: Standard error of the mean
- TBARS: thiobarbituric acid reactive substances.
- TNC: TUNEL negative cells
- TPC: TUNEL positive cells
- TUNEL: terminal deoxynucleotidyl transferase dUTP nick end labeling.
- UT: untreated
- WM: White matter